Student Research Accomplishments 2001 – 2002

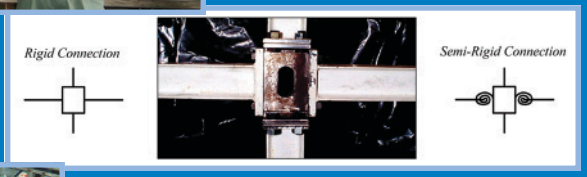

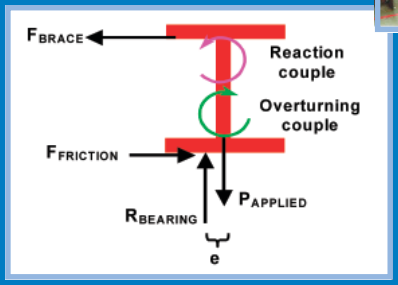

MCEER
MULTIDISCIPLINARY CENTER FOR EARTHQUAKE ENGINEERING RESEARCH
A National Center of Excellence in Advanced Technology Applications

October 2002

The Multidisciplinary Center for Earthquake Engineering Research

The Multidisciplinary Center for Earthquake Engineering Research (MCEER) is a national center of excellence in advanced technology applications that is dedicated to the reduction of earthquake losses nationwide. Headquartered at the University at Buffalo, State University of New York, the Center was originally established by the National Science Foundation (NSF) in 1986, as the National Center for Earthquake Engineering Research (NCEER).

Comprising a consortium of researchers from numerous disciplines and institutions throughout the United States, the Center's mission is to reduce earthquake losses through research and the application of advanced technologies that improve engineering, pre-earthquake planning and post-earthquake recovery strategies. Toward this end, the Center coordinates a nationwide program of multidisciplinary team research, education and outreach activities.

Funded principally by NSF, the State of New York and the Federal Highway Administration (FHWA), the Center derives additional support from the Federal Emergency Management Agency (FEMA), other state governments, academic institutions, foreign governments and private industry.

Student Research Accomplishments

2001-2002

Multidisciplinary Center for Earthquake Engineering Research
University at Buffalo, State University of New York

Edited by Diego Lopez Garcia

October 2002

MCEER-02-SP09

Red Jacket Quadrangle, Buffalo, New York 14261
Phone: (716) 645-3391; Fax: (716) 645-3399
E-mail: *mceer@mceermail.buffalo.edu*
World Wide Web: *http://mceer.buffalo.edu*

Foreword

The Student Leadership Council (SLC) is a formal incarnation of the students who are involved in performing MCEER research under a faculty advisor. Since its inception, MCEER has included and encouraged student efforts throughout its research program and in all of the disciplinary specialties concerned with earthquake engineering.

Throughout the years, students have been an integral component in advancing research in earthquake hazard mitigation. Many former students are now in academia, professional practice or government agencies applying knowledge gained during their exposure to MCEER research. While associated with MCEER, students participate in annual Center Investigator meetings, attend conferences, workshops and seminars, and have the opportunity to make presentations at these events. The SLC was formed in the year 2000 to formalize these programs and to afford students from many different institutions the opportunity to meet with each other and develop/improve interaction.

The idea for the *Student Research Accomplishments* was conceived by the SLC and features the work of some of MCEER's current students. Topics range from traditional civil and lifeline engineering to applications of advanced technologies to social impacts and economic modeling.

This issue was coordinated and edited by Diego Lopez Garcia, a Ph.D. candidate in the Department of Civil, Structural & Environmental Engineering at the University at Buffalo. MCEER acknowledges Mr. Lopez Garcia's efforts as well as those of the individual contributors. MCEER also wishes to extend its thanks to the Student Leadership Council for its endeavors, and in particular to A. Natali Sigaher, past president, and Jeffrey Berman, current president, for their able guidance of the SLC.

Contents

Contents (Cont'd)

1

On the Calibration of the Specific Barrier Model to Eastern North America Earthquakes

Benedikt Halldorsson

Department of Civil, Structural & Environmental Engineering, University at Buffalo

Research Supervisor: Apostolos S. Papageorgiou, Professor

Summary

The paucity of high-quality strong motion data for moderate and large earthquakes in Eastern North America (ENA) makes it difficult to reliably estimate strong ground motions for future earthquake events in the region. The stochastic modeling approach, which utilizes a seismological model to describe the spectral amplitudes of the ground motion and their relationship with the earthquake size, is arguably the only viable method of ground motion prediction in ENA. The source model used in the present study is the "specific barrier model" proposed and developed by Papageorgiou and Aki (1983a, 1983b, 1985) and Papageorgiou (1988). This paper presents results of the calibration of the "specific barrier model" using the available strong motion database of ENA earthquakes.

Introduction

Prediction of seismic hazard in tectonic regions of moderate-to-low seismicity, such as Eastern North America (ENA), is a difficult task due to the paucity of available data for such regions. The "stochastic modeling approach" has been extensively used in the past for the prediction of strong ground motion in ENA. Various earthquake source models such as the "ω^2 model" (Brune 1970, Frankel et al., 1996) have been employed for this purpose (Atkinson and Boore 1998). A more physically realistic source model is the "specific barrier model" proposed and developed by Papageorgiou and Aki (1983a, 1983b, 1985) and Papageorgiou (1988). This model may be used for "far-field" as well as for "near- source" strong motion prediction.

This paper presents results of the calibration of the "specific barrier model" using the available strong motion database of ENA earthquakes. Estimates of "global" and "local" stress drops believed to be representative of earthquake sources in ENA are presented and a "scaling law" (i.e., the variation of source spectrum scales with respect to the earthquake size) for the source spectra of ENA earthquakes is proposed.

Spectral Response Data

The strong motion database utilized in this study for the calibration of the "specific barrier model" comprises the pseudo-spectral acceleration data recorded on rock used by Atkinson and Boore (Tables 1 and 2 in Atkinson and Boore, 1998) for the evaluation of earthquake source models for ENA, with the exception of four historical ENA events. The remaining events are shown in Table 1. Events of magnitude greater than 5.8 occurred in other intraplate regions that are believed to be tectonically similar to ENA (Atkinson and Boore, 1998). Only PSV (= pseudo-velocity response)

data associated with frequencies of oscillation equal to 1, 2, 5 and 10 Hz were used because they were available.

Furthermore, four different variations of the datasets were considered for the calibration of the model for comparison purposes:

Dataset 1 (AB98): all the events included in Table 1 of Atkinson and Boore (1998).

Dataset 2: the dataset shown in Table 1.

Dataset 3: the dataset shown in Table 1 excluding the 1988 Saguenay mainshock.

Dataset 4: data for the Saguenay earthquake only.

Table 1. Seismic events from which response spectral data has been utilized in calibrating the "specific barrier model" to ENA earthquakes. *N* indicates the number of records for which spectral response data at frequencies 1, 2, 5 and 10 Hz is used.

Date	Event	*Mw*	*N*
05/17/76	Gazli, USSR	6.8	2
09/16/78	Tabas-e-Golshan, Iran	7.4	4
01/19/82	Gaza, NH	4.3	6
10/07/83	Newcomb, NY	5.0	16
01/31/85	Painesville, OH	4.8	9
12/23/85	Nahanni, NT, CA	6.8	6
07/12/86	St. Marys, OH	4.5	5
11/23/88	Saguenay (fs), QC, CA	4.2	11
11/25/88	Saguenay (ms), QC, CA	5.8	28
10/19/90	Mont Laurier, QC, CA	4.5	17
06/15/91	Georgia, USSR	6.2	2

Seismological Model

Central to the stochastic modeling approach is the spectral scaling of the seismic radiation of the seismological model implemented for the prediction of ground motion (Boore 1983, Boore and Atkinson, 1987). Use of random vibration theory allows for the prediction of extreme ground motion parameters such as the peak response of a harmonic oscillator (Cartwright and Longuet-Higgins, 1956, Boore 1983).

The "specific barrier model" is adopted as source model. Once the moment magnitude, average shear velocity of the medium and the rupture velocity are given, the "specific barrier model" is uniquely determined by two parameters: the "global" and "local" stress drops $\Delta\sigma_G$ and $\Delta\sigma_L$, respectively (Papageorgiou 1988). The ratio of rupture velocity to shear velocity is set equal to 0.8.

Other elements of our seismological model such as path and site effects were considered according to Atkinson and Boore (1995). However, since various investigators have accounted for path effects in different ways, it was decided to implement and test some of these descriptions. An attempt is made to discriminate among these various ways to account for path effects by evaluating the quality of fit of their predictions to the available data. Therefore, three variations of the seismological model mentioned before were used. Model I accounts for the attenuation of high-frequency waves by a low-pass exponential filter $P(f) = e^{-\pi\kappa f}$ (κ-filter) with $\kappa = 0.01$ in accordance with Frankel et al., (1996). Model II accounts for the attenuation of high-frequency waves by a Butterworth low-pass filter $P(f) = [1 + (f / f_{max})^8]^{-1/2}$ with $f_{max} = 50$ Hz (f_{max}-filter). Model III makes use of the abovementioned $f_{\max}$ filter and utilizes Boore and Atkinson's geometrical spreading factor (Boore and Atkinson 1987), which changes from $1/r$ to $1/(r\, r_x)^{1/2}$ at distance r_x in order to account for the observed transition of body waves to surface waves at around $r_x = 100$ km in ENA.

The quality factor $Q(f)$ is in all models expressed using an empirical functional form proposed by Boore (1985), which was fitted to match Atkinson and Boore's $Q(f) = 680\, f^{-0.36}$ (Atkinson and Boore, 1995) at intermediate and high frequencies. Site amplification factor was assumed equal to unity in all models, which is a reasonable assumption for "very hard rock" in ENA (Boore and Joyner, 1997).

Results

Calibration of the seismological model to spectral response data and calibration of the "specific barrier model" to inferred source spectra were performed using a "weighted" nonlinear least squares regression based on the modified Levenberg-Marquardt algorithm (VNI 1991).

Fitting of Model I to the datasets in Table 2 using both the "global" and "local" stress drop parameters of the "specific barrier model" as "free" inversion parameters resulted in "global" stress drops ranging from 30 to 50 bar. A "global" stress drop value of $\Delta\sigma_G = 45$ bar was then assumed, which is consistent with Haddon's estimate of the source area of the 1988 Saguenay mainshock event (Haddon 1995) and with empirical relationships between moment magnitude and fault area proposed by Wells and Coppersmith (1994).

In order to infer a similarly representative value of the "local" stress drop, $\Delta\sigma_G$ was set equal to 45 bar and then inversions of Models I, II and III were carried out using the spectral response datasets indicated in Table 2 and treating $\Delta\sigma_L$ as the only inversion parameter. Results are given in Table 2, where ${}^{i}\Delta\sigma_L$ and ${}^{i}\sigma$ correspond to seismological models i = I, II and III and ${}^{i}\sigma$ denotes the non-weighted standard deviation of the residual between the logarithm of measured values and the logarithm of predicted values (referred to in what follow simply as "the standard deviation").

Table 2 suggests that, except for Dataset 4, all the other datasets give a very stable value for $\Delta\sigma_L$. Judging from the standard deviations, Model III clearly has the largest residuals, hence Models I and II are preferred. It is observed that the inversions cannot clearly discriminate between Models I and

II (i.e., whether a high-frequency f_{max}-filter or a κ-filter is preferable). This is very likely related to the fact that the available data cover a rather narrow (ENA events) frequency range (1 to 10 Hz).

The standard deviation resulting from inversions using Dataset 2 is significantly reduced from that for Dataset 1, which means that exclusion of the data of the four historical events was warranted.

Table 2. Results of the calibration of the "specific barrier model" using spectral response data. $^{I}\sigma_{400}$ is the standard deviation of model I with $\Delta\sigma_L$ = 400 bar.

No.	Dataset	$^{I}\Delta\sigma_L$	$^{I}\sigma$	$^{II}\Delta\sigma_L$	$^{II}\sigma$	$^{III}\Delta\sigma_L$	$^{III}\sigma$	$^{I}\sigma_{400}$
1	AB98, Table 2	185	0.37	153	0.36	224	0.38	0.36
2	Table 1	213	0.32	171	0.32	224	0.36	0.31
3	Table 1 (except *)	183	0.25	151	0.25	197	0.27	0.30
4	Saguenay data*	935	0.28	682	0.27	987	0.33	0.32

Similar scrutiny of results for Datasets 2 and 3 shows that exclusion of the Saguenay data improves the fit even further. Finally, the very high "local" stress drop values for Dataset 4 as compared to the other datasets indicate high amplitudes of ground motion for this event, as compared to what is expected on the average from other events with the same seismic moment (see section entitled **Spectral Response Data**).

However, data for events of M_w = 5.0 or smaller in Table 1 include 64 records, while data for larger events include 42 records, 28 of which are provided for by the Saguenay event. The non-weighted standard deviation is therefore greatly affected. Besides, the Saguenay event is one of the largest recorded earthquakes in ENA over the last 50 years and researchers have debated over whether it was a "typical" ENA event or not (Haddon 1997). Discussion of this issue is out of the scope of this paper, but a note is made about the difference between the stress drop results for Datasets 2 and 3.

Discussion and Conclusions

Estimates of values of the "local" stress drop obtained from the inversions using the spectral response data of Datasets 1, 2 and 3 are equal to approximately 50% of the values corresponding to a "local" stress drop of 400 bars (see last column in Table 2). However, the corresponding difference between standard deviations is not large, as observed when comparing values of $^{I}\sigma$ and $^{I}\sigma_{400}$ (Table 2), especially for Datasets 1 and 2, which include the Saguenay data.

Taking into consideration the abovementioned limitations of the available spectral response data, the following values for the two key scaling parameters of the "specific barrier model" are tentatively proposed: $\Delta\sigma_G$ = 45 bar and $\Delta\sigma_L$ = 330 bar. Figure 1 shows the scaling laws of a few source models that have been proposed for ENA earthquakes (Atkinson and Boore 1998), including the "specific barrier model" for $\Delta\sigma_G$ = 45 bar and $\Delta\sigma_L$ = 330 bar.

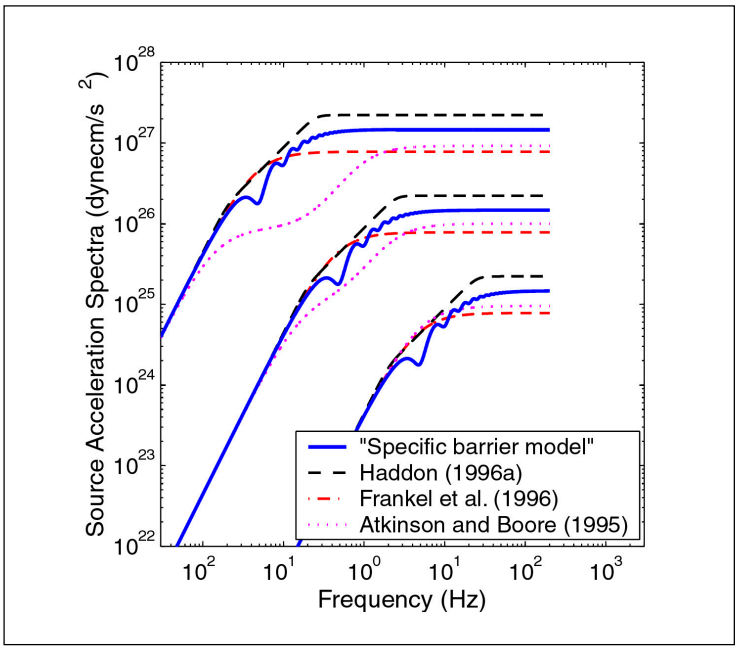

Figure 1. Acceleration source spectra for a few source models proposed for earthquakes in Eastern North America. The "specific barrier model" shown uses $\Delta\sigma_G$ = 45 bar and $\Delta\sigma_L$ = 330 bar.

Acknowledgements

This research was carried out under the supervision of Professor Apostolos S. Papageorgiou and supported by the Multidisciplinary Center for Earthquake Engineering Research through projects MCEER 99-0102, 00-0102 and 01-0102 under NSF Grant EEC-9701471.

References

Atkinson GM, Boore DM (1995): Ground-motion relations for Eastern North America. *Bulletin of the Seismological Society of America*, **85** (1), 17-30.

Atkinson GM, Boore DM (1998): Evaluation of models for earthquake source spectra in Eastern North America. *Bulletin of the Seismological Society of America*, **88** (4), 917-934.

Boore DM (1983): Stochastic simulation of high-frequency ground motions based on seismological models of the radiated spectra. *Bulletin of the Seismological Society of America*, **73** (6A), 1865-1894.

Boore DM (1985): The prediction of strong ground motion. *Proceedings of NATO Advanced Studies Institute on Strong Ground Motion Seismology,* Ankara, Turkey.

Boore DM, Atkinson GM (1987): Stochastic prediction of ground motion and spectral response parameters at hard-rock sites in Eastern North America. *Bulletin of the Seismological Society of America*, **77** (2), 440-467.

Boore DM, Joyner WB (1997): Site amplifications for generic rock sites. *Bulletin of the Seismological Society of America*, **87** (2), 327-341.

Brune JN (1970): Tectonic stress and the spectra of seismic shear waves from earthquakes. *Journal of Geophysical Research*, **75**, 4997-5009.

Cartwright DE, Longuet-Higgins MS (1956): The statistical distribution of the maxima of a random function. *Proceedings of the Royal Statistical Society*, **237**, 212-232.

Frankel A, Mueller C, Barnhard T, Perkins D, Leyendecker EV, Dickman N, Hanson S, Hopper M (1996): National seismic-hazard maps: Documentation. *Open-File Report 96-532*, U.S. Geological Survey, Reston, VA.

Haddon RAW (1995): Modeling of source rupture characteristics for the Saguenay earthquake of November 1988. *Bulletin of the Seismological Society of America*, **85** (2), 525-551.

Haddon RAW (1997): Reply to comment by G. M. Atkinson, et al., on "Earthquake source spectra in Eastern North America". *Bulletin of the Seismological Society of America*, **87** (6), 1703-1708.

Kanamori H, Anderson DL (1975): Theoretical basis of some empirical relations in seismology. *Bulletin of the Seismological Society of America*, **65** (5),1073-1095.

Papageorgiou AS (1988): On two characteristic frequencies of acceleration spectra: patch corner frequency and f_{max}. *Bulletin of the Seismological Society of America*, **78** (2), 509-529.

Papageorgiou AS, Aki K (1983a): A specific barrier model for the quantitative description of inhomogeneous faulting and the prediction of strong ground motion. I. Description of the model. *Bulletin of the Seismological Society of America*, **73** (3), 693-722.

Papageorgiou AS, Aki K (1983b): A specific barrier model for the quantitative description of inhomogeneous faulting and the prediction of strong ground motion. Part II. Applications of the model. *Bulletin of the Seismological Society of America*, **73** (4), 953-978.

Papageorgiou AS, Aki K (1985): Scaling law of far-field spectra based on observed parameters of the specific barrier model. *Pure and Applied Geophysics*, **123** (3), 354-374.

VNI (1991): *IMSL Stat/Library User's Manual - Version 2.0*. Visual Numerics, Inc., Houston, TX.

Wells DL, Coppersmith KJ (1994): New empirical relationships among magnitude, rupture length, rupture width, rupture area and surface displacement. *Bulletin of the Seismological Society of America*, **84** (4), 974-1002.

2

On Seismic Source Spectra from Complex Earthquakes

Benedikt Halldorsson

Department of Civil, Structural & Environmental Engineering, University at Buffalo

Research Supervisor: Apostolos S. Papageorgiou, Professor

Summary

Within the context of the stochastic modeling approach for ground motion prediction, the most important aspect is the seismic source model. The specific barrier model is a physically realistic source model that enables prediction of both far-field and near-source ground motion. It is a special case of a variable-size subevent earthquake source model, since it assumes identical size subevents distributed without overlap on a fault plane. In this study, the effects of variable-size subevents on the far-field seismic source spectrum are investigated.

Introduction

The stochastic modeling approach, which utilizes a seismological model to describe the spectral amplitudes of the ground motion and their scaling with earthquake size, is arguably the only viable method for prediction of ground motions in Eastern North America. The most important aspect of the seismological model is the source model, which quantifies the spectral seismic radiation from the source. The specific barrier model, proposed and developed by Papageorgiou and Aki (1983a, 1983b), is a physically realistic source model that enables prediction of both far-field and near-source ground motion. It is a special case of a variable-size subevent earthquake source model, since it assumes identical subevent sizes distributed without overlap on a fault plane. In this study, the effects of variable-size subevents on the far-field seismic source spectrum are investigated.

Framework

Consider a complex seismic source that is represented by an aggregate of N circular sub-sources (subevents). It is assumed that subevent j has a random radius R_j and ruptures at a random time instant t_j. Subevent sizes and rupture times are statistically independent of one another. In addition, it is assumed that:

1. The seismic spectral radiation of each subevent has the same functional form $S(\omega, R_j)$
2. Subevent sizes follow the same probability distribution defined in the range $[R_a; R_b]$
3. Rupture times for all subevents follow the same probability distribution, which is defined in the interval $[0; T]$ (T = total rupture time of the main event).

Joyner and Boore (1986) derived a simple analytical expression for the seismic radiation from a complex seismic source based on the above assumptions, except that they considered subevents of

equal size. This expression was adopted by Papageorgiou (1988) in deriving the source spectrum for the specific barrier model, which exhibits two characteristic frequencies, f_1 and f_2. Corner frequency f_1 is controlled by the duration of rupture of the entire fault and is related to a measure of the stress drop over the entire fault referred to as the "global" stress drop, $\Delta\sigma_G$. Corner frequency f_2 is controlled by the duration of rupture of individual subevents, on which a "local" stress drop $\Delta\sigma_L$ occurs. The "global" and "local" stress drops are key parameters of the model because they have been found to be stable for a given tectonic region.

In this study, the work of Joyner and Boore (1986) and Papageorgiou (1988) was extended by considering variable subevent sizes whose distribution follows uniform and fractal (Frankel 1991, Zeng et al., 1994) distributions. The corresponding analytical expressions for the far-field seismic radiation of the complex earthquake were derived. Although the analytical expressions greatly facilitate the calculations, they are lengthy and will not be presented here.

The deterministic variables of the complex seismic source spectrum are the seismic moment of the main event (M_0) and the "global" and "local" stress drops. These parameters are used to estimate the areal extent of the main event, represented by the radius R_m of a circular fault. In addition, the type and range of the size distribution are specified beforehand.

Example

Figure 1 shows an example of the effects of different distributions of subevent size on the source acceleration spectrum of a $M_w = 5.8$ earthquake having "global" and "local" stress drops equal to 60 bar and 320 bar, respectively.

The top right diagram of Figure 1 shows a single-size and three fractal ($D = 2$) probability density functions of subevent size. Lower limits of the fractal density functions are equal to 0.10, 0.25 and 0.40 R_m, and the upper limit is equal to 0.50 R_m for all distributions.

Source acceleration spectra for these subevent size distributions are shown in the left diagram of Figure 1. Notice how the different distribution types and the corresponding ranges affect the spectral shape at intermediate and high frequencies.

Realizations of the abovementioned distributions of subevents on the fault plane are shown in the bottom right diagram of Figure 1. The numbers at the lower left corners indicate the number of subevents needed for each size distribution. These realizations were generated following the procedure proposed by Zeng et al., (1994).

The solid density function denoted by an arrow at $R = 0.23\ R_m$ is the Dirac delta function. The corresponding source spectrum and areal distribution of subevents are exactly equal to those of the specific barrier model (Papageorgiou 1988) because the ratio of total subevent area to the area of the main event has been set equal to $\pi/4$.

In all cases, the total seismic moment of the subevents is close to or equal to the seismic moment for the $M_w = 5.8$ event. It should be noted that only the specific barrier model (blue or solid lines) specifies unambiguously how the subevents (i.e., the seismic moment) are distributed on the fault plane. In all the other cases shown in Figure 1, subevents have been manually arranged on the fault plane for illustration purposes.

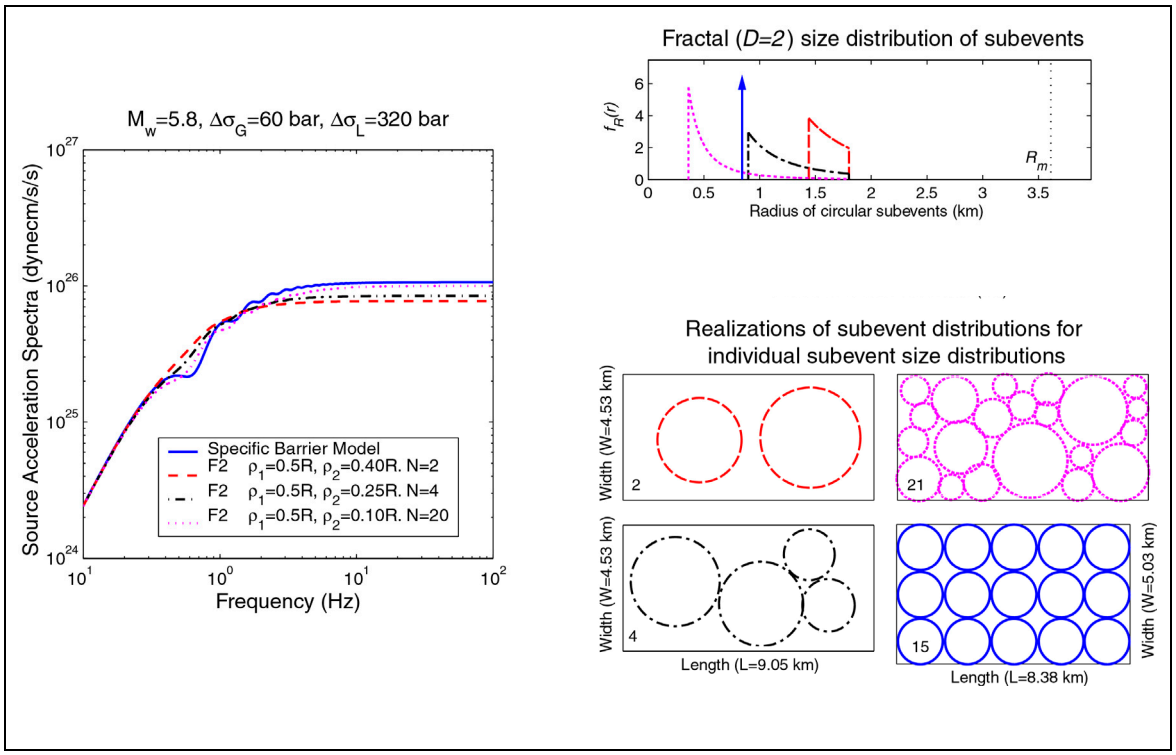

Figure 1. (top right) Four probability density functions of subevent size. The solid arrow denotes a Delta-function at R = 0.23 R_m and corresponds to the specific barrier model. The other density functions are fractal (D = 2) with an upper limit equal to 0.50 R_m and different lower limits. (bottom right) Realizations of the subevent size distributions for a Mw = 5.8 event with $\Delta\sigma_G$ = 60 and $\Delta\sigma_L$ = 320 bars. (left) The corresponding source acceleration spectra.

Main Conclusions

Seismic spectral shapes based on equal- and variable-size subevent distributions are self-similar.

When the width of the size density function approaches zero around a specific subevent size *R*, the seismic spectrum becomes equal to that of the specific barrier model if $(R_m / R)^2 = \pi/4$.

The number of subevents needed to achieve the moment condition is a function of the lower and upper limits of the size distribution and of the ratio of "global" and "local" stress drops.

The larger the number of subevents, the more pronounced the "oscillations" of the spectral shape between the two corner frequencies.

The high-frequency level of source acceleration spectra is a function of lower and upper limits of the size distribution, the ratio of "global" and "local" stress drops, the first corner frequency and the total seismic moment.

The shape of the seismic spectrum is not affected dramatically by the type or range of the size distribution of subevents.

Acknowledgements

This research was carried out under the supervision of Professor Apostolos S. Papageorgiou, and supported by the Multidisciplinary Center for Earthquake Engineering Research under projects MCEER 99-0102, 00-0102, 01-0102, NSF Grant No. EEC-9701471.

References

Atkinson GM, Boore DM (1995): Ground-motion relations for Eastern North America. *Bulletin of the Seismological Society of America*, **85** (1), 17-30.

Joyner WB, Boore DM (1986): On simulating large earthquakes by Green's function addition of smaller earthquakes. *Earthquake Source Mechanics,* American Geophysical Union, Washington, DC.

Frankel A (1991): High-frequency spectral falloff of earthquakes, fractal dimension of complex rupture, *b*-value, and the scaling of strength on faults. *Journal of Geophysical Research,* **96** (B4), 6291-6302.

Papageorgiou AS (1988): On two characteristic frequencies of acceleration spectra: patch corner frequency and f_{max}. *Bulletin of the Seismological Society of America*, **78** (2), 509-529.

Papageorgiou AS, Aki K (1983a): A specific barrier model for the quantitative description of inhomogeneous faulting and the prediction of strong ground motion. I. Description of the model. *Bulletin of the Seismological Society of America*, **73** (3), 693-722.

Papageorgiou AS, Aki K (1983b): A specific barrier model for the quantitative description of inhomogeneous faulting and the prediction of strong ground motion. Part II. Applications of the model. *Bulletin of the Seismological Society of America*, **73** (4), 953-978.

Zeng YH, Anderson JG, and Yu G (1994): A composite source model for computing realistic synthetic strong ground motions, *Geophysical Research Letters*, **21** (8), 725–728.

3

Analytical Study on Rehabilitation of Critical Electric Power System Components

Seyed Ali Ashrafi

Department of Civil and Environmental Engineering, New Jersey Institute of Technology

Research Supervisor: M. Ala Saadeghvaziri, Professor

Summary

This paper describes an experimental and analytical research project intended to study the behavior of substation equipment under earthquakes and their response when isolated using FPS bearings. Results show that the interaction between components of substation equipment has a significant effect on the response of the system as a whole, and that incorporation of FPS bearings is a promising retrofit strategy.

Research Motivation and Research Objectives

Substations sustained significant damage during past earthquakes. Substation equipment is designed and qualified for a specified level of base excitation. If the design level is exceeded or if the interaction among various electrical and structural components aggravates the seismic response, damage to the equipment is almost certain. This results in direct and indirect losses and in a significant impact to the regional economy. Raising the level of the design seismic excitation, even if economically feasible, might not remedy the situation because the complicated interaction among the different components of the entire system when subjected to seismic events is not fully understood.

The objective of this research is to develop the tools and a framework to evaluate and assess the seismic performance of various substation components and the influence of their interaction on the response of the system as a whole. This research is also intended to evaluate the application of technologies for the improvement of the seismic resiliency of substations and to perform research addressing structural and functional problems that are unique to a substation facility.

Description of Research

In light of the abovementioned objectives, the research project described in this paper includes analytical and experimental studies on critical substation components intended to obtain a better understanding of their dynamic characteristics and to evaluate their seismic response in order to develop effective rehabilitation strategies. Transformers, bushings and disconnect switches are the key components in a substation. Individual behavior of transformers and bushings, as well as their interaction, was studied through time history analyses using 3-D finite element models. Results indicate that the transformer flexibility has a significant effect on the dynamic characteristics and seismic response of the bushings. This effect explains the discrepancy between the bushings' good-to-excellent performance when supported on rigid frames in laboratory experiments and their poor

performance during past earthquakes. Analyses of typical transformer foundations indicate that it is very difficult to design foundations capable of resisting inertia forces caused by a major seismic event. New transformers tend to be even heavier due to the need for higher voltage transmission, which further compounds the design of seismically adequate foundations.

Shaking table tests were also performed to compare the response of a fixed-based transformer model supporting a bushing with that of the same system isolated with Friction Pendulum System (FPS) bearings (see Figure 1). 1-D, 2-D and 3-D excitations obtained from several earthquake records and scaled to different PGAs were used.

Experimental studies were followed by a parametric study on the response of a SDOF model of a typical transformer. Results demonstrate the effectiveness of base isolation using FPS bearings in reducing inertia forces and the response of the bushing. However, issues such as the effect of changes of the friction force due to changes of the normal force need further investigation. Large displacements associated with the use of base isolation can compound the interaction among transformer-bushing and interconnecting equipment. This can be addressed through proper design of conductor cables and possible modifications to the bushing flange. Based on analytical and experimental results, a simplified model has been developed to further study the interaction of the transformer-bushing system with interconnecting equipment. This interaction is studied parametrically for several earthquake excitations, isolation radii, interconnecting equipment frequencies, connecting cable stiffness and cable slacks for fixed-base and isolated cases (see Figure 2).

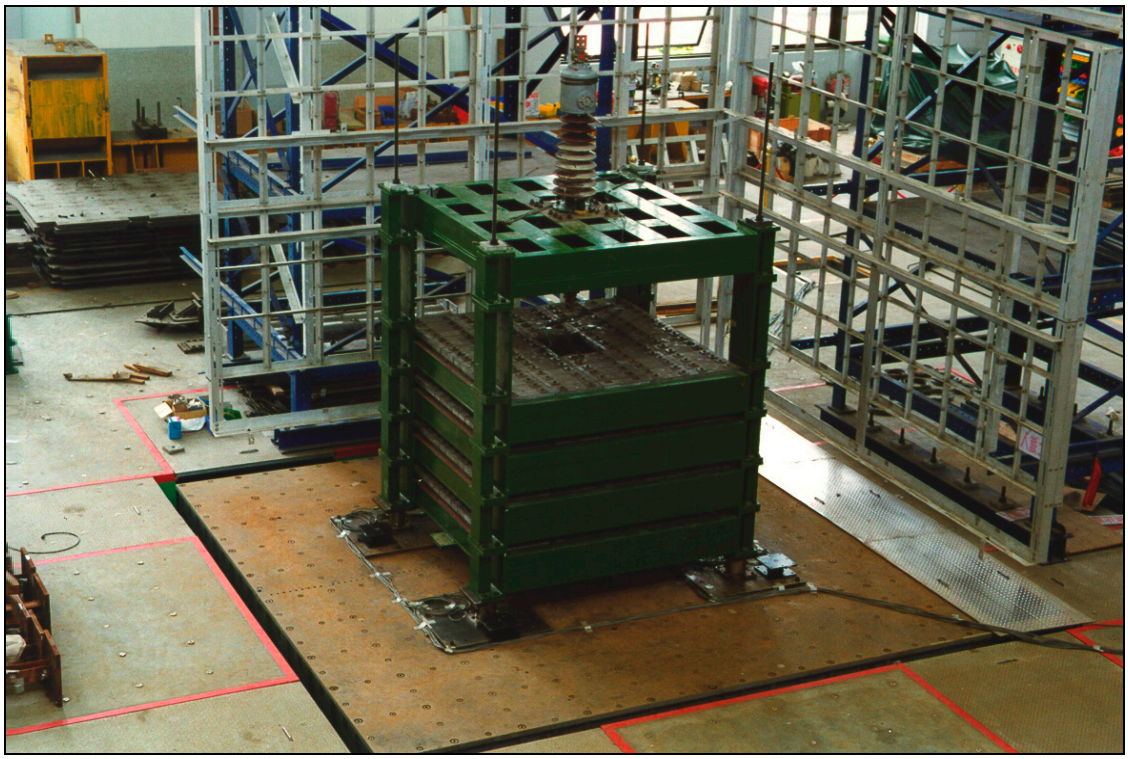

Figure 1. Experimental model of transformer-bushing on shaking table

Another ongoing task deals with the development of a finite element model for FPS bearings to be implemented into a general-purpose package such as ADINA. This element will be used to study the behavior of isolated transformer-bushing systems considering the effect of changes of the friction force on the transformer-bushing dynamic response (see Figures 3 and 4). It should be noted that FPS bearings have been widely investigated and some finite element formulations have already been presented. However, these are either not publicly available or possess restrictions on their applicability mainly because they were developed for building applications. Incorporation of the element into a general-purpose package will be beneficial to the general earthquake engineering community, since recent developments in seismic design of bridges will very likely require more use of advanced technologies such as FPS bearings.

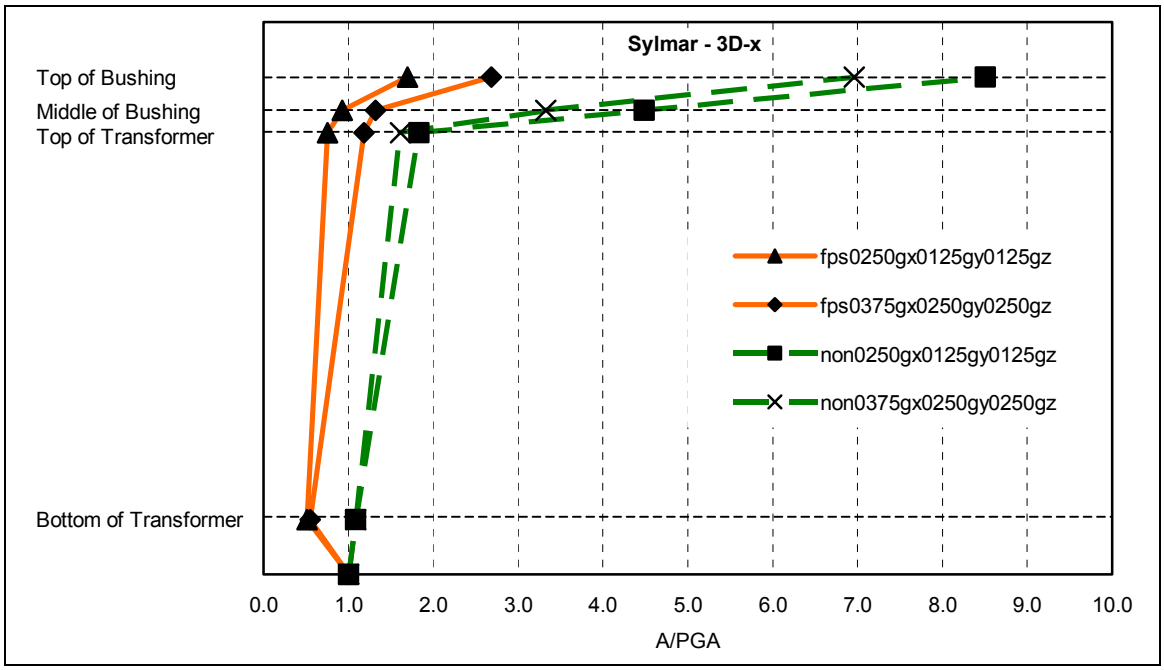

Figure 2. Acceleration response of transformer-bushing model to 3-D Sylmar excitation

Another task planned is the development of a new design criterion for the bushing flange so that the latter acts as a fuse during extreme events. In doing so, a yielding mechanism within the flange of the connection between the transformer/turret and the bushing prevents failure of the bushing and damage to the transformer should the relative displacement exceed the amount of slack provided. Future tasks include work on issues related to the seismic design of foundation and anchorage systems and cost-benefit analysis (vis-à-vis demand on foundations with and without base-isolation). The effect of seismic forces on the design of the anchorage between the core-coil assembly and the tank floor, as well as on the stability of these internal components, will be considered. On a long-term note, possible modifications of FPS bearings in order to minimize or eliminate displacements at the top of the bushing will be investigated.

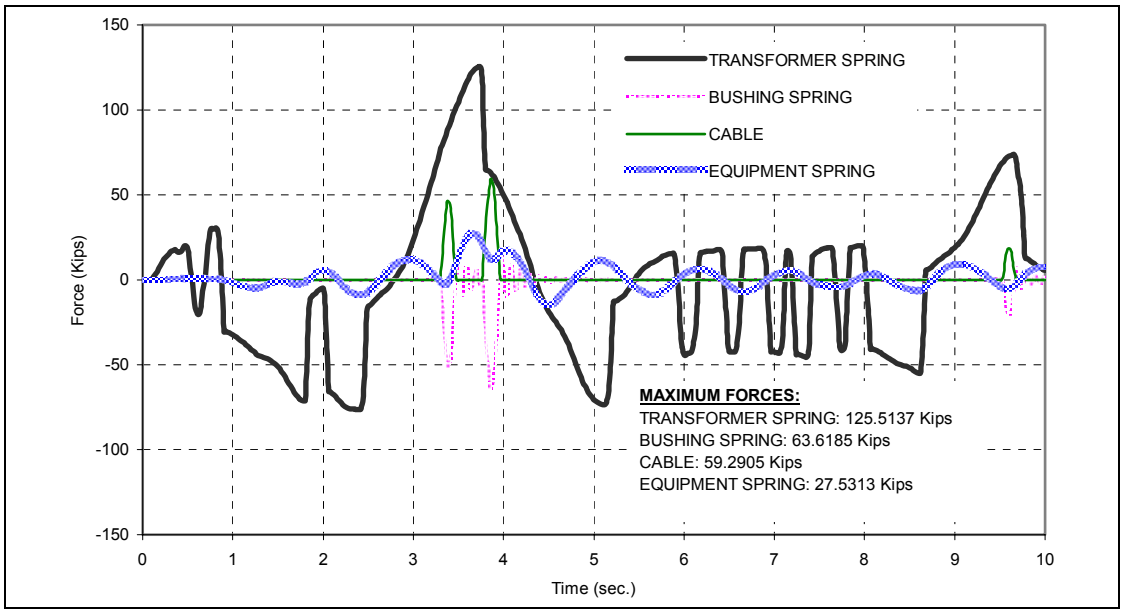

Figure 3. Time-history displacement response of a transformer-bushing system interacting with other elements in a power station

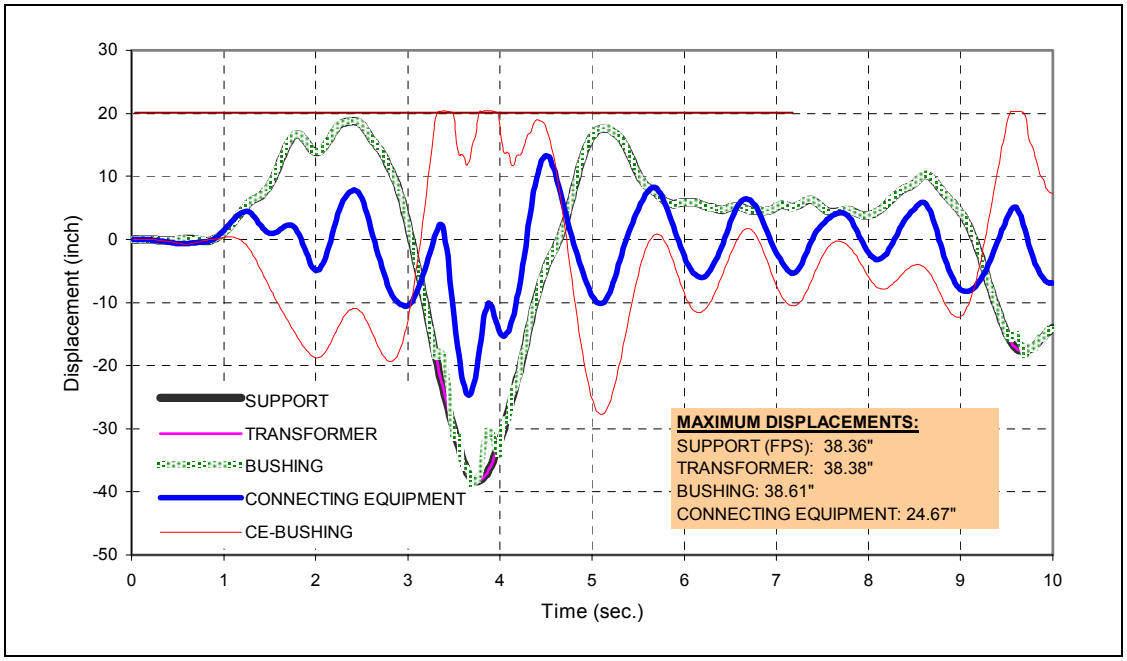

Figure 4. Time-history force response of a transformer-bushing system interacting with other elements in a power station

Acknowledgements

This research was carried out under the supervision of Professor M. Ala Saadeghvaziri, and supported in part by the Multidisciplinary Center for Earthquake Engineering Research.

4

Steel Truss Bridge Braced Pier and Substructure

Kangmin Lee

Department of Civil, Structural & Environmental Engineering, University at Buffalo

Research Supervisor: Michel Bruneau, Professor

Summary

Analytical and experimental research is conducted to investigate the behavior of bridge truss pier brace members. The objective is to generate knowledge and results that can be broadly applicable to evaluate the seismic performance of steel truss bridges of the type built during the first half of the 1900's throughout the United States. They were typically designed to resist wind forces, but not earthquakes. From a review of past practices, commonly used shapes and details that have been historically used for built-up members in steel truss bridge braced pier substructures were selected, and an experimental program has been devised whereby several cross-sectional shapes and geometric configurations of X-bracing are explored to ascertain the inelastic deformation capability of these critical elements. These tests are underway at the time of this writing. Knowledge from this experimental and analytical study will be also be used to develop retrofit measures for seismically vulnerable members.

Introduction

A large number of steel truss bridges have been built throughout the United States, many in zones of moderate to high seismicity. These bridges have typically been designed to resist wind forces, but not earthquakes. Structural analyses of such bridges often reveal that many key structural members along the load path followed by the seismically induced forces may buckle or suffer brittle fracture of their non-ductile connections. However, seismic evaluation remains difficult due to the lack of knowledge on the cyclic inelastic behavior of built-up members of the type typically found in these bridges, and on their riveted connections. Although some testing of bridge-specific latticed members has been conducted by other researchers, results to date have mostly been project specific. Consequently, it is difficult to draw general conclusions from those studies. The objective of this research is therefore to provide theories and results that can be broadly applicable to many steel truss bridges that share similar structural characteristics and details.

Research Approach

A survey was conducted to investigate those commonly used shapes and details that have been historically used for built-up members used in steel truss bridge braced pier substructures. This survey showed that braces in these bridges almost universally consist of latticed built-up members with riveted connections. Common cross-sectional shapes have been identified. Their potential failure modes are global buckling (in-plane or out-of-plane of the frame) or local buckling. To this end, based on representative details, an experimental program has been devised whereby several cross-sectional shapes and geometric configurations of X-bracing are explored to ascertain the inelastic deformation capability of these critical elements. These tests are underway at the time of this writing. Results from these tests will be used to develop simple strength and deformation

models based upon rational mechanics and able to predict strength and displacement limit states. Knowledge from this experimental and analytical study will also be used to develop retrofit measures for seismically vulnerable members.

Preliminary Results

As a result of discussion with the California, Oregon, Washington, Tennessee and New York DOTs, as well as with a few consulting engineering firms, drawings were obtained for a few existing bridges having truss substructures (bents, towers, etc.) with latticed members. Design provisions in the literature, particularly in steel design textbooks published at the turn of the century (Ketchum 1920, Wells 1913, Kunz 1915), were also reviewed, along with recent research work conducted for the major crossings in California (Uang and Kleiser 1997, Dietrich and Itani 1998, 1999). This allowed extraction of a range of parameters typically encountered for such members, including typical built-up member configurations and lacing geometry, typical width-to-thickness b/t and slenderness KL/r ratios for the built-up members and their lacings, connection details, and other lacing characteristics. Parameters worthy of experimental consideration (and their range) were then identified (Table 1 and Figure 1).

Table 1. Summary of experimental parameters to be considered

Built-up members			Lacings		
Configuration	***b/t* ratio**	***KL/r* ratio**	**Type**	**Angle**	***KL/r* ratio**
Type "A" **Type "B"**	8 – 16	60 – 120	**Single** **Lacing**	60°	100 – 120

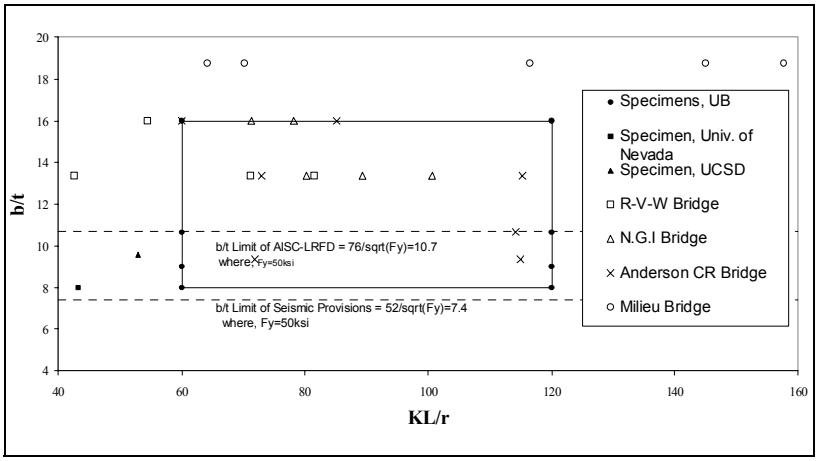

Figure 1. Distribution of *b/t* and *KL/r* ratios

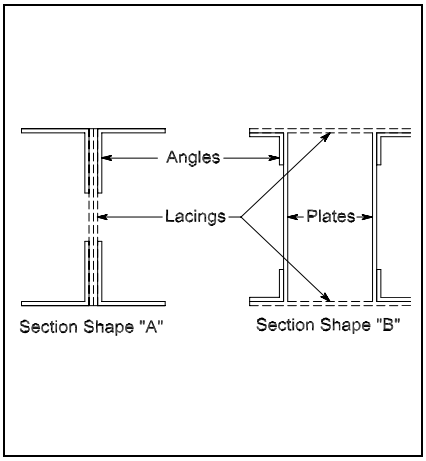

Figure 2. Section shapes

While some bridges were observed to have members having b/t ratios in excess of 16, it was decided to restrict testing to specimens having b/t values of 8 and 16 on the basis that this would allow comparison the cyclic performance of members having considerably different expectations in terms

of local buckling behavior. Note that the AISC recommended maximum b/t value for ductile seismic design is 7.6 for grade 50 steel.

Likewise, it was judged that testing braces having slenderness (KL/r) of 60 and 120 would encompass the range of member slenderness observed in bridges, while allowing comparison of the cyclic inelastic behavior of members expected to have significantly different levels of inelastic buckling. The resulting specimens designed based on these considerations are listed in Table 2. Note that only built-up members constructed of angles are considered. Specimens with section shape A (Ay8-60, Ay8-120, Ay16-60, and Ay16-120) and two specimens with shape B (Bx8-60 and Bx8-120) were instrumented with displacement and strain gages and tested. The corresponding test set-ups are shown in Figures 3 to 8. Note that the set-up for Ay8-60 was used to test two specimens having the same section type and b/t ratio, but two different values of the KL/r ratio (60 and 120). This was achieved by using the same members, and testing first in an X-bracing (KL/r = 60) configuration (but without connecting the upper end of one brace), and second, in a single brace (KL/r of 120) configuration.

Table 2. Specimen names

Name	Section shape	Buckling axis	b/t ratio	KL/r
Ay8-60, Ay8-120	A	Y	8	60 and 120
Ay16-60, Ay16-120	A	Y	16	60 and 120
By8-60, By8-120	B	Y	8	60 and 120
By16-60, By16-120	B	Y	16	60 and 120
Bx8-60, Bx8-120	B	X	8	60 and 120
Bx16-60, Bx16-120	B	X	16	60 and 120

Axial gravity loads were applied at the top of the frame for specimens Ay16-60 and Ay16-120 to reduce slippage in the hinges in the set-up and reduce the global frame horizontal displacements observed during testing of the other two specimens. Replacement of the reinforced concrete foundation beam by a steel beam, as well as use of high-precision hinges, made the use of axial gravity loads unnecessary for all subsequent tests. For all specimens in the X-bracing configuration except Ay8-60 specimen, a dummy member was used instead of the previously used approach of using a specimen brace unconnected at its upper end to prevent damage to the member to be used as a slender specimen (e.g., Ay16-120). Figures 9 to 14 show the axial force–displacement curve experimentally obtained for the specimens. These hysteretic curves exhibit the typical behavior of bracing members observed in previous studies. The Ay16-60 and Ay16-120 specimens bucked locally instead of globally, because of their large width-to-thickness ratio (b/t = 16). Repeated buckling and straightening of the braces (reversed cyclic loading) at the local buckling location led to failure by fracture.

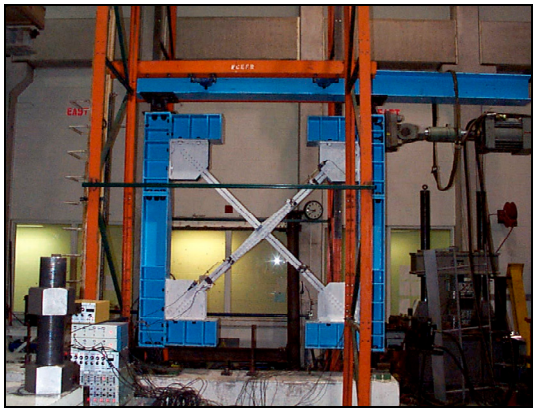

Figure 3. Test set-up for specimen Ay8-60

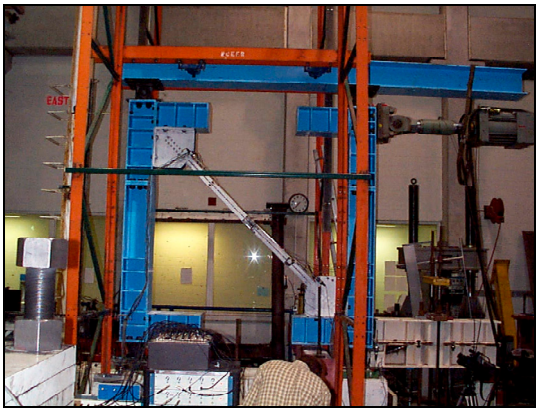

Figure 4. Test set-up for specimen Ay8-120

Figure 5. Test set-up for specimen Ay16-60

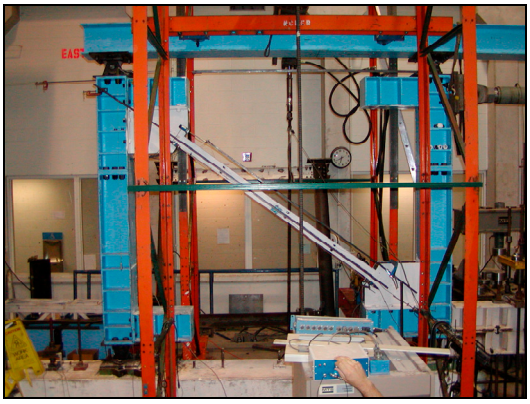

Figure 6. Test set-up for specimen Ay16-120

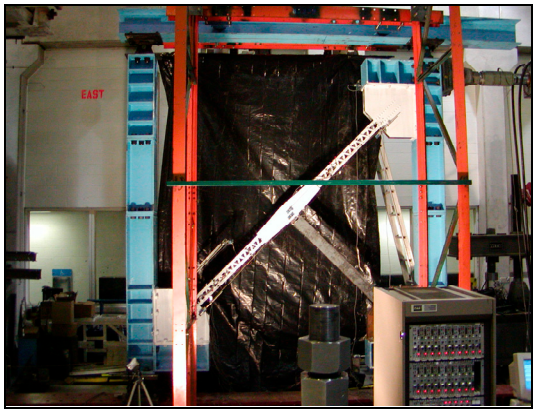

Figure 7. Test set-up for specimen Bx8-60

Figure 8. Test set-up for specimen Bx8-120

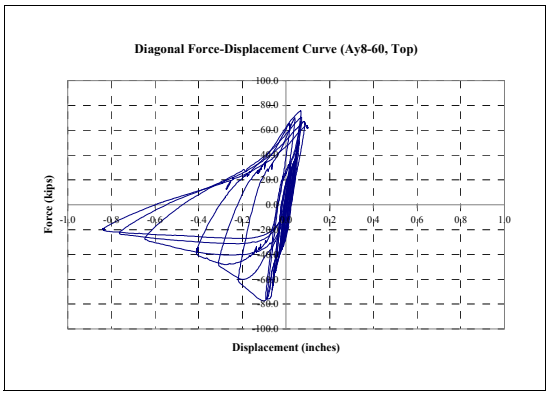

Figure 9. Hysteretic curve for Ay8-60

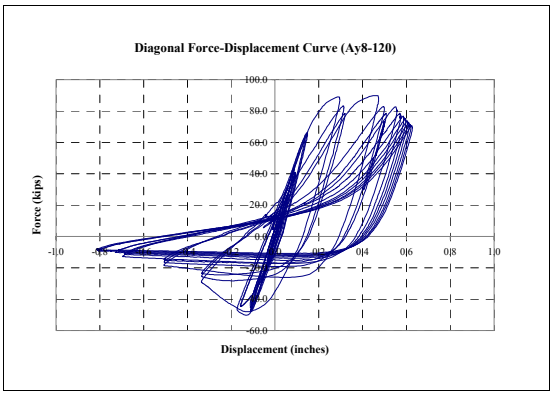

Figure 10. Hysteretic curve for Ay8-120

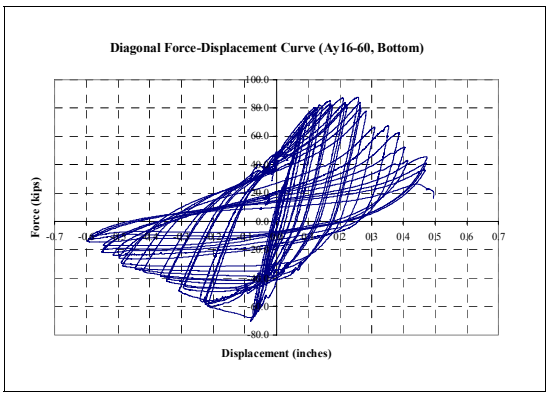

Figure 11. Hysteretic curve for Ay16-60

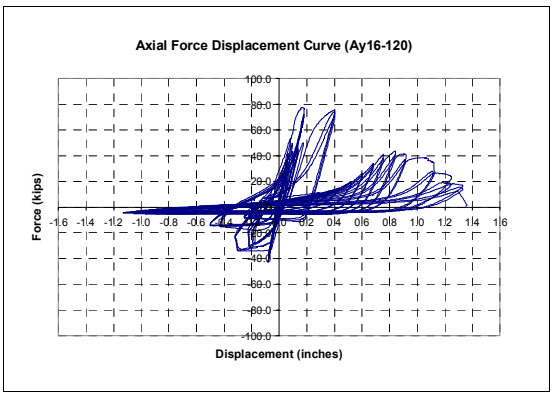

Figure 12. Hysteretic curve for Ay16-120

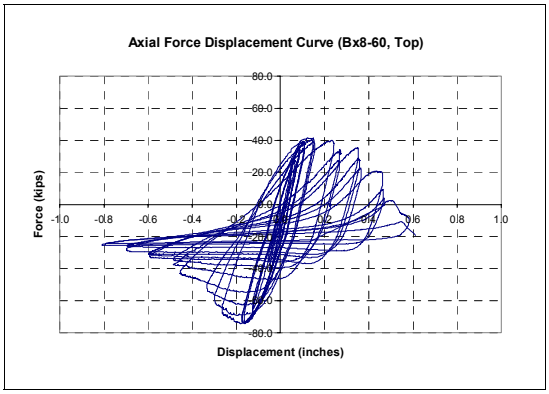

Figure 13. Hysteretic curve for Bx8-60

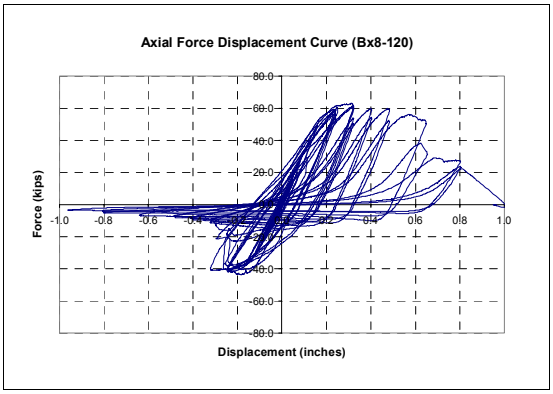

Figure 14. Hysteretic curve for Bx8-120

Figures 15 and 16 show the different buckled shapes at maximum compressive deformation of the braces for the Ay8-60 and Ay16-60 specimens, respectively. The Ay8-60 specimen globally bent (Figure 15), while the Ay16-60 specimen remained almost straight except at the location of local buckling (Figure 16). Global buckled shapes of the other specimens are shown in Figures 17 to 20. Damaged and fractured specimens are also shown in Figures 21 to 26.

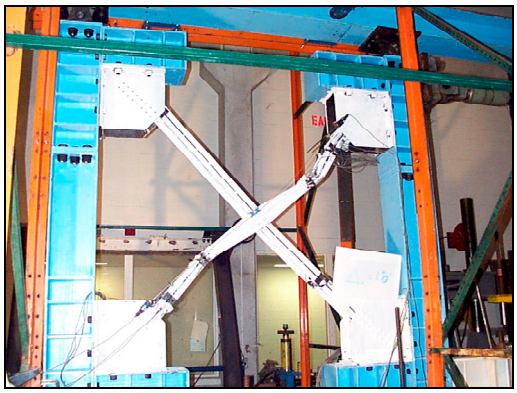

Figure 15. Buckled shape for Ay8-60

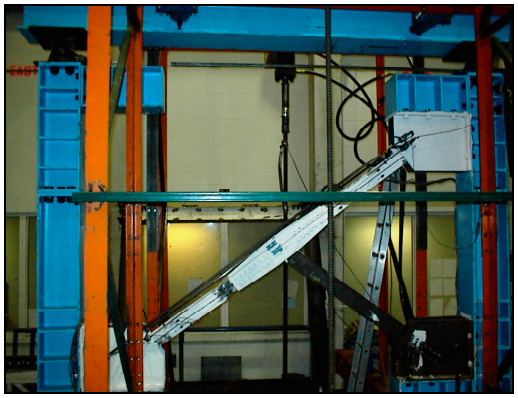

Figure 16. Buckled shape for Ay16-60

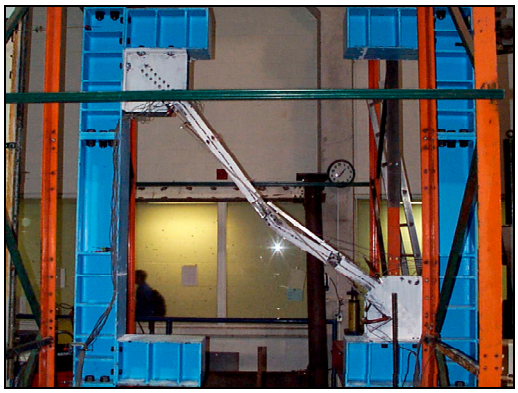

Figure 17. Global buckling for Ay8-120

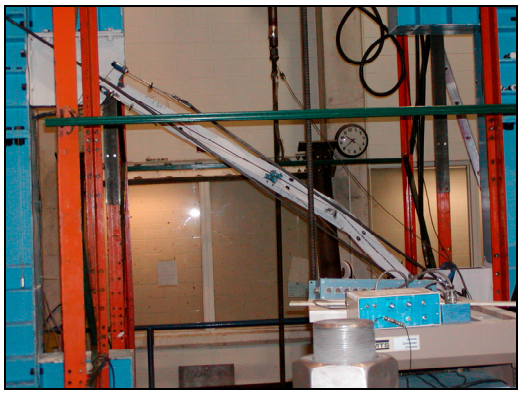

Figure 18. Global buckling for Ay16-120

Figure 19. Global buckling for Bx8-60

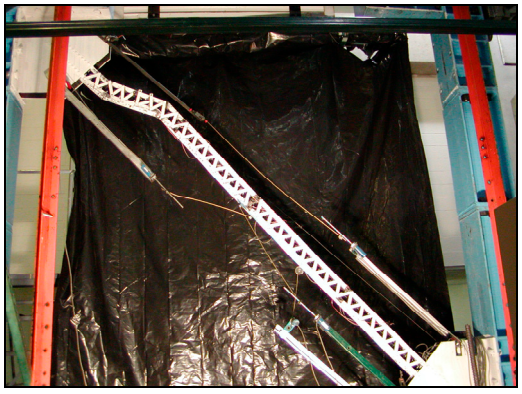

Figure 20. Global buckling for Bx8-120

To investigate fracture life of the bracing member under cyclic loading, the test results of the Ay8-120 specimen were compared with fracture life models of bracing members suggested by Hassan and Goel (1991) and by Archambault et al., (1995). Although these fracture life models have been developed for structural tubular sections, preliminary results obtained so far suggest that these models predict well the fracture life of the Ay8-120 specimen (results for other specimens were not available at time of writing).

Figure 21. Buckling for Ay8-60

Figure 22. Fracture of Ay8-120

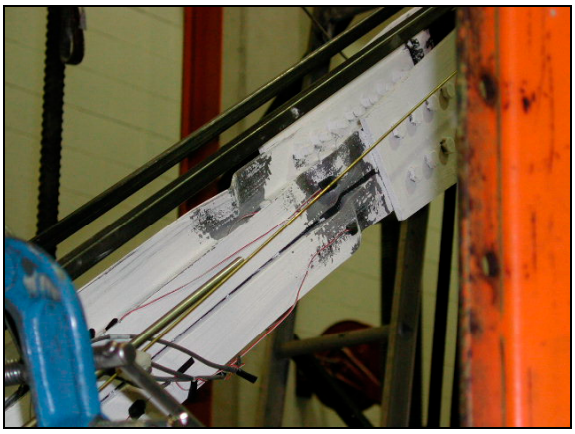

Figure 23. Buckling for Ay16-60

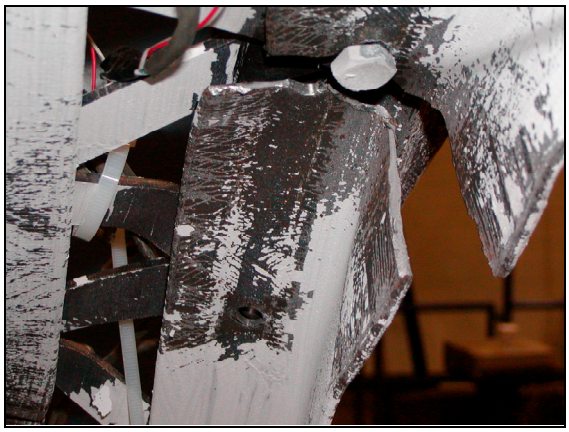

Figure 24. Fracture of Ay16-120

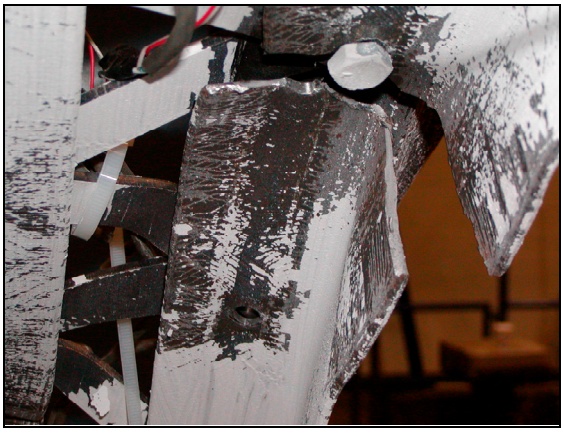

Figure 25. Buckling of Bx8-60

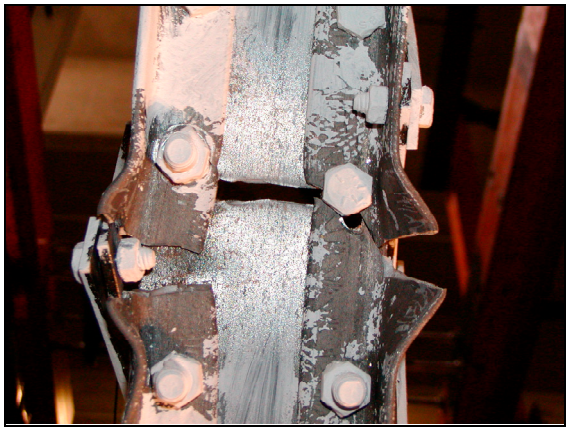

Figure 26. Fracture of Bx8-120

Conclusions

Because this research program is still in progress, firm conclusions would be premature. However, preliminary results suggest that models developed by other researchers for the prediction of fracture life of steel tubes might also work for built-up members typically used in truss bridges. Upon subsequent experimental validation of this finding, existing models could then be used to assess the seismic resiliency of truss bridges. This research is also expected to provide detailed information about maximum cyclic ductility and maximum energy dissipation capacity of built-up braces. Quantitative information will be generated using hysteretic curves of the type presented in this paper. This information will also contribute to the assessment of seismic performance of steel truss bridge systems.

Acknowledgements

This research is carried out under the supervision of Dr. Michel Bruneau, and supported in part by the Federal Highway Administration under a grant awarded to the Multidisciplinary Center for Earthquake Engineering Research.

References

Archambault MH, Tremblay R, Filiatrault A (1995): Etude du comportment seismique des contreventements ductiles en X avec profiles tubulaires en acier. *Rapport EPM/GCS-1995-09*, Departement de Genie Civil Section Structures, Ecole Polytechnique de Montreal, Montreal, Quebec, Canada.

Dietrich AM, Itani AM (1998): Cyclic behavior of built-up and steel members and their connections. *Report CCEER 98-10*, Department of Civil Engineering, University of Nevada at Reno, Reno, NV.

Dietrich AM, Itani AM (1999): Cyclic behavior of built-up and perforated steel members on the San Francisco-Oakland Bay bridge. *Report CCEER 99-9*, Department of Civil Engineering, University of Nevada at Reno, Reno, NV.

Hassan OF, Goel SC (1991): Modeling of bracing members and seismic behavior of concentrically braced steel structures. *Report UMCE 91-1*, Department of Civil Engineering, The University of Michigan, Ann Arbor, MI.

Ketchum MS (1920): *The design of highway bridges of steel, timber and concrete*. McGraw-Hill Co., New York, NY.

Kunz FC (1915): *Design of steel bridges: theory and practice for use of civil engineers and students*. McGraw-Hill Co., New York, NY.

Uang CM, Kleiser M (1997): Cyclic performance of latticed members for the San Francisco-Oakland Bay bridge. *Report SSRP-97/01*, Division of Structural Engineering, University of California at San Diego, La Jolla, CA.

Wells MB (1913): *Steel bridge designing*. The Myron C. Clark Publishing Co., Chicago, IL.

5

Assessment of Performance of Bolu Viaduct in the 1999 Duzce Earthquake

Panayiotis C. Roussis

Department of Civil, Structural & Environmental Engineering, University at Buffalo

Research Supervisor: Michael C. Constantinou, Professor and Chairman

Summary

The Bolu viaduct is a 2.3 km long seismically isolated structure whose construction was nearly complete when it was struck by the 1999 Duzce earthquake in Turkey. It suffered complete failure of the seismic isolation system and narrowly avoided total collapse due to excessive superstructure movement. This paper presents an evaluation of the design of the viaduct's seismic isolation system and an assessment of its performance in the Duzce earthquake. The evaluation revealed that the seismic isolation system did not meet the requirements of the AASHTO Guide Specifications for Seismic Isolation Design. Analysis of the viaduct with motions scaled in accordance to the AASHTO Guide Specifications resulted in a displacement demand equal to 820 mm, which is far more than the 210 mm displacement capacity of the existing isolation system. Analysis of the viaduct for a simulated near-fault ground motion with characteristics consistent with the site conditions resulted in an isolation system displacement demand equal to 1400 mm. This indicates that even if the isolation system had been designed in compliance with the AASHTO Guide Specifications it would have still suffered damage in the earthquake.

Introduction

The Bolu viaduct (Figure 1) forms a small segment of the Trans European Motorway (TEM), which runs from Turkey's capital city (Ankara) to Europe parallel to the North Anatolian Fault (NAF). The viaduct is a seismically isolated structure whose construction was nearly complete at the time of the 1999 Duzce earthquake. It suffered complete failure of the seismic isolation system and narrowly avoided total collapse due to excessive superstructure movement.

This paper presents an evaluation of the design of the viaduct's seismic isolation system and an assessment of its performance in the Duzce earthquake. For more details, the reader is referred to the report by Roussis et al., (2002). The outcome of this study becomes important in validating the AASHTO Guide Specifications (AASHTO 1991, 1999) and in developing experience in the seismic behavior of this type of structures.

Description of the Viaduct

The viaduct is a typical 10-span segment (Figure 2) and it incorporates an energy dissipation system in the form of yielding steel devices (YSD) installed on each pier cap to form, together with multi-directional sliding bearings, a seismic isolation system (Marioni 1997, 2000). Details of the YSD are displayed in Figure 3. The YSD is composed of an inner and outer ring interconnected by sixteen steel C-elements in a radially symmetric configuration. The inner and outer rings are connected to the substructure and the superstructure, respectively. As the superstructure moves relative to the

substructure, the C-elements deform, yield and dissipate energy. Moreover, shock transmission devices are incorporated between the YSD and the substructure in the longitudinal viaduct direction. This system allows free longitudinal movement of the superstructure relative to the substructure due to creep, shrinkage, and temperature change, and locks up under high-speed movement to engage the YSD (Ciampi and Marioni 1991, Tsopelas and Constantinou 1997).

Figure 1. General View of Bolu Viaduct

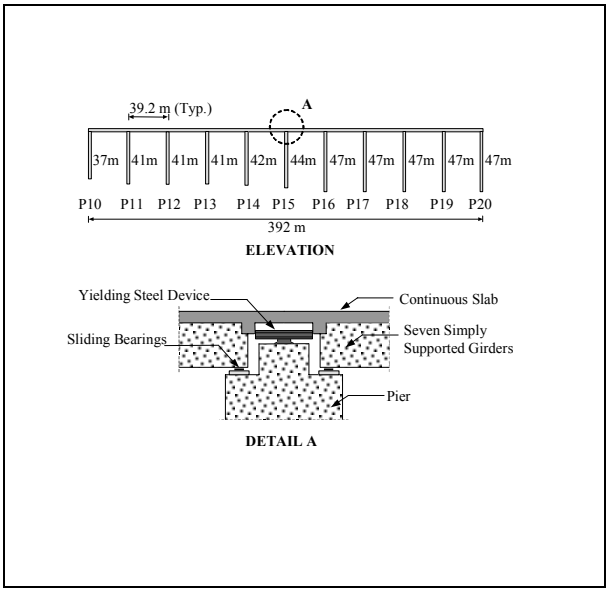

Figure 2. Elevation of viaduct at piers

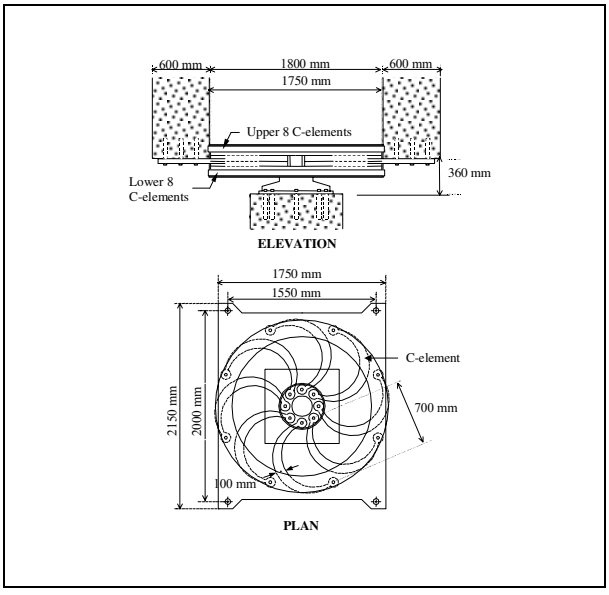

Figure 3. Details of yielding steel device

Design of the Seismic Isolation System

Turkey is an affiliated AASHTO State. However, the design concept for the viaduct involved the application of mixed criteria using the then applicable AASHTO Standard Specifications and seismic isolation guidelines developed by the designer. The design seismic forces and displacements were determined by means of nonlinear time history analyses performed using seven uni-directional artificial accelerograms. The structure was designed for the mean values of maximum forces and displacements obtained from the seven analyses (Marioni 1997, 2000).

Based on test results of the YSD, the seismic isolation system was modeled assuming a bilinear hysteretic behavior as shown in Figure 4 (Astaldi SpA 2000). This behavior is the combination of the inelastic behavior of the YSD and of the sliding bearings.

The design displacement of the seismic isolation system was calculated as equal to 320 mm. However, the bearings had a displacement capacity equal to only 210 mm and the YSD had an ultimate deformation capacity equal to 480 mm (Marioni 1997, 2000). Clearly, there is an apparent inconsistency in the design of the seismic isolation system as the displacement capacity of the bearings is much smaller than the design displacement, while the ultimate deformation capacity of YSD is larger.

It should also be noted that the assumed post-elastic stiffness does not meet the criteria for the lateral restoring force of either the 1991 or the 1999 AASHTO Guide Specifications. A direct application of the minimum requirements of the 1991 AASHTO Guide Specifications resulted in a required displacement capacity equal to 790 mm. This figure is greater than both the 210 mm displacement capacity of the installed system and the 320 mm calculated response. Moreover, the 1999 AASHTO Guide Specifications require that three-dimensional nonlinear dynamic analysis must be used if the seismic isolation system has insufficient restoring force capability. Such an analysis requires at least three pairs of horizontal ground motion histories selected from recorded events and scaled to represent the applicable response spectrum. Yet, the design of the structure was performed using only uni-directional ground motion inputs ignoring the three-dimensional effect of pairs of ground motion components simultaneously applied on the structure.

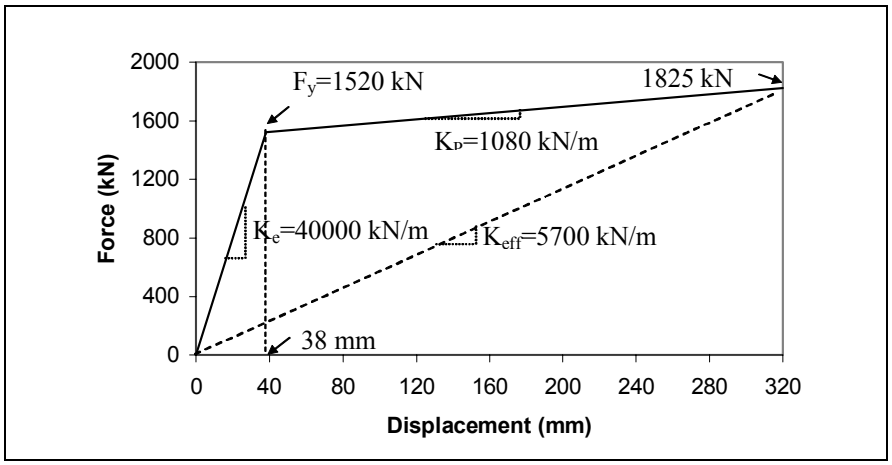

Figure 4. Assumed bilinear hysteretic behavior of seismic isolation system

Damage to Seismic Isolation System in the 1999 Duzce Earthquake

The viaduct was subjected to a near-fault, pulse-type ground motion as the ruptured fault crossed the viaduct at 25-degree angle with respect to the viaduct's longitudinal direction. Thus, the structure might have been exposed to significant directivity and fling effects, with associated large velocity pulses and permanent tectonic deformations. Consequently, the viaduct superstructure experienced a westward permanent displacement relative to the piers, leaving all ends of the girders offset from their supports in the order of 1000 mm longitudinally and 500 mm transversely. At nearly all locations, the sliding bearings suffered complete failure with their parts dislocated and ejected from the bearing pedestals. The observed scratch signs on the surface of the bearing's stainless steel plates resembled the number six, indicating that the bearings slid off probably at a very early stage before any significant cyclic movement.

Analysis of the Viaduct

A typical 10-span segment of the viaduct (Figure 2) was analyzed using the finite element program ANSYS (SAS 1996). The analysis was based on a three-dimensional finite element model. Nonlinear dynamic analyses were carried out to estimate the response of the viaduct in the 1999 Duzce earthquake. The two records at Bolu and Duzce were first used to assess the performance of the viaduct during the Duzce earthquake. However, it was recognized that neither of the two records truly represent the conditions experienced by the viaduct in the vicinity of the fault. Accordingly, the ground motion at the viaduct's site was simulated based on stipulated earthquake source parameters and it was then used for the assessment of the performance of the viaduct.

In addition, nonlinear time history analyses were performed to calculate the design displacements for the isolation system in compliance with the AASHTO Guide Specifications. The calculated displacements were used to determine whether the structure would have survived the earthquake had it been designed in compliance with the AASHTO Guide Specifications. The analyses were conducted using three pairs of scaled horizontal ground motions selected from different recorded events. These ground motions are: (i) 360 and 270 components of 1992 Landers earthquake recorded at Yermo station; (ii) 90 and 0 components of 1989 Loma Prieta earthquake recorded at Hollister station; and (iii) S00W and S90W components of 1971 San Fernando earthquake recorded at station 458.

Analysis of Results

Calculated maximum resultant displacements of the isolation system at each pier are summarized in Table 1. Note that the calculated peak displacement response of the isolation system in the simulated near-fault motion is on the order of 1400 mm. While this figure may be a conservative estimate, it demonstrates that the demand in the Duzce earthquake far exceeded the capacity of the isolation system. Furthermore, results for ground motions scaled in accordance to the AASHTO Guide Specifications demonstrate that the displacement capacity of the isolation system should have been equal to at least 820 mm. This value is substantially larger than the 210 mm capacity provided to the isolated viaduct.

Figure 5 presents graphs of the calculated displacement paths of the isolation bearings at Pier 15 during the initial portion of movement for the simulated, Bolu station, and Duzce station ground motions. The calculated paths of the isolation system displacement for the Bolu station and the simulated near-fault ground motions consist of a half cycle of displacement whose amplitude is

equal to about 100-150 mm, followed by movement in the opposite direction that exceeds the displacement capacity of the bearings. Observations of the scoring on the stainless steel plates of the sliding bearings of the viaduct are consistent with the calculated displacement paths. In contrast, the calculated paths of the isolation system displacement for the Duzce station ground motion show no resemblance to the observed traces on the stainless steel plates of the bearings.

Table 1. Calculated maximum isolation system resultant displacements

Ground motion	Maximum Isolation System Resultant Displacement (mm)											
	P10	**P11**	**P12**	**P13**	**P14**	**P15**	**P16**	**P17**	**P18**	**P19**	**P20**	**Max**
Bolu	325	325	329	337	344	346	342	355	367	380	393	393
Duzce	530	525	521	516	515	514	504	511	513	511	509	530
Simulated	1297	1291	1302	1308	1322	1336	1354	1375	1391	1409	1425	1425
Scaled Yermo	487	489	496	506	514	522	531	543	557	569	581	581
Scaled Hollister	644	743	742	734	756	790	820	818	815	812	810	820
Scaled San Fernando	325	341	353	363	372	379	379	385	388	392	397	397

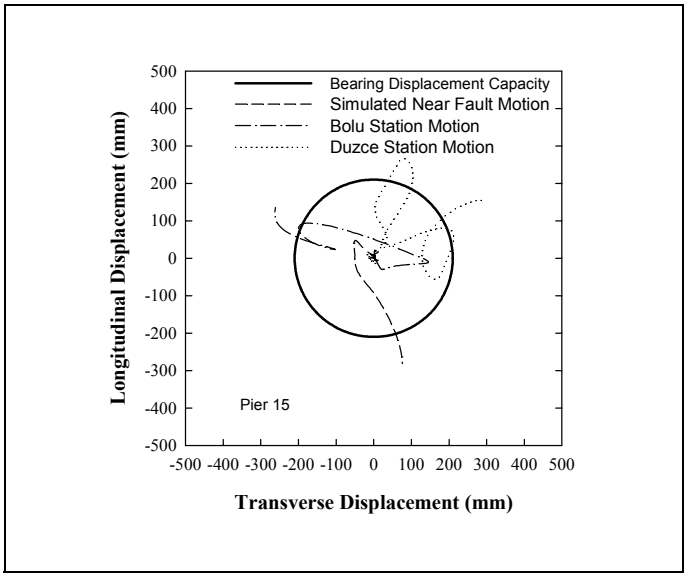

Figure 5. Isolation system displacement paths at Pier 15

Conclusions

Results of this study demonstrate the following: (1) the seismic isolation system of the Bolu viaduct did not meet the requirements of either the 1991 or the 1999 AASHTO Guide Specifications; (2)

analysis of the seismically isolated viaduct with motions scaled in accordance to the 1999 AASHTO Guide Specifications resulted in a required displacement capacity equal to 820 mm. Moreover, a direct application of the minimum requirements of the 1991 AASHTO Guide Specifications resulted in a displacement capacity equal to 790 mm. Either value of the displacement capacity is substantially larger than the 210 mm capacity provided; (3) analysis of the viaduct for the Duzce and Bolu records resulted in isolation system displacements that exceeded the displacement capacity by a factor of two or more. The Bolu record contained clear near-fault characteristics and the calculated displacement paths closely resembled the observed paths. However, realistic results are believed to have been obtained in the analysis for a simulated near-fault ground motion that resulted in isolation system displacement demands of up to 1400 mm; and (4) it appears that had the isolation system been designed in accordance with the AASHTO Guide Specifications to have a displacement capacity equal to 820 mm, it would have still suffered damage in the Duzce earthquake, given that the displacement demand was likely of the order of 1400 mm.

Acknowledgements

This research was carried out under the supervision of Professor Michael Constantinou, and supported in part by the Multidisciplinary Center for Earthquake Engineering Research. Professor Mustafa Erdik and Doctor Ester Durakal of Bogazici University (Istanbul, Turkey) and Professor Murat Dicleli of Bradley University contributed to this work.

References

AASHTO (1991, 1999): *Guide specifications for seismic isolation design*. American Association of State Highway and Transportation Officials, Washington, DC.

SAS (1996): *ANSYS User's Manual, Version 5.3*. Swanson Analysis Systems, Inc., Houston, PA.

Astaldi SpA (2000): Miscellaneous documents and diagrams related to the Bolu Viaduct in Duzce, Turkey.

Ciampi V, Marioni A (1991): New types of energy dissipating devices for seismic protection of bridges. *Proceedings of the Third World Congress on Joint Sealing and Bearing Systems for Concrete Structures*, National Center for Earthquake Engineering Research, **2**, 1225-1245.

Marioni A (1997): Development of a new type of hysteretic damper for the seismic protection of bridges. *Proceedings of the Fourth World Congress on Joint Sealing and Bearing Systems for Concrete Structures*, American Concrete Institute, **2**, 955-976.

Marioni A (2000): Behaviour of large base isolated prestressed concrete bridges during the recent exceptional earthquakes in Turkey. *Proceedings of the Seminar "Difendiamoci dai terremoti: le piu recenti applicazioni italiane delle nuove tecnologie antisismiche d'isolamento e dissipazione energetica"*, Bologna, Italy.

Roussis PC, Constantinou MC, Erdik M, Durukal E, Dicleli M (2002): Assessment of performance of Bolu viaduct in the 1999 Duzce earthquake in Turkey. *Technical Report MCEER-02-0001*, Multidisciplinary Center for Earthquake Engineering Research, Buffalo, NY.

Tsopelas P, Constantinou MC (1997): Study of elastoplastic bridge seismic isolation system. *ASCE Journal of Structural Engineering*, **123** (4), 489-498.

6

Displacement Estimates in Isolated Bridge Structures

Gordon P. Warn

Department of Civil, Structural & Environmental Engineering, University at Buffalo

Research Supervisor: Andrew S. Whittaker, Associate Professor

Summary

The AASHTO equation for calculating displacements in seismically isolated bridges is based on the work of Kelly at UC Berkeley in the 1980s, whose focus was building structures. The equation assumes linearly increasing displacements in the constant-velocity region of the design spectrum and accounts for the effects of energy dissipation (hysteretic or viscous) by using properties of the equivalent viscoelastic system. The seismic input is assumed unidirectional for the AASHTO calculation. Recent work done under the direction of Whittaker while at UC Berkeley indicates that simultaneous seismic excitation along each horizontal axis of a bridge can substantially increase the maximum isolator displacement over that calculated assuming unidirectional excitation, especially if the isolators are (correctly) modeled using coupled plasticity or Bouc-Wen models.

Introduction

The objective of this research is to revise the AASHTO equation for displacements in seismically isolated bridges (AASHTO 1999, Section 7, Equation 3a) to account for bi-directional seismic input and for improved estimates of damping displacement-reduction factor *B* as proposed by Ramirez et al., (2000).

Five bins of earthquake ground motions have been selected and organized to perform linear and nonlinear response-history analysis. The mean spectrum for each of the bins matches well the assumed shape of the AASHTO design spectrum for isolated bridges. Results of analyses performed using binned ground motions, on average, will be assumed to represent well the response of an isolated bridge structure subjected to earthquake excitation.

The assumption of linearly increasing displacements in the constant-velocity region of the design spectrum is addressed. A relationship that better estimates unidirectional displacement demands based on the 5% damped, 1.0 sec spectral displacement is proposed.

Currently, recommendations to better estimate displacements in linear and nonlinear systems subjected to simultaneous bi-directional excitation based on unidirectional excitation are being developed. Likely, the result of this work will be a coefficient in the form of a unidirectional displacement multiplier. This multiplier is likely to be a function of magnitude, distance to fault, as well as of isolator properties. Preliminary results of linear and nonlinear response-history analyses are presented herein.

Ground Motion Components

A total of 52 recorded earthquake ground motions were utilized for this study. Ground motions have been organized into five bins based on magnitude and distance to fault. Earthquake time histories were extracted from two sources: the Pacific Earthquake Engineering Research (PEER) database (http://peer.berkeley.edu/smcat/) and the SAC steel project database (http://quiver.eerc.berkeley.edu:8080/studies/system/ground_motions.html).

Ground motions have been grouped into 5 bins based on magnitude and distance to fault: (1) Near-Field, (2) Large Magnitude Small Distance, (3) Large Magnitude Large Distance, (4) Small Magnitude Small Distance, and (5) Small Magnitude Large Distance (Krawinkler 2001). Each bin contains 20 acceleration time histories corresponding to 10 earthquake events with the exception of Bin 1, which contains 24 acceleration time histories. Each earthquake event consists of two perpendicular horizontal components. Table 1 is a summary of the ground motions bins and ground motion information including event magnitude and distance to fault.

Table 1. Ground motion bins

Bin	Name	Event Magnitude	Distance to Fault (km)	Soil Type	Soil Classification
1	NF	6.7 – 7.4	< 10	D	NEHRP
2	LMSR	6.7 – 7.3	10 – 30	A,C	USGS
3	LMLR	6.7 – 7.3	30 – 60	A,C	USGS
4	SMSR	5.8 – 6.5	10 – 30	A,C	USGS
5	SMLR	5.8 – 6.5	30 – 60	A,C	USGS

Elastic Response Spectrum

Binned ground motions used in this study produce, on average, a response spectrum that matches well the assumed shape of the AASHTO design spectrum. Short period mean spectral accelerations range from 1.0 g for near-field (Bin 1) to 0.2 g for small-magnitude, small-distance (Bin 5). This range of spectral demand is representative of seismic hazard levels throughout the United States.

Mean and mean $\pm 1\sigma$ (σ = sample standard deviation assuming a normal distribution) spectral information has been generated for all five bins. Figure 1 shows acceleration response spectra for all ground motion components in Bin 2 as well as the mean spectrum (shown by the heavy black line). Bin 2 spectra have been plotted to show scatter about the mean. Information for the remaining bins is not presented for brevity. Results of analyses performed using binned ground motions, on average, will be assumed to represent well the response of an isolated bridge structure subjected to earthquake excitation.

Spectral Displacements

The equation for calculating design displacements in isolated bridge structures is given by Equation 3a of the *Guide Specification for Seismic Isolation Design* (AASHTO 1999). This equation assumes linearly increasing displacements in the constant-velocity region of the design spectrum.

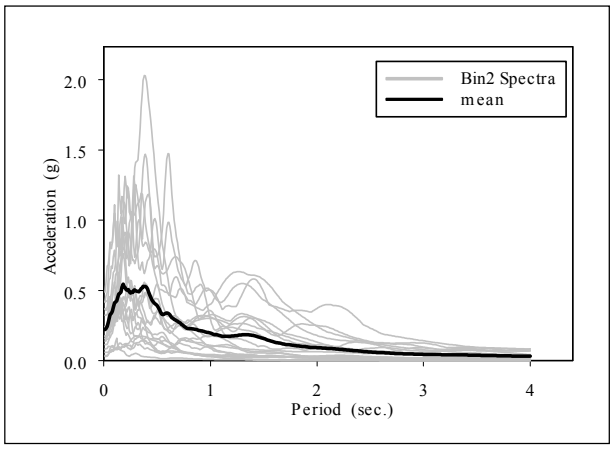

Figure 1. Acceleration response spectra for Bin 2 ground motions

Displacements obtained using the AASHTO formula, although conservative, tend to be inaccurate and significantly overestimate displacement demands. A relationship is proposed to better estimate the displacement demand in the constant-velocity region of the design spectrum based on the 5% damped, 1.0 sec displacement. The proposed relationship is given by:

$$d(T) = d(T = 1.0)\,T^{\alpha} \tag{1}$$

where $d(T)$ is the displacement demand for the period of interest, $d(T = 1.0)$; is the 5% damped, 1.0 sec displacement, T is the period of interest and α is an exponent of the period, which is less than or equal to unity for all bins. Regression analysis was performed on the constant-velocity portion of the mean acceleration spectrum for each of the five bins to determine the value of the exponent α. Results of the regression analysis confirm Equation 3a to be conservative. Values of α ranged from 0.75 for near-field to 0.08 for small-magnitude, small-distance. Note that smaller values of α represent larger deviation (smaller demand) from those obtained assuming linearly increasing displacement. Shown below in Figure 2 are results of regression analysis performed on Bin 2. The dashed line represents a value of α = 1.0 (i.e., linearly increasing displacements), which corresponds to the displacements obtained using Equation 3a with 5% damping. The solid line represents displacements that would be obtained using the relationship presented in Eq. 1 above with $\alpha = 0.74$.

Linear Response-History Analysis

Response-history analysis of linear systems with 5% damping was undertaken utilizing horizontal ground motion pairs from the five bins mentioned previously. Displacements in each of the two horizontal orthogonal directions were combined using linear superposition theory to determine the maximum horizontal displacement. Maximum horizontal displacements were then statistically sorted to determine, on average, the increase in displacement due to consideration of bi-directional excitation for a linear system. Currently, regression analysis is being utilized to determine a coefficient that will serve as a multiplier to calculated unidirectional displacement to account for bi-directional earthquake loading for linear systems. This multiplier is expected to be a function of earthquake magnitude, distance and natural period of the linear system.

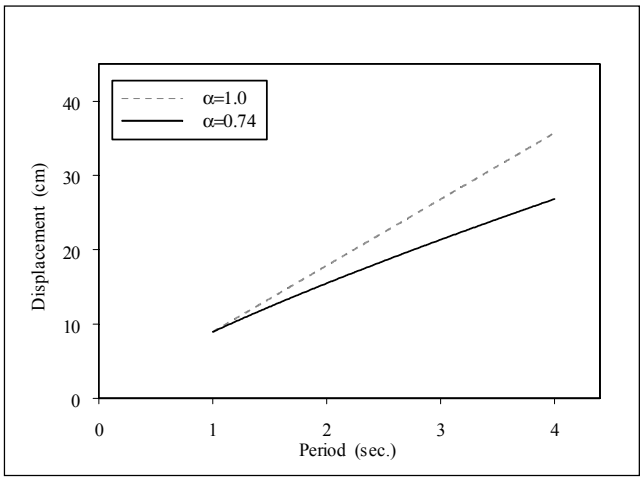

Figure 2. Design displacements for 5% critical damping based on Bin 2 mean spectrum

Preliminary results of the response history data suggest that consideration of simultaneous bi-direction excitation results in horizontal displacements that are significantly larger than those obtained from unidirectional considerations only. For example, preliminary analysis of data suggests a unidirectional multiplier of approximately 1.4 for Bin 2 (LMSR) assuming a constant linear best fit. Although results are preliminary, a multiplier of 1.4 suggest that bi-directional excitation has a significant effect on the maximum displacement.

Nonlinear Response-History Analysis

Nonlinear response-history analysis was performed using a mathematical model of an isolated bridge structure. Response-history analysis was performed for each of the ground motion pairs mentioned previously. Properties for the bridge model (i.e., mass, length, width) are based on a single span of a multi-span bridge that was proposed in an Applied Technology Council report (ATC 1981). Isolator parameters (i.e., normalized characteristic strength and second slope period) were varied to ensure broad applicability of results for isolated bridges in the United States. Four values of the characteristic strength Q_d/W (normalized by the weight acting on the isolator) were chosen and range from 0.03 to 0.12. Similarly, five values of the second slope period, T_d, were chosen and range from 1.5 sec to 4.0 sec resulting in 20 combinations of isolation parameters.

A Matlab model of a rigid superstructure supported by four seismic isolators was used to study the response of the isolation system subjected to unidirectional and bi-directional seismic input (Mosqueda 2001). This model represents the simplest of isolation systems so that a clear understanding of the response of the isolators subjected to bi-directional excitation is possible. The isolators were explicitly modeled using a rate-independent coupled plasticity model also implemented in Matlab (Huang 2000).

Shown in Figure 3 are some preliminary results of the nonlinear response history analysis for unidirectional and bi-directional excitation with isolator parameters $Q_d/W = 0.09$ and $T_d = 4.0$ sec. The ground motions used for the analyses shown in Figure 3 are from the Northridge earthquake, Canoga Park station. These ground motions were extracted from PEER's database and have been included in Bin2. Two important results of bi-directional excitation are shown in Figure 3. The first

one is the effect on unidirectional isolator properties (i.e., Q_d) and the second one is the increase in displacement along the x-direction horizontal axis. Due to the coupled behavior of the isolator, the contribution of yield force along the x-direction horizontal axis varies (always less than or equal to the unidirectional yield force) corresponding to the phasing of the horizontal ground motion in the perpendicular direction. The result of the bi-directional analysis is shown below by the solid black line. The result of this reduction in yield force along a single axis is an increase in isolator displacement along that axis.

Although the results shown in Figure 3 are preliminary, they suggest that bi-directional loading has a significant effect on maximum isolator displacement. Currently, nonlinear response history analysis is being performed for the remaining bins of ground motions. Likely, a displacement multiplier will be proposed to account for this increase in displacement due to bi-directional excitation in yielding systems. This multiplier is expected to be a function of earthquake magnitude, distance to fault and isolator parameters, namely, Q_d and T_d.

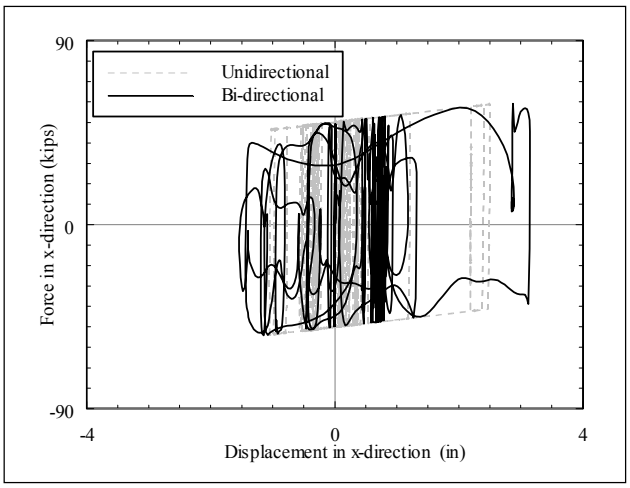

Figure 3. Results of nonlinear response-history analysis for unidirectional and bi-directional excitation

Concluding Remarks

Although this research is still in progress, preliminary results are in agreement with its objectives. The assumption of linearly increasing displacement is the constant-velocity region of the design spectrum is conservative, however, displacement demand is significantly overestimated. Both linear and nonlinear response history analysis indicate that bi-directional earthquake excitation significantly increases maximum horizontal isolator displacements. Finally, recommendations to improve the AASHTO equation for displacements in seismically isolated bridges to account for bi-directional excitation will be presented upon completion of this research.

Acknowledgements

This research was carried out under the supervision of Professor Andrew Whittaker, and supported in part by the Multidisciplinary Center for Earthquake Engineering Research.

References

AASHTO (1999): *Guide specifications for seismic isolation design*. American Association of State Highway and Transportation Officials, Washington, DC.

ATC (1981): Seismic design guidelines for highway bridges. *Report ATC-6*, Applied Technology Council, Redwood City, CA.

Huang WH, Fenves GL, Whittaker, AS, Mahin, SA (2000): Characterization of seismic isolation bearings for bridges from bi-directional testing. *Proceedings of the 12th World Conference on Earthquake Engineering*, New Zealand Society for Earthquake Engineering, Upper Hutt, New Zealand, Paper No. 2047.

Krawinkler H (2001): Private communication.

Mosqueda G (2001): *Experimental and analytical studies of the friction pendulum system for the seismic protection of bridges*. Department of Civil and Environmental Engineering, University of California at Berkeley, Berkeley, CA.

Ramirez OM, Constantinou MC, Kircher CA, Whittaker AS, Johnson MW, Gomez JD, Chrysostomou CZ (2000): Development and evaluation of simplified procedures for analysis and design of buildings with passive energy dissipation systems - Revision 01. *Report MCEER-00-0010,* Multidisciplinary Center for Earthquake Engineering Research, Buffalo, NY.

7

Plastic Analysis and Design of Steel Plate Shear Walls

Jeffrey Berman

Department of Civil, Structural & Environmental Engineering, University at Buffalo

Research Supervisor: Michel Bruneau, Professor

Summary

A revised procedure for the design of steel plate shear walls is proposed. In this procedure, the thickness of the infill plate is found using equations that are derived from plastic analysis of the strip model, which is widely accepted for the representation of steel plate shear walls. Equations are derived from a basic steel plate shear wall configuration but are shown to be conservative for more complex configurations. Fundamental plastic collapse mechanisms for several wall configurations are also given.

Introduction

Steel plate shear walls (SPSW) have sometimes been used as the lateral load resisting system in buildings. Until recently, the failure mode of SPSW was considered to be the out-of-plane buckling of the infill plates. This led engineers to design heavily stiffened plates that offered little economic advantage over reinforced concrete shear walls. However, as Basler (1961) demonstrated for plate girder webs, the post-buckling tension field action of SPSW can provide substantial strength, stiffness and ductility. The idea of utilizing the post-buckling strength of SPSW was first developed analytically by Thorburn et al., (1983) and verified experimentally by Timler and Kulak (1983). Studies performed to evaluate the strength, ductility, and hysteretic behavior of such SPSW designed with unstiffened infill plates have demonstrated their significant energy dissipation capabilities (Timler and Kulak 1983) and substantial economic advantages (Timler 1998).

At the time of this writing, there are no U.S. specifications or codes addressing the design of SPSW. The 2002 Canadian standard CAN/CSA S16-2002 (CSA 2002) now incorporates mandatory clauses for the design of SPSW. One of the models recommended to represent SPSW is the strip model developed by Thorburn et al., (1983). This model is generally recognized for providing reliable assessments of ultimate strength. In this study, the strip model is used as a basis to investigate the feasibility of plastic analysis as an alternative for the design of SPSW. Fundamental plastic collapse mechanisms are described for single story and multistory SPSW with either simple or rigid beam-to-column connections.

Single Story Frames with Simple Beam-to-Column Connections

Consider the frame with inclined strips and simple beam-to-column connections shown in Figure 1. When the shear force, V, displaces the top beam by a value Δ sufficiently large to yield all the strips, the external work done is equal to $V\,\Delta$ (Figure 2).

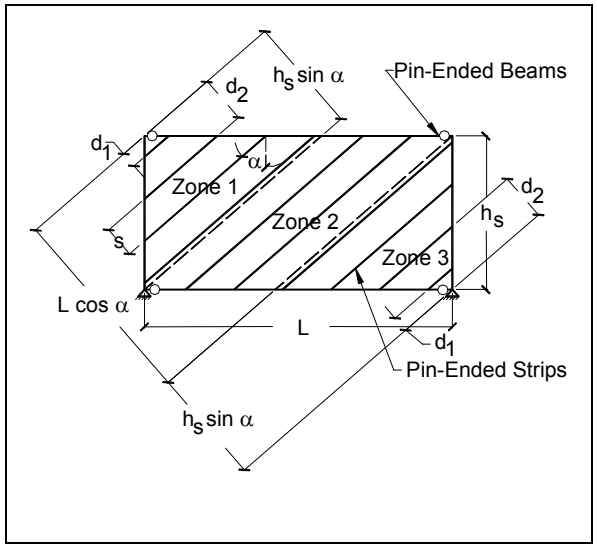

Figure 1. Strip model of single story wall

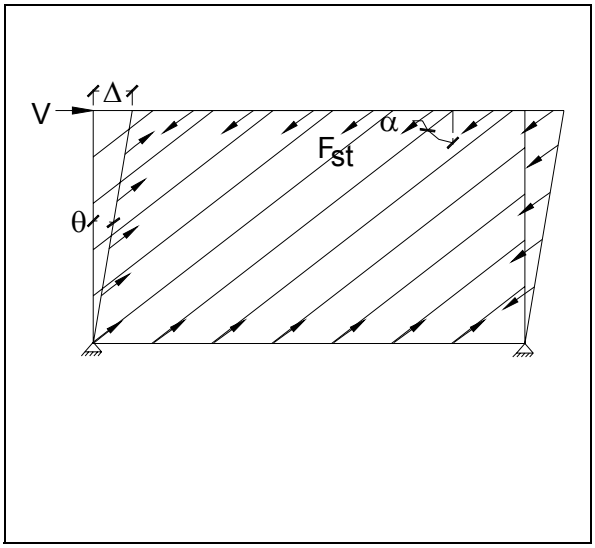

Figure 2. Single story collapse mechanism

If the beams and columns are assumed to remain elastic, their contribution to the internal work may be neglected when compared to the internal work done by the braces. Hence, the internal work is $[n_b\, A_{st}\, F_y \sin(\alpha)]\,\Delta$, where n_b is the number of strips anchored to the top beam, A_{st} is the strip area, F_y is the strip yield stress, and α is the angle of inclination of the strips measured from vertical. This result can be obtained by the product of the yield force times the yield displacement of the strips, but for simplicity it can also be found using the horizontal and vertical components of these values. Note that the horizontal components of the yield forces of the strips on the columns cancel (the forces on the left column do negative internal work and the forces on the right column do positive internal work) and the vertical components of all the yield forces do no internal work because there is no vertical deflection. Therefore, the only internal work done is that due to the horizontal components of the strip yield forces anchored to the top beam. Equating the external and internal work gives:

$$V = n_b\ F_{st}\ \sin(\alpha) \tag{1}$$

Using the geometry shown in Figure 1, $n_b = [L \cos(\alpha)]\ /\ s$ and the strip force F_{st} is again $F_y\, t\, s$. Substituting these into Eq. 1 and knowing that $(1/2)\ \sin(2\alpha) = \cos(\alpha)\ \sin(\alpha)$, the resulting base shear relationship is:

$$V = \frac{1}{2}\, F_y\ t\ L \sin(2\alpha) \tag{2}$$

Single Story Frames with Rigid Beam-to-Column Connections

In single story SPSW having rigid beam-to-column connections (as opposed to simple connections), plastic hinges also need to form in the boundary frame to produce a collapse mechanism. The corresponding additional internal work is $4\ M_p\ \theta$, where $\theta = \Delta\ h_s$ is the story displacement over the story height and M_p is the smaller of the plastic moment capacity of the beams (M_{pb}) or columns (M_{pc}). For most single-story frames that are wider than tall, if the beams have sufficient strength and stiffness to anchor the tension field, plastic hinges will typically form at the top and bottom of the columns and not in the beams. The ultimate strength of a single-story SPSW in a moment frame with plastic hinges in the columns becomes:

$$V = \frac{1}{2}\ F_y\ t\ L\ \sin(2\alpha) + \frac{4\ M_{pc}}{h_s} \tag{3}$$

In a design process, failure to account for the additional strength provided by the beams or columns results in larger plate thicknesses than necessary. In turn, larger thickness would translate into lower ductility demands in the walls and frame members. Therefore, neglect of additional strength provided by the beams or columns could be considered a conservative approach.

Multistory Frames

For multistory SPSW with pin-ended beams, plastic analysis can also be used to predict the ultimate capacity. The purpose here is not to present closed-form solutions for all possible failure mechanisms, but to identify some key plastic mechanisms that should be considered in estimating the ultimate capacity of a SPSW. These could be used to define a desirable failure mode in a capacity design perspective and/or to prevent an undesirable failure mode, as well as to complement traditional design approaches.

In soft-story plastic mechanisms (Figure 3), the plastic hinges that would form in the columns at the mechanism level could be included in the plastic analysis. Calculating and equaling the internal and external work, the following general expression could be used for soft-story i in which all flexural hinges develop in columns:

$$\sum_{j=i}^{n_s} V_j = \frac{1}{2}\ F_y\ t_i\ L\ \sin(2\alpha) + \frac{M_{pci}}{h_{si}} \tag{4}$$

where V_j are the applied lateral forces above the soft-story i, t_i is the plate thickness at the soft-story, M_{pci} is the plastic moment capacity of the columns at the soft-story, h_{si} is the height of the soft-story, and n_s is the total number of stories. Note that only the applied lateral forces above the soft-story do external work and they all move the same distance (Δ). The internal work is done only by the strips on the soft-story itself and by column hinges forming at the top and bottom of the soft-story. Using the above equation, the possibility of a soft-story mechanism should be checked at every story in which there is a significant change in plate thickness or column size. Additionally, the soft-story mechanism is independent of the beam connection type (simple or rigid) because hinges must form in the columns, not in the beams.

A second (and more desirable) possible collapse mechanism involves uniform yielding of the plates over every story (Figure 4). For this mechanism, each applied lateral force V_i moves a distance

$\Delta_i = \theta\, h_i$, and does an external work equal to $V_i\, \theta\, h_i$, where h_i is the elevation of the i^{th} story. The internal work is done by the strips of each yielding story. It is important to note that the strip forces acting on the bottom of a story beam do positive internal work and the strip forces acting on top of the same beam do negative internal work. Therefore, the internal work at any story i is equal to the work done by strip yield forces along the bottom of the story beam minus the work done by strip yield forces on the top of the same beam. This indicates that in order for every plate at every story to contribute to the internal work, the plate thicknesses would have to vary at each story in direct proportion to the demands from the applied lateral forces. Even with this in mind, this mechanism provides insight into the capacity and failure mechanism of the wall. The general equation for the ultimate strength of a multistory SPSW with simple beam-to-column connections and this plastic mechanism (equating the internal and external work) is:

$$\sum_{i=1}^{n_s} V_i\ h_i = \sum_{i=1}^{n_s} \frac{1}{2}\, F_y\, \left(t_i - t_{i+1}\right) L\ h_i\ \sin\left(2\alpha\right) \tag{5}$$

where h_i is the i^{th} story elevation, n_s is the total number of stories, and t_i is the thickness of the plate on the i^{th} story.

After examining results of several different pushover analyses for such multistory SPSW, it has been observed that the actual failure mechanism is typically somewhere between a soft-story mechanism and uniform yielding of the plates on all stories. Finding the actual failure mechanism is difficult if hand calculations are performed. Therefore, a computerized pushover analysis should be used. However, the mechanisms described above will provide a rough estimate of the ultimate capacity. They will also provide some insight as to whether a soft story is likely to develop (by comparing the ultimate capacity found from the soft story mechanism with that of the uniform yielding mechanism).

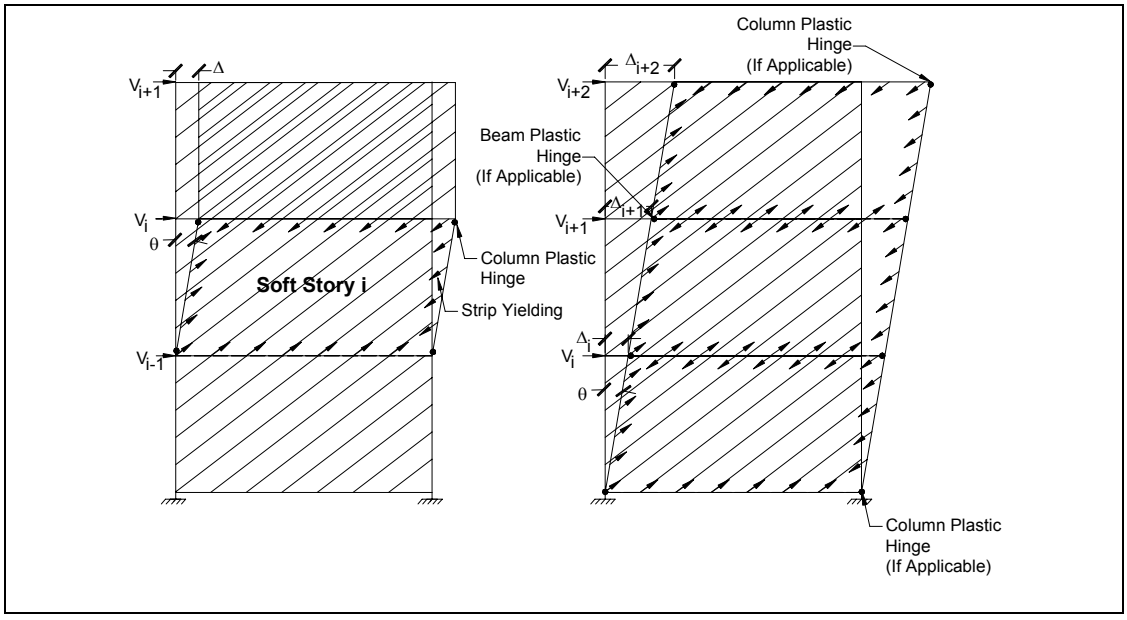

Figure 3. Soft-story mechanism

Figure 4. Uniform yielding mechanism

Proposed Design Procedure

Using the results of the plastic analyses described previously, the infill plates of SPSW can be sized to consistently achieve the desired ultimate strength. The procedure is simple, even for a multistory SPSW, and neglecting the contribution of plastic hinges in beams and columns will always give a conservative design in the case of rigid beam-to-column connections. The proposed procedure requires the designer to:

1. Calculate the design base shear, and distribute it along the height of the building as described by the applicable building code;

2. Use the following equation to calculate the minimum plate thicknesses required for each story:

$$t = \frac{2 V_s \Omega_s}{F_y L \sin(2\alpha)} \tag{6}$$

   where Ω_s is the system overstrength factor described in FEMA 369 (BSSC 2001) and V_s is the design story shear found using the equivalent lateral force method;

3. Develop the strip model for computer (elastic) analysis using the equation from Timler et al., (1983) to calculate the angle of inclination of the strips;

4. Design beams and columns according to capacity design principles (to insure the utmost ductility) or other rational methods using plate thicknesses specified (in case these thicknesses exceed the minimum required for practical reasons);

5. Check story drifts against allowable values from the applicable building code;

Conclusions

Plastic collapse mechanisms for single and multistory SPSW with simple and rigid beam-to-column connections have been investigated and simple equations that capture the ultimate strength of SPSW have been developed. Using the results of these plastic analyses, a new procedure for the sizing of the infill plates has been proposed. The proposed procedure allows the engineer to control the ultimate failure mechanism of the SPSW, and directly accounts for structural overstrength.

Acknowledgements

This research was carried out under the supervision of Dr. Michel Bruneau, and supported in full by the Multidisciplinary Center for Earthquake Engineering Research.

References

Basler K (1961): Strength of plate girders in shear. *ASCE Journal of the Structural Division*, **87** (7), 150-180.

CSA (2002): *Limit states design of steel structures*. Standard CAN/CSA S16-2001, Canadian Standards Association, Willowdale, Ontario, Canada.

BSSC (2001): *NEHRP Recommended provisions for seismic regulations for new buildings and other structures: Part-2-Commentary*. Report FEMA 369, prepared by the Building Seismic Safety Council for the Federal Emergency Management Agency, Washington, DC.

Thorburn LJ, Kulak GL, Montgomery CJ (1983): Analysis of steel plate shear walls. *Structural Engineering Report No. 107*, Department of Civil Engineering, Universtiy of Alberta, Edmonton, Alberta, Canada.

Timler PA, Kulak GL (1983): Experimental study of steel plate shear walls. *Structural Engineering Report No. 114*, Department of Civil Engineering, University of Alberta, Edmonton, Alberta, Canada.

Timler PA (1998): Design procedures development, analytical verification and cost evaluation of steel plate shear wall structures. *Earthquake Engineering Research Facility Technical Report No. 98-01*, Department of Civil Engineering, University of British Columbia, Vancouver, British Columbia, Canada.

8

A Combined Honeycomb and Solid Viscoelastic Material for Structural Damping Applications

WooYoung Jung

Department of Civil, Structural & Environmental Engineering, University at Buffalo

Research Supervisor: Amjad J. Aref, Assistant Professor

Summary

The goal of the research described in this paper is to investigate the feasibility of a new combined polymer composite damping system, which consists of a polymer honeycomb material and a viscoelastic solid material. This new combined viscoelastic system, which is intended primarily for energy dissipation and vibration control, serves as an interface layer within lightweight composite panels subjected to in-plane shear. The basic concept and mechanical properties of the combination of polymer honeycomb and solid viscoelastic materials were experimentally investigated under different strain and frequencies inputs. Numerical models in which the effect of temperature and frequency are taken into account were then established. Analytical results given by a simplified numerical model agreed well with experimental results. This study also led to useful information about the optimum design of the combined damping system.

Description of Research

A multi-layer energy-dissipating panel was recently proposed by Aref and Jung (2001) for the retrofit of semi-rigidly connected steel frames. These multi-layer composite panels are characterized by shear interface layers, which are composed of polymer honeycomb material placed between composite laminates consisting of several plies. A characteristic feature of this composite panel system is its ability to provide a significant level of damping due to interface slip at contact surfaces.

The design of composite infill panels as a damping component for seismic applications faces the following challenge. If the interface material is sufficiently stiff, deformations at the interface might not be large enough as to provide a significant level of energy dissipation. On the other hand, materials such as a solid viscoelastic material dissipate a significant amount of energy but at the expense of making the structure too flexible. The new interfacing damping system described in this paper seeks to comply with both of the desired properties (i.e., stiffness and energy dissipation capability) by combining two composite materials. A schematic representation of the idealized force-displacement relationship is shown in Figure 1. Once incorporated into a structure, the enhanced passive damping of this new interface layers modifies key structural design parameters such as structural mass, stiffness, and damping characteristics.

The effectiveness of the combined composite damping material system in increasing the energy dissipated between fiber reinforced polymer (FRP) skin plates is the primary interest of this research. This new layer configuration consists of two different styles of composite materials: a polymer honeycomb material and a solid viscoelastic material. This configuration is intended to increase the level of damping provided. The honeycomb material is expected to enhance the stiffness of the

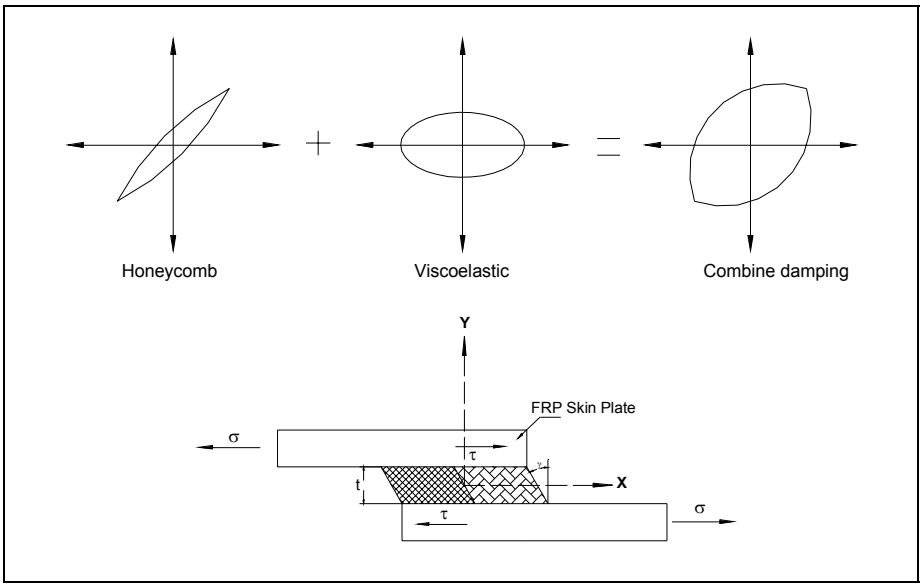

Figure 1. Schematic presentation of the idealized force-displacement relationship

entire structure, whereas the solid viscoelastic material is expected to improve the energy dissipation capability of the multi-layer panel system when subjected to in-plane shear loading. Figure 2 presents experimental force-displacement relationships for two different damping systems. Figure 3 shows the amount of energy dissipated by each of the three systems considered at different frequencies. Both figures show that, except at very low frequencies, the energy dissipation capability of the combined system is significantly better than that of systems consisting of only one of either composite materials (polymer honeycomb or solid viscoelastic).

Finally, the optimal design of the proposed combined polymer composite damping system was investigated. Several cases were considered in order to find the best combination of several relevant factors such as cost and fabrication. Numerous experimental and analytical studies were performed. Based on these results, simplified design procedures were developed to improve the stiffness and the damping characteristics of the energy dissipating material.

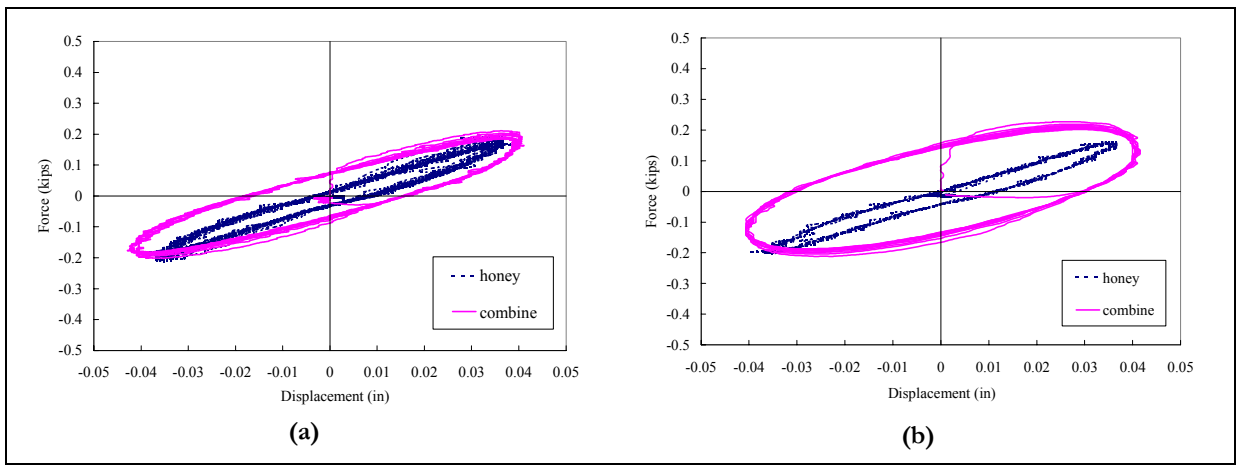

Figure 2. Experimental force-displacement relationships: (a) f = 1 Hz; (b) f = 3 Hz

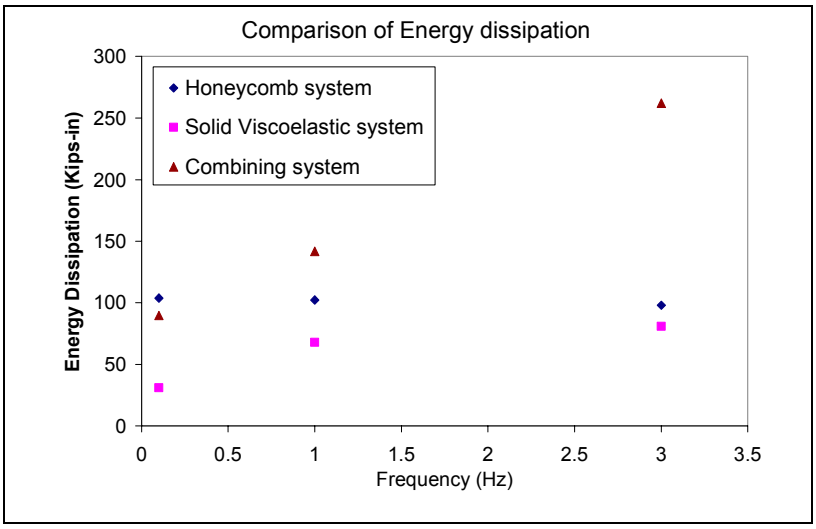

Figure 3. Energy-dissipation-versus-frequency relationship

Acknowledgements

This research was carried out under the supervision of Professor Amjad Aref, and supported in part by the Multidisciplinary Center for Earthquake Engineering Research. This financial support is gratefully acknowledged.

References

Aref AJ, Jung WY (2001): Polymer matrix composite infill walls for seismic retrofit. *Proceedings of the 2001 Structures Congress & Exposition*, American Society of Civil Engineers, Reston, VA.

9

Ductile Fiber Reinforced Panels for Seismic Retrofit

Keith E. Kesner

School of Civil & Environmental Engineering, Cornell University

Research Supervisor: Sarah L. Billington, Assistant Professor

Summary

An infill system consisting of ductile fiber reinforced composite panels with bolted connections is being developed for seismic retrofits. A combination of laboratory and numerical studies are being used to evaluate and develop components of the infill system. Initial results suggest that the composite infill panels are capable of increasing the lateral load capacity, the stiffness and the energy dissipation capability of a steel frame subjected to cyclic lateral loads.

Introduction

Ductile cement-based composite materials or engineered cementitious composite (ECC) materials, which are comprised of a Portland cement or mortar matrix and low volume fraction of polymeric fibers, represent a new kind of material for use in seismic retrofits. Ductile cement-based composites are unique due to their high tensile strain capacity. The material was originally developed from micromechanical tailoring of fiber and matrix properties and the resulting composites show multiple, fine (steady-state) cracking and significantly higher tensile ductility than that of conventional cementitious materials. The material also exhibits pseudo-strain hardening and therefore energy dissipation (Li 1998).

In the current research, two types of infill wall panel systems are being evaluated for use in steel framed structures, as shown in Figure 1. The different infill systems are a complete bay infill (Figure 1a) and a beam-type infill (Figure 1b). The infill panels are constructed using the ECC material in lieu of a traditional concrete or brick masonry. This research builds upon previous research by Kanda et al., (1998). The panel systems are unique in their use of bolted connections between panels, with either bolted or welded connections to the frame. The system has several advantages in retrofit applications including rapid installation, ability for relocation (if necessary) and ease of replacement after damage during seismic events. In this paper, the combination of ongoing numerical and laboratory studies, which are being used to evaluate and develop the infill panel system, are described.

To develop the ECC infill panel system, there are three focus areas in the ongoing research:

1. Evaluation of the cyclic response of ECC materials.

2. Evaluation of the panel connection capacity.

3. Optimization of panel geometry and layout in retrofit applications.

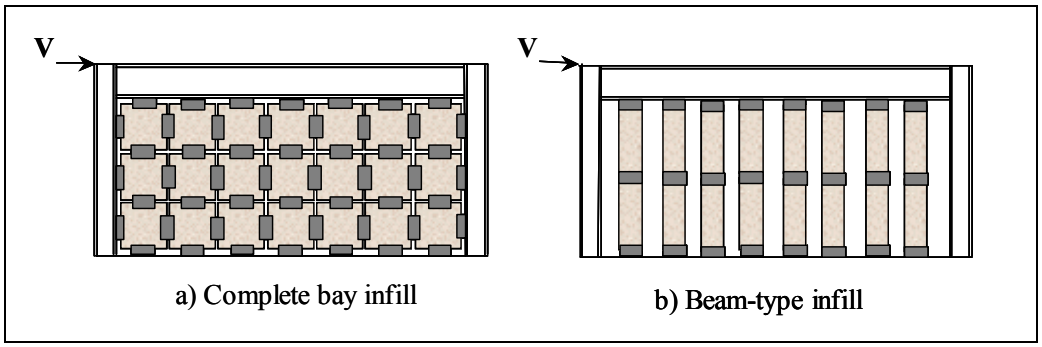

Figure 1. Panel infill systems under development

Results presented in this paper describe ongoing efforts in focus areas 2 and 3.

Panel Connection Tests

The infill panel concept being developed uses pre-tensioned bolted connections both between the panels and at the connection of the panels to the frame. In this application, the behavior of the bolted connections is conceptually similar to slip-critical connections in steel structures. Kanda et al., (1998) were the first to investigate the use of pre-tensioned bolted connections. The geometry of their tested specimens resulted in a compression failure of the specimens outside of the connection region.

In the current research, compression and shear capacities of ECC panels with pre-tensioned bolted connections are being investigated. Figure 2 shows the geometry of some of the specimens tested. This represents the compression capacity in a connection such as that shown in Figure 1b. The bolts used in the connections are 19 mm ASTM A490 high strength bolts with the pre-tensioning load slightly below AISC specifications (AISC 1988) for slip critical connections. The pre-tensioning load is selected to limit the compressive stresses within the connection region. This is necessary to prevent localized crushing during bolt tensioning. The pre-tensioning load in the bolts is monitored using load cell washers, which allow the variation of bolt load to be recorded during testing. In order to provide additional space for alignment of the connections, bolt holes in both the steel angles and the ECC blocks are 22 mm in diameter, which is 2 mm larger than AISC specifications. The testing is performed in a displacement controlled, 2670 kN MTS test frame at an approximate displacement rate of 4 mm per minute. The displacement was stopped during the testing to allow for photographs of the specimens to be taken. The loading is applied perpendicular to the axis of the bolts. Six displacement transducers (three per side) are used during testing to monitor the deformation and the slip of the specimen. The location of the transducers is shown in Figure 2.

Two different interface conditions were studied. During the initial testing, the ECC specimens were tested without any modification to the formed surfaces. Figure 3 shows the load displacement response of a test specimen with a plain-formed surface. The specimen began to slip at a load equal to approximately 338 kN. After the specimen began to slip, the load gradually increased until a

compressive failure occurred in the top section. The compressive failure initiated as the ECC began bearing on the bolts in the connection region.

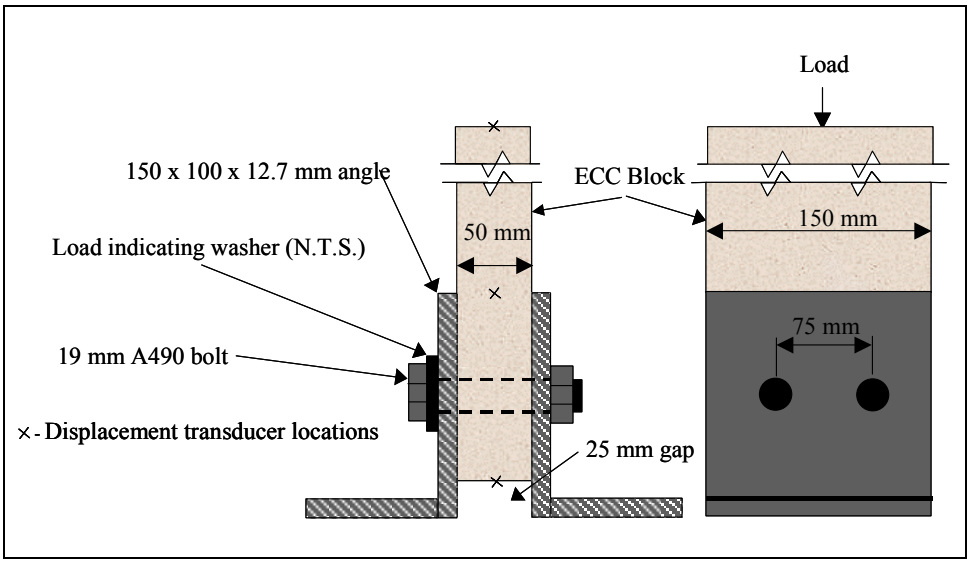

Figure 2. Schematic representation of ECC shear connection test

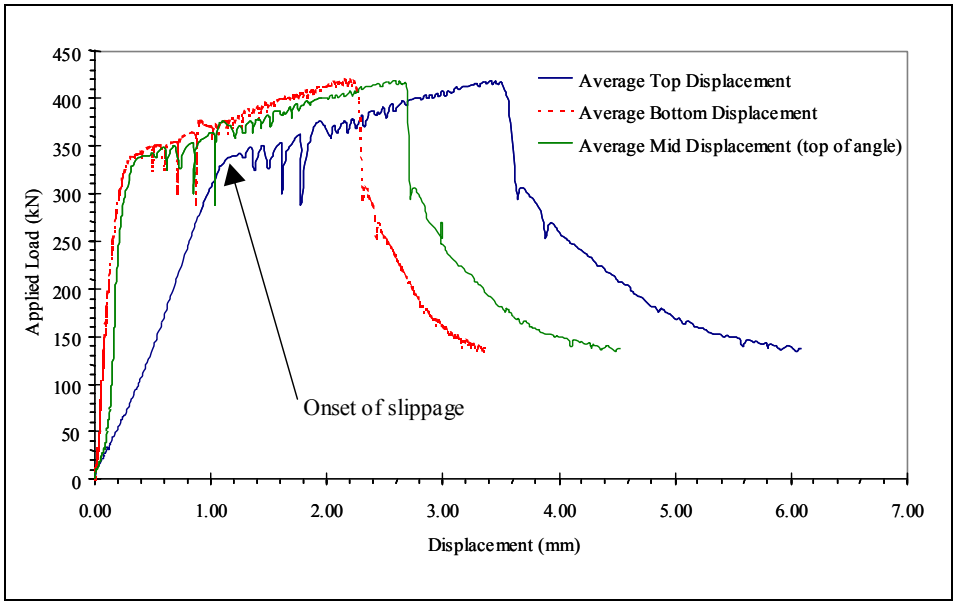

Figure 3. Load displacement results from connection test

In subsequent testing, both the ECC specimens and the steel angles were sandblasted to increase the friction between the ECC block and the steel angle. Test results indicate that sandblasting increases the shear capacity of the connection region. Table 1 shows a summary of the bolted connection test results. In Table 1, the slip coefficient was calculated using Eq. 1, which was adopted from the AISC specifications for the use of high strength bolts:

$$k_s = \frac{sl}{2cf} \quad (1)$$

where k_s = slip (interface friction) coefficient, cf = total bolt pretensioning force and sl = load at which the deformation rate increases.

Table 1. Summary of average panel connection tests

Interface type	Clamping force [kN]	Slip load [kN]	Slip coefficient
Formed	267	338	0.63
Sandblasted	267	463	0.87

Values of the slip coefficient obtained from testing are being used to evaluate the size and number of required bolts between precast panels and at the connections to steel frames. Test results are also being used to model the confined ECC material in the connection regions. Additional tests are underway to evaluate the effect of loading in line with the axis of the bolts (shear strength of the connection shown in Figure 1b), as well as the effect of creep in the connection region.

Preliminary Retrofit Analysis

The infill installation can be used to increase the stiffness and the energy dissipation capacity of a structure, as well as to limit deflections. The primary goals of such installations are to protect the existing structure as well as critical secondary systems such as piping systems and hospital equipment. To contribute to the achievement of these goals, a clear understanding of the ways by which the ECC panel retrofit alters the structural properties (stiffness, strength and energy dissipation) must be developed. At the same time, the panel geometry must be selected so that it minimizes the number of panels per frame while maintaining the portability and flexibility of the system.

To begin the evaluation of the effect of added infill walls, a finite element model of a single bay of a steel frame from MCEER's demonstration hospital was created. Multi-bay frame models are also being investigated. Frame members for the single bay model are 2-noded beam elements. The infill panels and the steel connections are modeled using 4-noded plane stress elements. For the steel frame and panel connection members, an elastoplastic material model with isotropic hardening is used. Panel reinforcement is modeled as embedded grid reinforcement. ECC material is modeled using a simplified material model that includes a multilinear stress-strain curve wherein the transition points on the stress strain diagram are obtained from uniaxial tension tests. The tension model used in the current analysis is based on a total strain fixed-crack model. A parabolic softening model is used for the compression branch. The model has secant unloading and reloading in both tension and compression.

A beam-type infill panel addition (as shown in Figure 1b) is being evaluated. An infilled frame is cyclically displaced to three drift levels: 0.25%, 0.5% and 1%. In the simulation, 0.5% grid reinforcement in each direction is used in the panels. The panel thickness is equal to 100 mm. Figure 4 shows some results from the simulations. In the figure, results for three different panel

aspect (panel height (l)/panel depth (d)) ratios are shown. The number of panels is varied to keep the ratio of infill panel area to total panel area approximately constant. The percentage of infilled frame area is indicated in the figure legend. For comparison, the result from an evaluation of the bare frame is also shown.

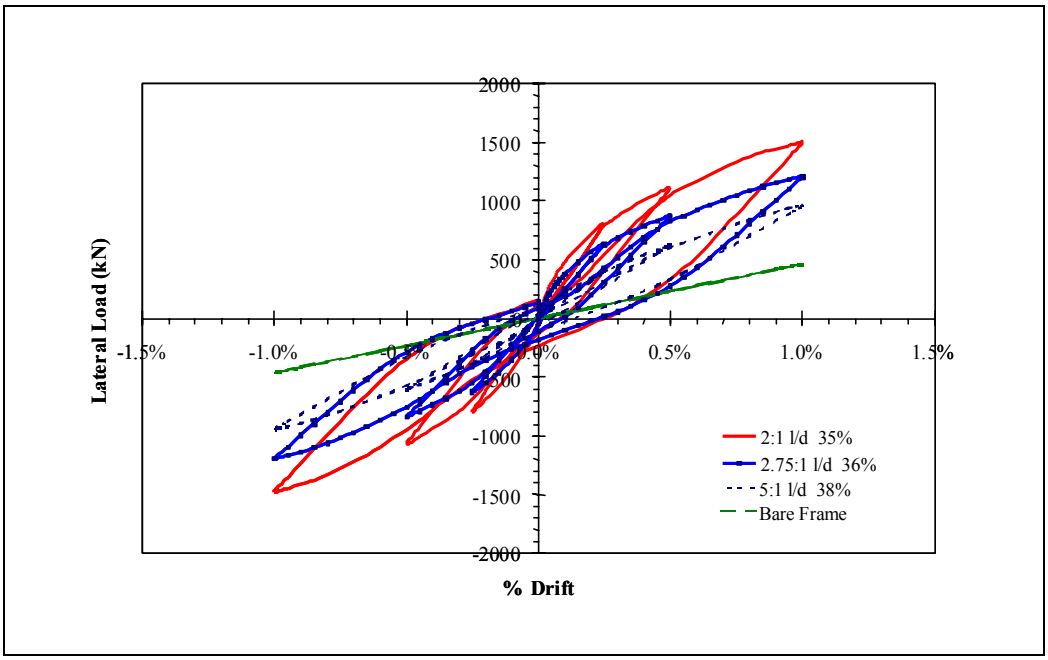

Figure 4. Summary of finite element simulation results from beam-type infill system

Results indicate that beam-type infill panel systems can significantly increase the stiffness of the frame, as well as the energy dissipation during cyclic loadings. In the analysis of the bare frame, yielding is observed to occur at the base of the columns at approximately 1% drift. In the infilled frames, yielding was observed to occur at similar drift levels. This indicates that the infill addition can simultaneously protect the frames and increase the stiffness.

Results from numerical studies are being used to identify promising systems for experimental investigations. Further development of ECC material models will allow for more accurate and efficient evaluation of ECC infill panels for seismic strengthening, stiffening and energy dissipation.

Concluding Remarks

An infill system of ECC panels with bolted connections is being developed for seismic retrofit. A combination of laboratory and numerical studies are being used to evaluate and develop components of the infill system. ECC infill panels are capable of increasing the lateral load capacity, stiffness and energy dissipation capability of a steel frame subjected to cyclic lateral loads.

The feasibility of bolted connections between panels has been demonstrated experimentally. Values of the slip coefficients calculated from test results allow for simple design of ECC panel connections. These test results demonstrate the viability of the infill panel concept.

Acknowledgements

This research is being performed under the direction of Professor Sarah L. Billington of Cornell University and is sponsored by the Multidisciplinary Center for Earthquake Engineering Research (MCEER). The author gratefully acknowledges the support of both Professor Billington and his committee members at Cornell University and the support of MCEER.

References

AISC (1988): *Specification for structural joints using ASTM A325 or A490 bolts*. American Institute of Iron and Steel Construction, Chicago, IL.

Kanda T, Watanabe W, Li VC (1998): Application of pseudo strain hardening cementitious composites to shear resistant structural elements. *Fracture Mechanics of Concrete Structures*, Proceedings of FRAMCOS-3, AEDIFICATIO Publishers, Freiburg, Germany, 1477-1490.

Li VC (1998): Engineered cementitious composites – Tailored composites through micromechanical modeling. *Fiber Reinforced Concrete: Present and the Future*, Canadian Society for Civil Engineering, Montreal, Canada, 64-97.

10

Development of a Benchmark Model for Irregular Structures

Dyah Kusumastuti

Department of Civil, Structural & Environmental Engineering, University at Buffalo

Research Supervisor: Andrei M. Reinhorn, Clifford C. Furnas Professor

Summary

Many building structures have non-symmetric floor plans or multiple towers and setback floors. Such buildings are prone to earthquake damage due to coupled lateral and torsional movements producing non-uniform displacement demands in building elements and concentrations of stresses and forces on structural members. Current codes fall short of providing recommendations for irregular structures. Thus, there is an apparent need to develop a simple analysis procedure based on rigorous analytical and experimental information on the inelastic seismic response of irregular structures. An experiment was designed and carried out to better understand the nonlinear inelastic seismic response of irregular structures. A new structural (benchmark) model was designed in such a way that damage affects sacrificial elements only while most parts are retained for further use. The model was also designed for easy reconfiguration. Test results show that permanent deformations and asymmetric mode shapes are visible and that damage occurs due to irregularities. Results from a recent shaking table experiment are used to develop a simplified analytical tool for irregular structures based on the "spectral capacity analysis" concept.

Introduction

Structural irregularities are commonly found in constructions and structures. Architectural demands are usually the cause of such irregularities. The analysis of the seismic response of irregular structures is complex due to nonlinear and inelastic response and more difficult than that of regular structures. There are very few experiments on globally irregular assemblies. A shaking table study was performed using a new reconfigurable model to obtain data for calibration and benchmark of analytical studies. The experiment is intended to provide a better understanding of the effect of irregularities on the structural seismic response near collapse. Results are also used to calibrate analytical models currently under development. Moreover, the model developed for this study will be used further as a test-bed for hybrid structures and new protective systems and energy dissipation devices.

Objectives

The objectives of this study are:

1. Develop a model with separated vertical and lateral load resisting systems and capable to sustain damage in sacrificial elements without collapse (the model is developed as a BENCHMARK MODEL for the analysis and testing through the Networking Program)

2. Develop a retrofit strategy for hybrid structures with separated lateral and vertical supporting systems using supplemental energy dissipation devices

3. Develop simplified evaluation procedures for irregular structures

4. Determine performance limits for irregular structures, i.e., calibration of techniques of fragility evaluation (Barron-Corvera 2000).

Methods

The model is a 3-story steel structure with two unequal towers, i.e., it has a vertical irregularity. The scale of the model is 1:3. The model is designed to behave in a ductile manner and to allow collapse to occur in the lateral load resisting system. The plan dimensions of the model (6m x 2m) were defined in accordance with the size of the shaking table. Views of the benchmark model are presented in Figure 1. The undamageable gravity load resisting system is separated from the damageable lateral load resisting frames. The gravity load resisting system consists of rocking columns and slotted connections are implemented in the lateral load resisting frames. Special features of the model such as the gravity load columns, the slotted connections and the 5-directional load cell used to measure the structural response are shown in Figure 2. The model has a versatile configuration due to its removable elements and can be used for experimental studies of different structural configurations, protective systems or energy dissipation devices. Figure 3 shows possible layout arrangements of the model.

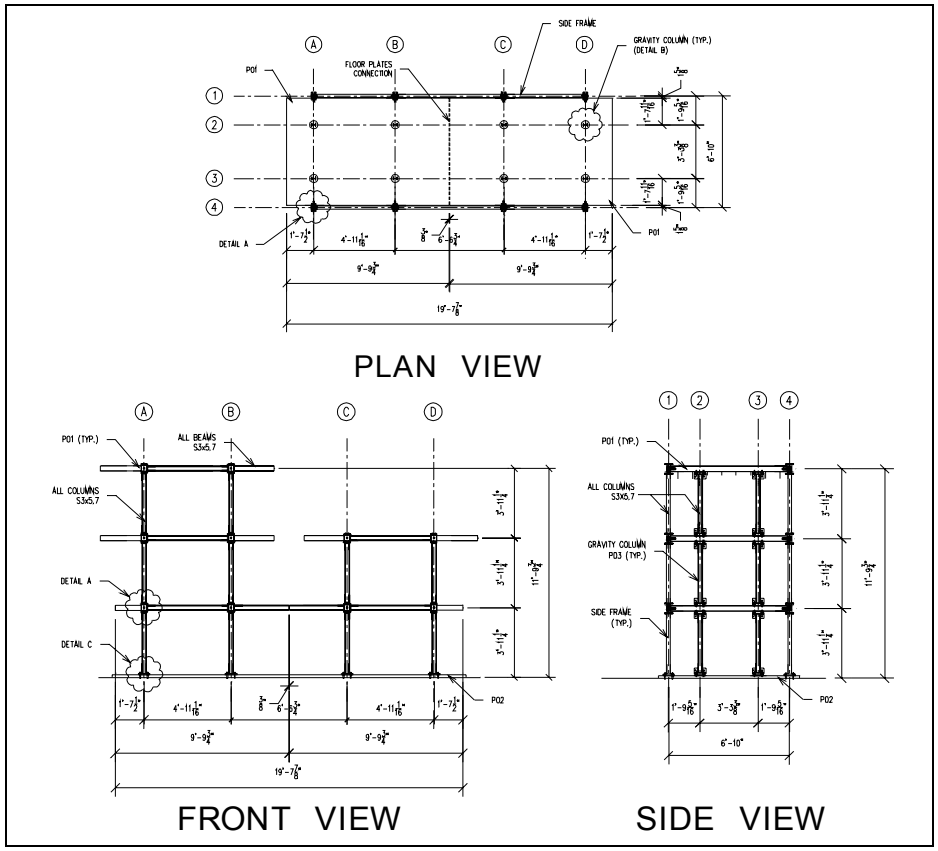

Figure 1. Structural drawings of the model

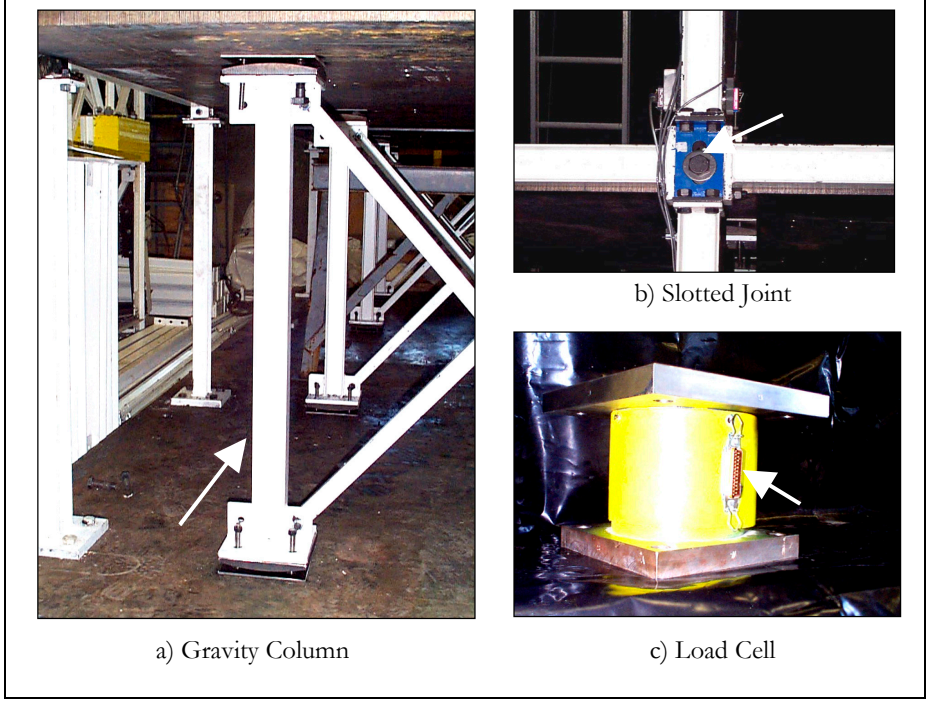

Figure 2. Special features of the benchmark model

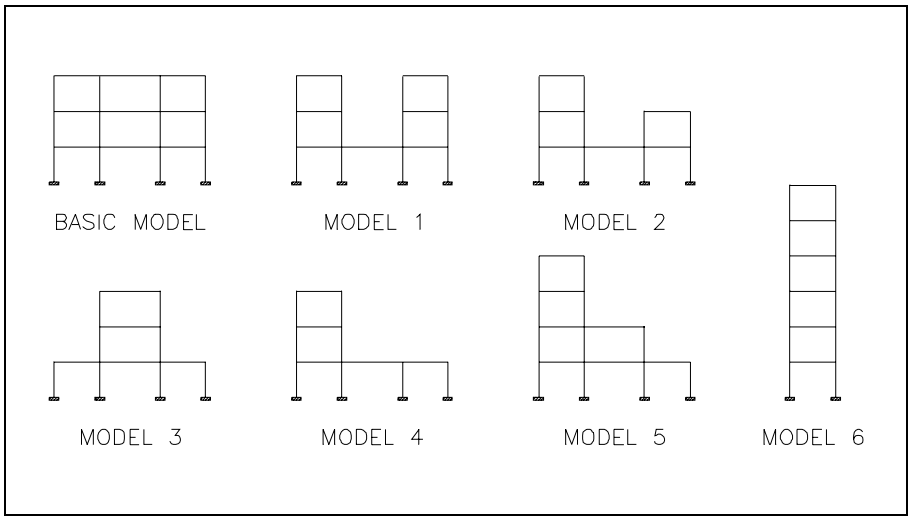

Figure 3. Possible layout arrangements of the model

Test and Analysis

The model (type 2) was subjected to the Rinaldi Station (LA16) earthquake record of the 1994 Northridge earthquake scaled to increasing values of PGA. Static and Dynamic (Incremental) Pushover Analyses were performed using IDARC2D and LARSA software platforms. Initial analyses show that the model develops irregular response in terms of curvatures and generalized forces (Figure 4).

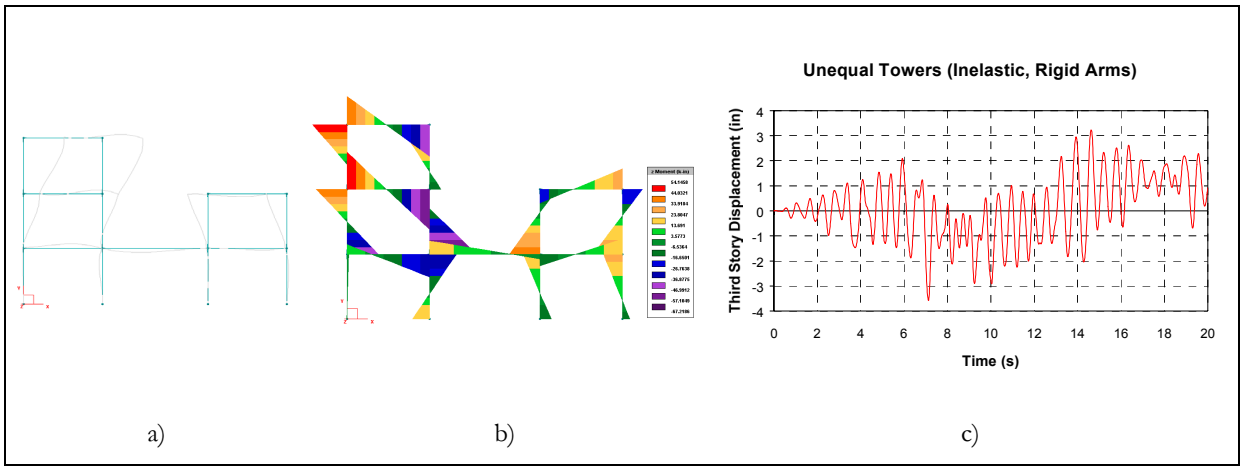

Figure 4. Inelastic displacements and forces

An experimental study was conducted following the Dynamic Pushover Analysis approach. The model (Figure 5) was subjected to the same ground acceleration history mentioned before (LA16) scaled to increasing values of PGA. Test results show that the fundamental period of the model is 0.60 sec and that the model behaves inelastically when the base shear is greater than 20% of the weight of the model. The experiment shows that damage occurs mostly on beam-column connections in the form of prying effects in column end plates and welding failures of rigid connection (Figure 6).

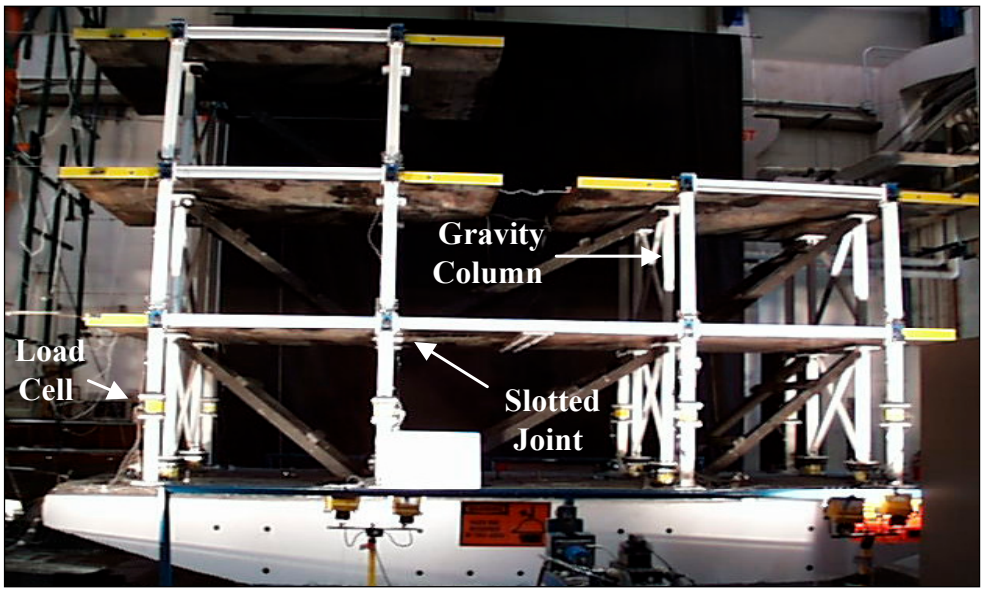

Figure 5. View of the test setup

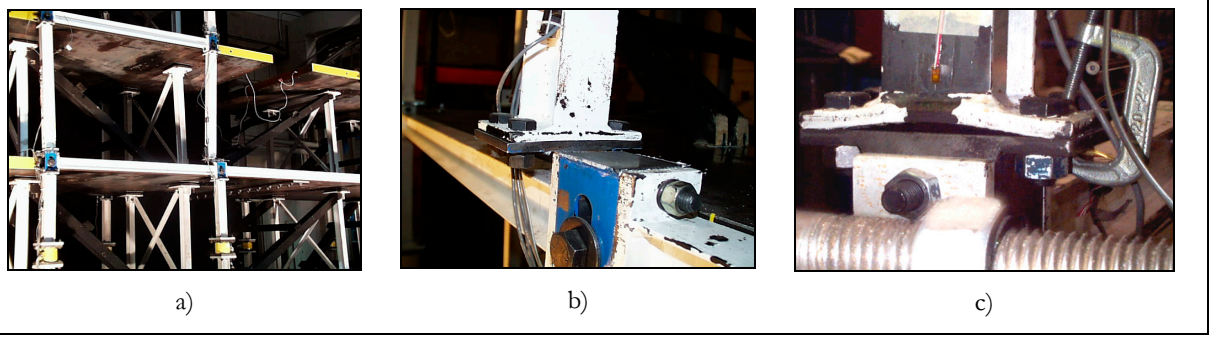

a) b) c)

Figure 6. Damage on elements of the model

Work in Progress

Preliminary testing of joints and components indicated that the benchmark model has actually semi-rigid connections. A new computational model for these connections was developed and the structure was re-evaluated. As a result, more fail-safe guards were added to the benchmark model and the computer program (IDARC2D) was enhanced by incorporating an additional connectivity model (Figure 7).

Comparison between experimental and analytical results (Figure 8) shows that the new computational model predicts well the behavior of the model under seismic excitations. In contrast, the original computational model with adjusted parameters ("strong" or "weak" in Figure 8) would not be able to predict the response to ground shaking.

Upon completion of the analyses, the model will be retrofitted with dampers attached to the rocking columns. This work will be done in cooperation with Taylor Devices, Inc. (Tonawanda, NY).

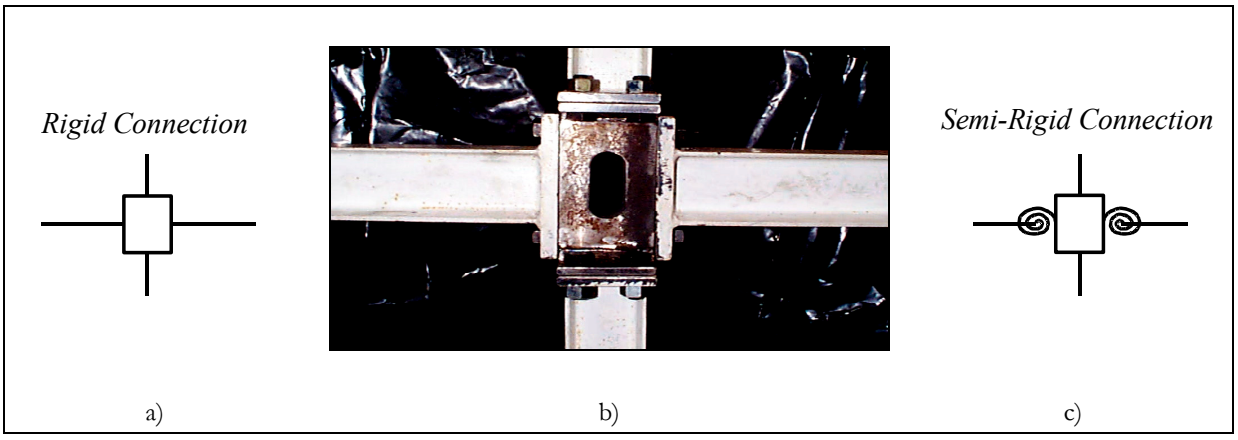

Figure 7. Computational model for connectivity

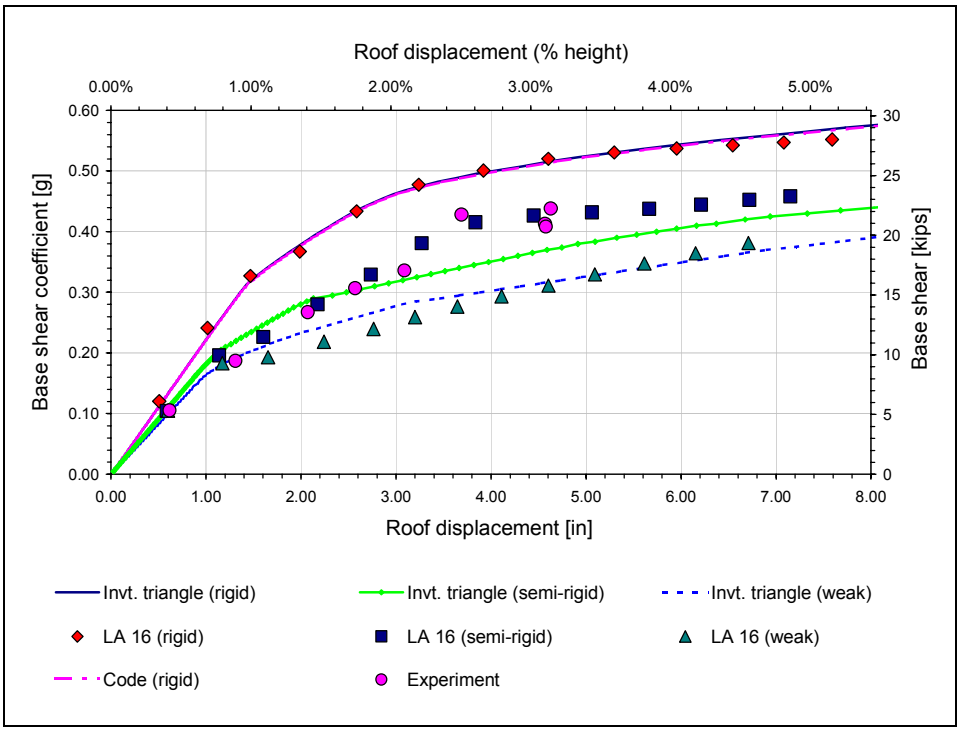

Figure 8. Comparison of analytical and experimental results

Conclusion

Experience shows that buildings with irregularities are prone to earthquake damage, as observed in many earthquake occurrences. Since current codes fall short of providing simplified analytical tools for irregular structures, it is necessary to develop a simple analytical procedure based on rigorous inelastic computations and experiments on the seismic response of irregular structures. Since there are very few analytical models validated by experiments, an experiment was carried out to better understand the nonlinear inelastic behavior of irregular structures under seismic excitations. Test results show that damage occurs due to irregularities. Further studies will be carried out to develop a simplified analytical tool for irregular structures based on the "spectral capacity analysis" concept.

Acknowledgements

This work is being carried out at the University at Buffalo under the supervision of Prof. A. M. Reinhorn, and is supported by the Multidisciplinary Center for Earthquake Engineering Research under program area Seismic Retrofit of Hospitals –Technology Portfolio and the Networking Program, Tasks number 2.4a and 4.1. This support is gratefully appreciated. Part of the design of the benchmark model was done in collaboration with Professor A. Rutenberg of Technion - Israel Institute of Technology.

References

Barron-Corvera R (2000): Spectral evaluation of seismic fragility of structures. *Ph.D. Dissertation*, Department of Civil, Structural & Environmental Engineering, University at Buffalo, Buffalo, NY.

11

A Strategy for the Optimization of Damper Configurations based on Building Performance Indices

Wei "Wanda" Liu

Department of Civil, Structural & Environmental Engineering, University at Buffalo

Research Supervisor: George C. Lee, Samuel P. Capen Professor

Summary

The objective of this research is to develop an effective and efficient design methodology for optimizing the configurations of energy dissipation devices (EDD) based on building performance objectives. Current design codes do not provide any guidelines for the optimization of EDD configurations. Previous research efforts are either limited in addressing different performance indices or not efficient. The proposed methodology uniquely combines the evolutionary approach and engineering knowledge to optimize EDD configurations for optimal structural performance under earthquake excitations. It is effective in that resulting optimal configurations minimize the response of different performance indices such as interstory drift or acceleration. It is also efficient in that the probabilistic-based exploration of the evolutionary approach is guided by modal-analysis-based heuristic knowledge.

Introduction

Addition of energy dissipation devices (EDDs) is considered one of the viable strategies for enhancing the seismic performance of building structures. It is known that the EDD configuration can have a significant effect on the structure response under earthquake excitations. For many building structures, optimal configurations of EDDs may provide considerable performance improvement or cost saving. For instance, given a fixed number of EDDs, some configurations may allow the structure to achieve its performance objective while some may not. Similarly, an optimized configuration may reduce the number of EDDs required to achieve a target performance objective.

Current design provisions (FEMA 2000, 2001) provide some design procedures for structures with added EDDs. Supplemental damping provided by added EDDs is accounted for through an effective damping ratio, which in turn is used to reduce the design seismic forces. Structural members can then be designed for the reduced seismic forces. However, no guidelines for the optimization of EDD configurations are provided.

Brief Review of Previous Research

Several parametric studies on the effect of damper capacity and damper location have been conducted. Chang et al., (1995) investigated the seismic behavior of a steel frame structure with added viscoelastic dampers. Hahn and Sathiavageeswarm (1992) showed that dampers should be placed in the lower-half floors of buildings having uniform story stiffnesses. Because these studies always use simple and regular structures, their results cannot be used for optimization.

Some researchers investigated the optimal capacity of EDDs based on analytical optimization approaches. Several objective functions have been considered: maximum displacement under white noise excitation (Constantinou and Tadjbakhsh 1983), energy (Gurgoze and Muller 1992), system response and control gain matrix (Gluck et al., 1996), pre-assigned modal damping and natural frequency (De Silva 1981), norm of the transfer function (Spencer et al., 1994, Takewaki 1997), total story stiffness (Tsuji and Nakamura 1996) or the desired level of response reduction (Singh and Moreschi 2001). These approaches lead to device sizes that may not be practical for commercial products. Furthermore, it is not possible to define analytical objective functions valid for any arbitrary ground motion.

Some researchers have used heuristic approaches to obtain the optimal placement and capacity of EDDs. Zhang and Soong (1992) and Shukla and Datta (1999) proposed and extended the sequential seismic design method to find the optimal configuration of viscous dampers for buildings with specified story stiffnesses. They used an intuitive criterion to place additional dampers sequentially on the story at which the interstory drift response is a maximum. Lopez Garcia (2001) simplified this approach and showed that it is effective for drift response. These heuristic approaches are practical. However, results from Singh and Moreschi (2001) showed that the sequential approach proposed by Zhang and Soong obtains very low reduction of acceleration response, especially for buildings with non-uniform story stiffnesses.

Singh and Moreschi (1999) used a genetic algorithm to obtain the optimal configuration of EDDs for a desired level of response reduction. They showed that genetic algorithms are powerful tools that lead to optimal configurations if the number of iterations is large enough. However, this approach is computationally expensive.

Proposed Methodology

In this research, a new optimization methodology is proposed for the optimization of EDD configurations. It combines the efficiency of heuristic procedures with the effectiveness of evolutionary approaches. The proposed method searches the optimal solution by generating new configurations, which are obtained by improving previous configurations. This is achieved by increasing the damping ratio of the modes dominating the response. In doing so, the indexed structural response is reduced. The derived optimization procedure can be implemented in computer programs so that it can be used routinely by designers.

Once a performance index is selected depending on the building performance objective, an initial EDD configuration is defined. Modal analysis is then performed and the contribution of each mode to the response quantity of interest (performance index) is obtained. EDDs are then redistributed in such a way that damping ratios of the modes dominating the response are maximized. The procedure is an iterative process intended to explore the solution space and to escape local optima.

Current Status of Research Project

The developed optimization procedure is being implemented into a software package intended to provide the optimal EDD configuration given a structural model, external loads and a performance index. Results will be compared with results given by other available optimization strategies. Both the sequential approach and the genetic algorithm will be considered.

Contribution to the State-of-the-art

The proposed methodology provides an optimal solution for the EDD design problem under earthquake excitations. Different from other procedures for earthquake engineering applications, the proposed methodology uses a new approach to integrate the design of EDDs with performance-based engineering. The benefits of this new approach includes:

- It provides either the best performance or the most cost-effective design.
- It is effective for different performance indices.
- It is more efficient than random search. It adapts the powerful evolutionary approach but adds problem-specific knowledge to guide the search. Therefore, the optimal solution is obtained more efficiently.
- It is theoretically sound because the heuristics is based on structural dynamics theory and practice.

Example

The proposed optimization procedure is applied to a 10-story building structure having uniform mass and stiffness properties along its height. The story mass is equal to 2.5×10^5 kg and the story stiffness is equal to 4.5×10^5 kN/m. The natural period of the first mode is 1.0 sec. The damping ratio is assumed equal to 3%. The design load is an artificial ground acceleration history whose peak acceleration is equal to 0.40 g.

The selected initial configuration consists of 80 linear viscous dampers uniformly distributed along the stories. The damping coefficient of each damper is equal to 5×10^5 Ns/m. Two different performance indices are considered: interstory drift and absolute acceleration. Different optimal configurations are obtained for each performance index. Figure 1 shows results for performance index interstory drift. Figure 1a shows interstory drift response at each story for different EDD configurations. Maximum interstory drift is reduced by 20% after the optimization. Figure 1b shows the EDD configuration before and after optimization. Figure 2 shows results for performance index absolute acceleration. Figure 2a shows absolute acceleration response at each story for different EDD configurations. Maximum story acceleration is reduced by 8% after the optimization. Figure 2b shows the EDD configuration before and after optimization.

Future Research

There are several directions for future research.

- Improvement of heuristic search in order to use not only modal damping but also mode shapes.
- Although the methodology can be extended to other devices such as yielding metallic or friction dampers, the current formulation is limited to viscous devices only. The location effectiveness must be formulated based on different device characteristics.
- Extension of the modal-analysis-based optimization to other dynamic design problems.

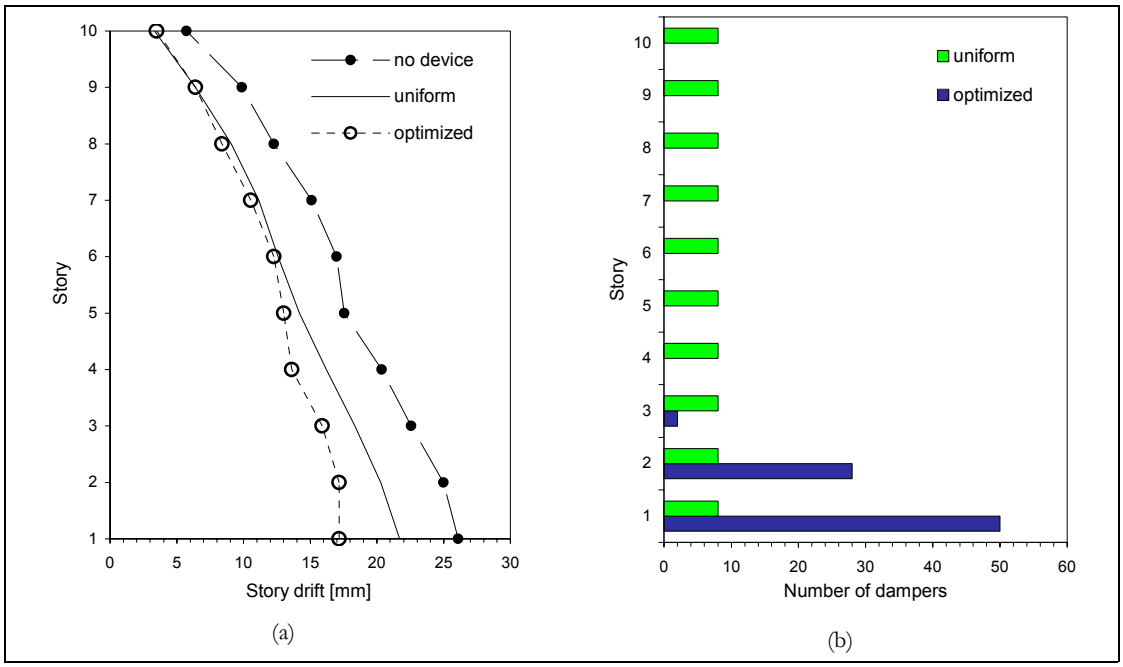

Figure 1. Optimization of EED configuration for performance index interstory drift

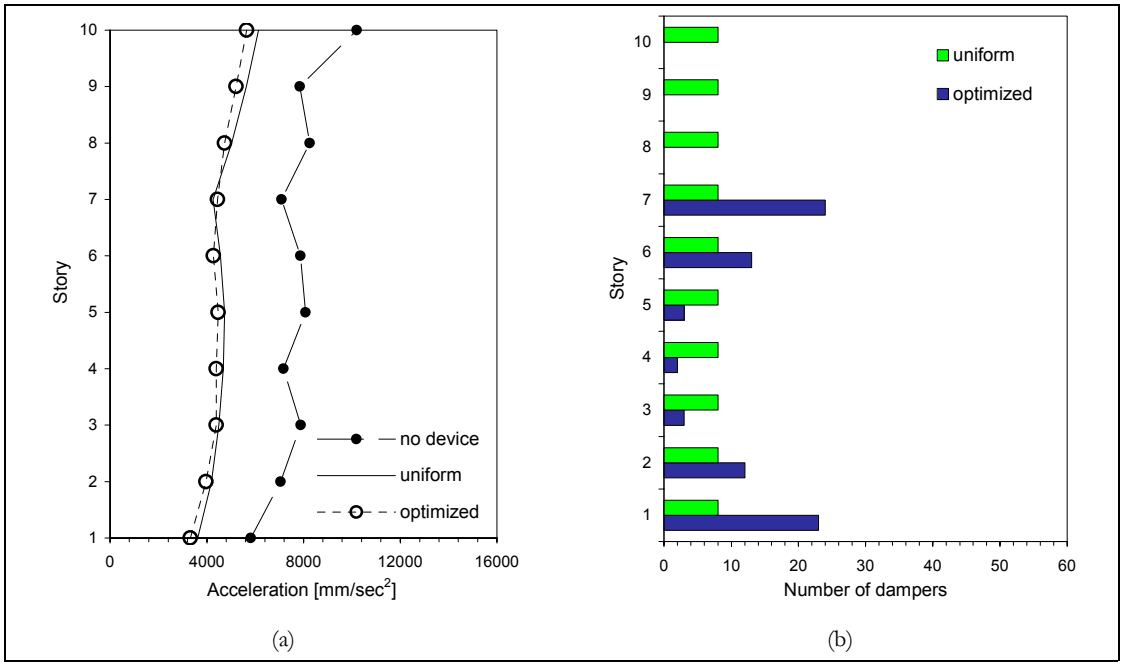

Figure 2. Optimization of EED configuration for performance index absolute acceleration

Concluding Remarks

Results of this research indicate that the optimization of EDD configurations can improve the structural performance under earthquake excitations. For a given performance level, the optimization may also reduce the cost of supplemental EDDs. The proposed optimization methodology can effectively obtain the optimal device configuration for different performance indices.

Acknowledgements

This research was carried out under the supervision of Dr. George C. Lee and Dr. Mai Tong, and supported by the Multidisciplinary Center for Earthquake Engineering Research.

References

Chang KC, Soong TT, Oh ST, Lai ML (1995): Seismic behavior of steel frame with added viscoelastic dampers. *ASCE Journal of Structural Engineering*, **121** (10), 1418-1426.

Constantinou MC, Tadjbakhsh IG (1983): Optimum design of first story damping systems. *Computers & Structures*, **17** (2), 305-310.

De Silva CW (1981): An algorithm for the optimal design of passive vibration controllers for flexible systems. *Journal of Sound and Vibration*, **74** (4), 495-502.

FEMA (2000): Prestandard and commentary for the seismic rehabilitation of buildings. *Report FEMA 356*, Federal Emergency Management Agency, Washington, DC.

FEMA (2001): NEHRP recommended provisions for seismic regulations for new buildings and other structures. Part 1: Provisions. *Report FEMA 368*, Federal Emergency Management Agency, Washington, DC.

Gluck N, Reinhorn AM, Gluck J, Levy R (1996): Design of supplemental dampers for control of structures. *ASCE Journal of Structural Engineering*, **122** (12), 1394-1399.

Gurgoze M, Muller OC (1992): Optimal positioning of dampers in multi-body systems. *Journal of Sound and Vibration*, **158** (3), 517-530.

Hahn GD, Sathiavageeswarm KR (1992): Effects of added-damper distribution on the seismic response of buildings. *Computers & Structures*, **43** (5), 941-950.

Lopez Garcia D (2001): A simple method for the design of optimal damper configurations in MDOF structures. *Earthquake Spectra*, **17** (3), 387-398.

Shukla AK, Datta TK (1999): Optimal use of viscoelastic dampers in building frames for seismic force. *ASCE Journal of Structural Engineering*, **125** (4), 401-409.

Singh MP, Moreschi LM (1999): Genetic algorithm-based control of structures for dynamic loads. *Proceedings of IA-99: International Seminar on Quasi-Impulsive Analysis*, Osaka University, Osaka, Japan.

Singh MP, Moreschi LM (2001): Optimal seismic response control with dampers. *Earthquake Engineering & Structural Dynamics*, **30** (4), 553-572.

Spencer BF, Suhardjo J, Sain MK (1994): Frequency domain optimal control strategies for aseismic protection. *Journal of Engineering Mechanics*, **120** (1), 135-157.

Takewaki I (1997): Optimal damper placement for minimum transfer functions. *Earthquake Engineering & Structural Dynamics*, **26** (11), 1113-1124.

Tsuji M, Nakamura T (1996): Optimal viscous dampers for stiffness design of shear buildings. *The Structural Design of Tall Buildings*, **5** (3), 217-234.

Zhang RH, Soong TT (1992): Seismic design of viscoelastic dampers for structural applications. *Journal of Structural Engineering*, **118** (5), 1375-1392.

12

Probabilistic Evaluation of the Separation Distance Between Adjacent Systems

Diego Lopez Garcia

Department of Civil, Structural & Environmental Engineering, University at Buffalo

Research Supervisor: Tsu-Teh Soong, Samuel P. Capen Professor

Summary

The ABS(ABSolute sum), SRSS(Square Root of Sum of Squares) and DDC (Double Difference Combination) rules for the assessment of the separation distance between adjacent structures are probabilistically evaluated through numerical simulations. Structures are modeled as SDOF systems, both linear and nonlinear. Ground acceleration histories are synthetically generated from modified Kanai-Tajimi power spectral density functions. Both wide-band and narrow-band excitations are considered. Results show that none of the rules considered in this study are satisfactory in the sense that they indicate separation distances whose probability of exceedance (i.e., the probability of pounding or collision) is not equal to the probability of exceedance of the displacement response of the individual systems. The ABS rule is consistently conservative, but its degree of conservatism is generally excessive. The SRSS and DDC rules provide conservative or unconservative results depending on the characteristics of the excitation and the relationship between the fundamental periods of the systems.

Introduction

Observations of the effects of past earthquakes indicate that pounding between adjacent structures is generally negative in the sense it leads to higher levels of damage. In some cases, pounding has been identified as the primary cause of collapse. Consequently, it has been widely recognized that pounding during earthquakes is always undesirable.

Pounding may be prevented by providing adequate separation distances between the potentially colliding structures. However, maximization of land use in metropolitan areas creates strong opposition to generous separation distances, which are then very difficult to effectively implement. The problem to be solved is then the estimation of the *minimum* separation distance necessary to preclude pounding, which is obviously equal to the relative displacement demand of the two potentially colliding structural systems.

Existing Rules for the Assessment of the Separation Distance

The International Building Code (ICB) 2000 specifies that the separation distance between adjacent buildings located on different properties (i.e., buildings separated by a property line) shall be given by:

$$S = \Delta_1 + \Delta_2 \tag{1}$$

where S is the separation distance and Δ_1, Δ_2 are the displacement responses of the buildings at the potential pounding location (i.e., at the top of the shorter building). Eq. 1 will subsequently be referred to as the ABS rule. In the case of buildings located on the same property, IBC 2000 specifies that the separation distance between adjacent buildings shall be given by:

$$S = \sqrt{\Delta_1^2 + \Delta_2^2} \tag{2}$$

Eq. 2 will subsequently be referred to as the SRSS rule.

A more rational approach is the Spectral Difference Method presented by Jeng et al., (1992), according to which the separation distance is given by:

$$S = \sqrt{\Delta_1^2 + \Delta_2^2 - 2\,\rho\,\Delta_1\,\Delta_2} \tag{3}$$

where ρ is the same correlation coefficient used by the well-known CQC modal combination rule. In a probabilistic sense, Eq. 3, which will subsequently be referred to as the Double Difference Combination (DDC) rule, is the exact solution for linear systems subjected to stationary white-noise excitations. The expression "in a probabilistic sense" means that the probability that the relative displacement response exceeds the separation distance S is the same probability of exceedance of the displacement responses Δ_1 and Δ_2. It must be noted that the DDC rule and the SRSS rule coincide when $\rho = 0$ (i.e., when the displacement responses are uncorrelated). Kasai et al., (1996) suggested that the DDC rule can still be used for nonlinear systems as long as modified natural periods T_1*, T_2* and modified damping ratios ξ_1*, ξ_2* are used when calculating the correlation coefficient ρ. In their proposed equations, T_i* and ξ_i* (i = 1, 2) are functions of the displacement ductility μ.

Probabilistic Evaluation of Assessment Rules for the Separation Distance

Due to the intrinsic random nature of earthquakes, none of the abovementioned rules gives the separation distance needed to "avoid" pounding. Rather, there is always a finite probability that, during a given period, the relative displacement response exceeds the separation distance indicated by any of the rules mentioned above. Therefore, it is more appropriate to consider that an assessment rule is accurate when it gives a separation distance S that has the same probability of exceedance as the displacement responses of the individual systems, Δ_1 and Δ_2.

A probabilistic evaluation of the aforementioned rules for the assessment of the separation distance is then numerically performed as follows. Earthquake excitation is characterized as a random process in terms of modified Kanai-Tajimi power spectral density (PSD) functions, from which ground acceleration histories are generated using an appropriate envelope function (Figure 1). The displacement response of SDOF systems is then obtained by performing time history analysis and the relative displacement response is then given by:

$$\Delta_{rel} = \max_t \left| x_1(t) - x_2(t) \right| \tag{4}$$

where x_1(t), x_2(t) are the displacement response histories of systems 1 and 2. The relative displacement response is calculated for each of the sample acceleration histories and the

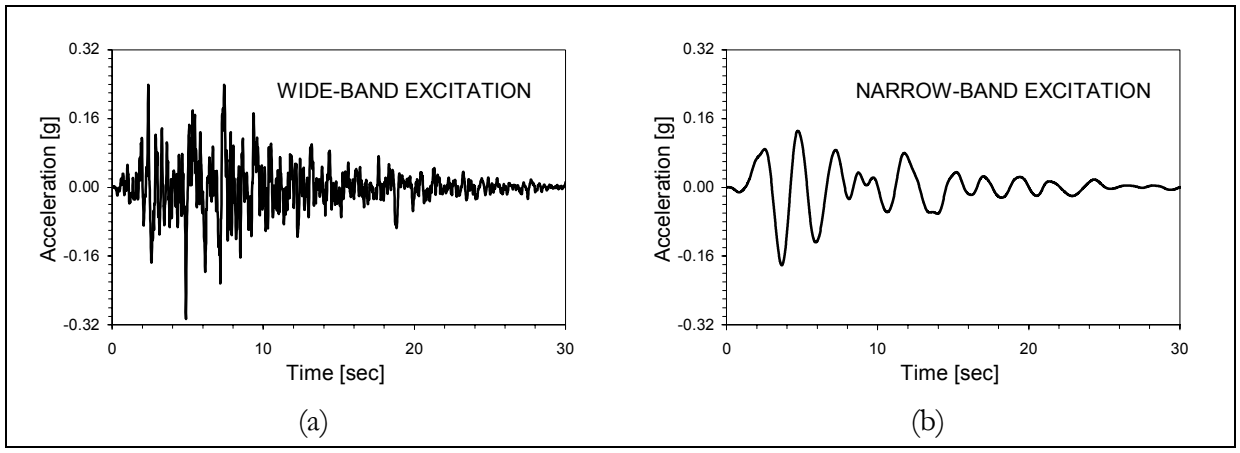

Figure 1. Sample ground acceleration histories

corresponding statistics are computed, from which the relative displacement demand for a 10% probability of exceedance is obtained. Finally, separation distances given by the assessment rules mentioned before are calculated using values of Δ_1 and Δ_2 for which the probability of exceedance is also equal to 10%.

Linear Systems

Examples of results for linear systems are shown in Figure 2. On the one hand, the analysis confirms some results already noticed by other researchers, i.e.: (1) the ABS rule always gives conservative results and its degree of conservatism is generally excessive, particularly when T_1 and T_2 are close to each other; (2) the SRSS rule gives conservative results when T_1 and T_2 are close to each other; (3) the DDC rule gives the most accurate results, particularly when T_1 and T_2 are close to each other. On the other hand, the analysis provides some new information, i.e.: (1) for wide-band excitations, the SRSS and DDC rules give unconservative results when T_1 and T_2 are not close to each other; (2) for narrow-band excitations, results given by the SRSS and DDC rules may be conservative or unconservative when T_1 and T_2 are not close to each other. Results for damping ratios greater than 5% show the same tendencies mentioned above.

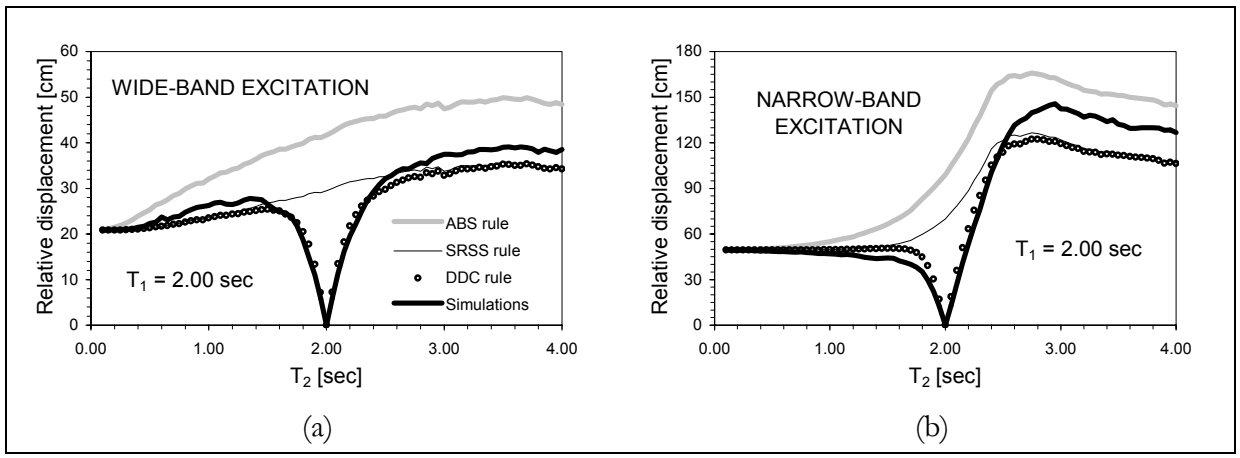

Figure 2. Relative displacement response of linear systems ($\xi_1 = \xi_2 = 0.05$)

Nonlinear Systems

The relative displacement response for nonlinear systems is evaluated assuming that the SDOF systems considered in this study have a bilinear force-displacement relationship, where the post-yielding stiffness is equal to 0.05 times the initial (elastic) stiffness. The systems yield at a force level equal to the elastic force demand divided by a given value of R, the force reduction factor. In doing so, the displacement ductility demand μ is different for each of the sample acceleration histories. In accordance with the probabilistic approach explained before, the statistics of μ are calculated and then modified natural periods T_1*, T_2* and modified damping ratios ξ_1*, ξ_2* for the application of the DDC rule are obtained using values of μ_1, μ_2 that have a 10% probability of exceedance. This is a significant departure from the approach followed by Kasai et al., (1996), who derived the equations to calculate T_i* and ξ_i* (i = 1, 2) from results obtained through time-history analysis where the yielding force of the SDOF systems was adjusted for each ground motion in order to obtain predefined values of μ. The approach followed in this study, however, is more representative of an actual case scenario.

Examples of results for nonlinear systems and for the same value of R are shown in Figure 3, where it can be seen that: (1) the ABS rule always gives results that are even more conservative than those for the linear case; (2) for wide-band excitations, the SRSS rule gives results exhibiting the same tendencies as those for linear systems, i.e., they are conservative when T_1 and T_2 are close to each other and unconservative otherwise; (3) for narrow-band excitations, the SRSS rule always gives conservative results; (4) while results given by the DDC rule are again the most accurate, they are always unconservative for wide-band excitations and may be either conservative or unconservative for narrow-band excitations regardless of whether T_1 and T_2 are close to each other or not.

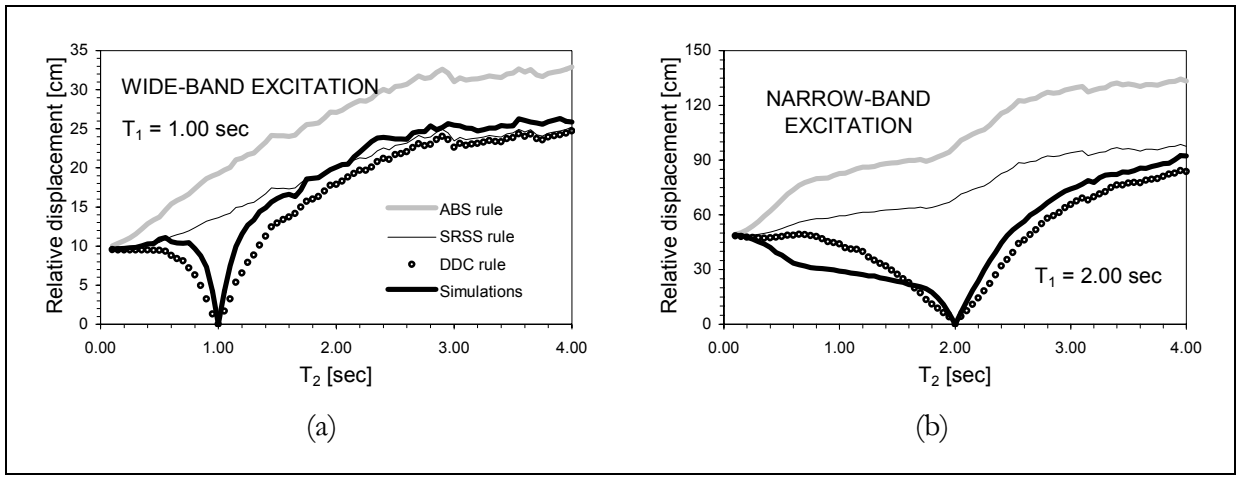

Figure 3. Relative displacement response of nonlinear systems ($R_1 = R_2 = 3$)

Results for damping ratios greater than 5% show the same tendencies mentioned above. However, in the case of narrow-band excitations, the accuracy of the DDC rules improves significantly as the damping ratio increases.

Examples of results for nonlinear systems and for different values of *R* are shown in Figure 4. This is the most general case studied and the most representative of an actual case scenario. It can be seen that results show the same tendencies as for the case where *R* is the same for both systems.

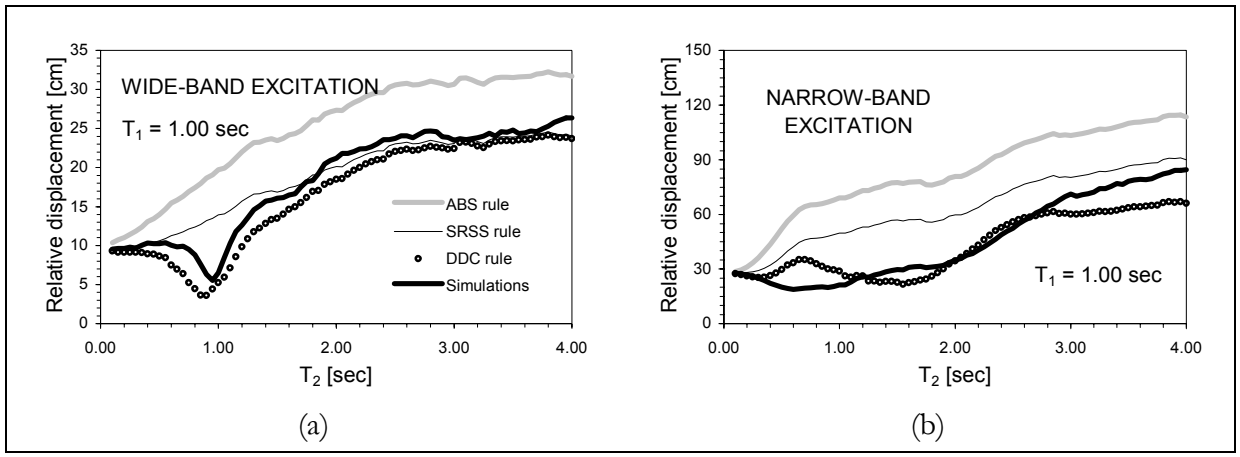

Figure 4. Relative displacement response of nonlinear systems (R_1 = 2.5, R_2 = 4.0)

Concluding Discussion

The analytical study described in this paper clearly shows that none of the existing rules is completely satisfactory in the sense that they cannot accurately predict the relative displacement demand between two adjacent systems. The SRSS and DDC rules give results that are conservative or unconservative depending on the characteristics of the excitation and the relationship between the natural periods of the systems. In other words, the actual risk of pounding or collision is unknown. On the other hand, the ABS rule gives consistently conservative results, but its implementation is difficult because of its generally excessive degree of conservatism.

It must be noted that, from a performance-based design point of view, the appropriate separation distance may or may not have the same probability of exceedance as the displacement response of the individual systems depending on the performance level (i.e., life safety, collapse prevention, etc.). Consequently, the most useful design tool is the complete relationship between the separation distance and the probability of exceedance (for a given period), so that *S* can be chosen for any desired probability of exceedance. An example can be seen in Figure 5, where *S* for a 10% probability of exceedance is also indicated. For comparison purposes, values of *S* given by the SRSS and DDC rules (using Δ_1, Δ_2 having 10% probability of exceedance) are shown as well. It can be seen that the corresponding probabilities of pounding are very different from the target 10% probability.

The probability-of-pounding vs. separation-distance relationship shown in Figure 5 was obtained through numerical simulations, which is a useful approach for research purposes but clearly not practical for real case applications. Further research is currently being carried out to find a theoretical expression for the probability-of-exceedance vs. separation-distance relationship so that the separation distance can be assessed directly based solely on the displacement response of the individual systems.

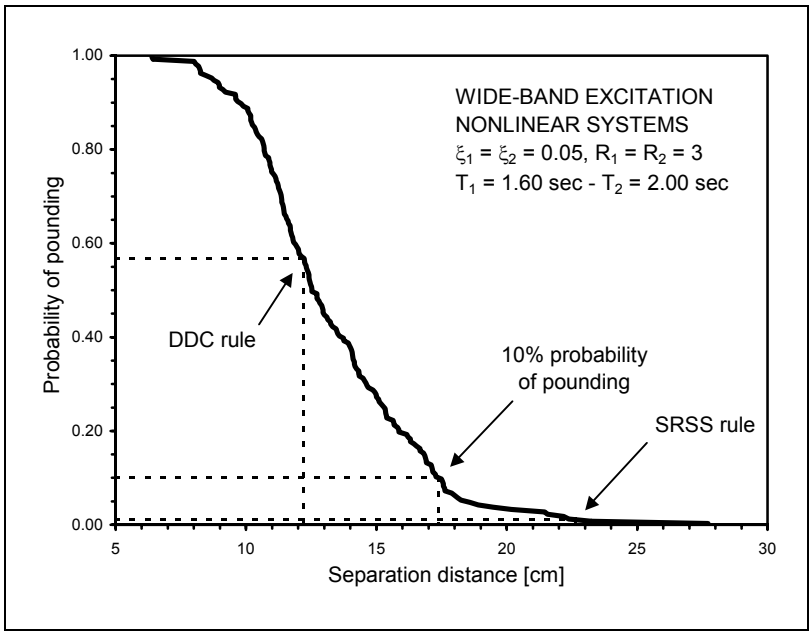

Figure 5. Probability of pounding vs. separation distance

Acknowledgements

This research was carried out under the supervision of Professor Tsu-Teh Soong, and supported in part by the Multidisciplinary Center for Earthquake Engineering Research through Program Area 2, Task Project MCEER-01-2042D. This financial support is gratefully acknowledged.

References

Jeng V, Kasai K, Maison BF (1992): A spectral difference method to estimate building separations to avoid pounding. *Earthquake Spectra*, **8** (2), 201-223.

Kasai K, Jagiasi AR, Jeng V (1996): Inelastic vibration phase theory for seismic pounding mitigation. *ASCE Journal of Structural Engineering*, **122** (10), 1136-1146.

13

Experimental Investigation of P-Delta Effects to Collapse during Earthquakes

Darren Vian

Department of Civil, Structural & Environmental Engineering, University at Buffalo

Research Supervisor: Michel Bruneau, Professor

Summary

Results of tests on fifteen four-column frame specimens subjected to progressive unidirectional ground shaking up to collapse are analyzed. Test structure performance is compared with proposed drift limits for the minimization of P-Δ effects in highway bridge piers. The stability factor θ is found to be strongly related to the relative structural performance in this regard. Specimens for which values of θ are less than 0.25 satisfied the criterion proposed by the National Cooperative Highway Research Program (NCHRP) for at least a portion of their respective test schedule. The drift limit is violated prior to the final test, in which complete specimen collapse occurs.

Introduction

Arbitrary lateral drift limits prescribed by modern design codes to limit nonstructural damage also indirectly ensure that structural performance is minimally affected by the effect of gravity loads on the lateral force resisting system of the structure (a.k.a. P-Δ effect). However, as conventional drift limits are being progressively eliminated and replaced by other performance-based limits, inelastic behavior is to a greater extent relied upon the dissipation of seismic input energy. Accurate quantification of the destabilizing effect of gravity loads is therefore becoming more significant for structural design. As a result, it may be desirable to investigate the destabilizing effect of gravity loads in order to enhance our understanding of the condition ultimately leading to structural collapse and to ensure public safety during extreme events.

A recently published report (Vian and Bruneau 2001) discusses a program of shaking table testing of simple frames through collapse. This series of tests provides well-documented data (freely available at *http://civil.eng.buffalo.edu/users_ntwk/experimental/case_studies/vian*), which may be used to develop or validate algorithms capable of modeling the inelastic behavior of steel frames up to collapse. Fifteen specimens having different properties were tested in an attempt to identify some of the general parameters responsible for trends in the behavior of SDOF structures to collapse under earthquake loading. Peak responses are compared with a drift limit proposed by other researchers to minimize P-Δ effects in bridge piers. Experimental results are also compared with results obtained using a simple analytical model in order to illustrate the use of the generated experimental data for the development and calibration of models of inelastic behavior to collapse.

P-Δ Behavior

Some concepts for characterizing P-Δ effects in inelastic SDOF structures under lateral load are described below, along with an overall view of the fundamental structural behavior. Figure 1a shows a column from a single bay, single story structure with an infinitely stiff beam, thereby resulting in a lateral stiffness of the column K_o, ignoring P-Δ effect, equal to 12 $E I / L^3$. A bilinear SDOF model is shown in Figure 1b. Elastic-perfectly plastic structural response (neglecting P-Δ effect) is shown, as well as the response modified by the influence of P-Δ effect. A summary of additional concepts on P-Δ effects on simple structures during earthquakes can be seen in MacRae et al., (1993).

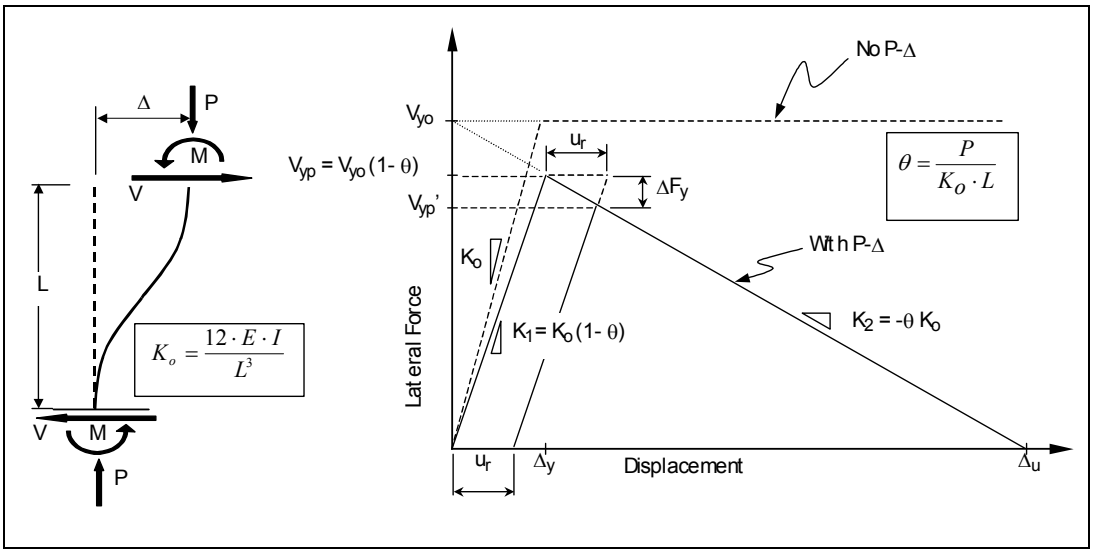

Figure 1. Bilinear lateral-force-versus-displacement model for SDOF structure

Overview of Experimental Program

A SDOF shaking table located at the University at Buffalo Structural Engineering and Earthquake Simulation Laboratory (UB-SEESL) was used to conduct the testing program whose results are analyzed in this paper. The 1940 El Centro S00E ground acceleration time history was used in this study. A displacement record was then generated and used as input to the displacement-controlled actuator. Note that unscaled ground motions were used as the specimens were designed to fit actual parameters of interest rather than intended to be scaled models of actual structures.

Description of Specimens

Fifteen four-column specimens were fabricated at the University of Ottawa and tested to failure at the UB-SEESL in the course of this research. The specimens were divided into three groups of five specimens each. The slenderness ratio of the specimens of each group was equal to 100, 150, and 200, respectively. A range of values of capacity/demand ratios for axial load in columns was chosen for each slenderness ratio. In order to fully document considered imperfections, each column of each specimen was measured in numerous ways prior to testing (Vian and Bruneau 2001).

Instrumentation

Instrumentation was designed to record structural response in a number of ways. A strain gage was mounted on one column of each specimen for estimation of forces during testing. Displacement transducers (LVDTs) were used to measure table displacements, vertical mass displacements and total horizontal mass displacements. Special modifications to the LVDTs setup were required to allow measurements of structural mass displacements during the entire response history, including much of the collapse. A schematic of the test setup and instrumentation is shown in Figure 2.

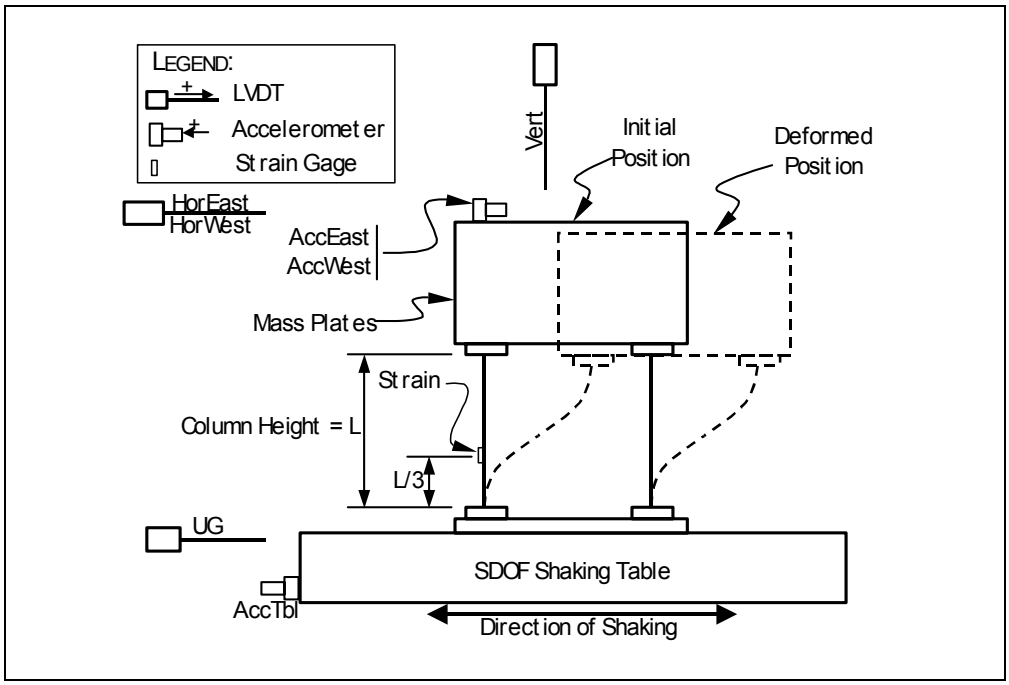

Figure 2. Schematic of test setup and instrumentation

Shaking Table Testing

A free vibration test was performed on each specimen prior to the initiation of its respective schedule of shaking table tests. Shaking table test schedules were established for each specimen, creating a series of progressively more severe shaking table tests until the specimen collapsed. Approximately five levels of ground motion intensity were selected and applied to each specimen. All specimens were investigated in the perspective of the entire series of tests to which they were subjected.

Behavioral Trends

The value of the stability factor θ has a significant effect on the response of the structure. In actual bridge and building structures, the value of θ is unlikely to be greater than 0.10 and is generally less than 0.06 (MacRae et al., 1993). Specimen 1 was found to be the only one whose value of θ (= 0.065) was close to the abovementioned range. Specimens 2, 6 and 11 have stability factors

whose values are slightly larger than the likely upper limit (= 0.123, 0.101 and 0.138, respectively). For all other specimens, $\theta \geq 0.155$.

Results of a graphical study of peak response parameters are summarized below. Values of three response parameters (spectral acceleration $S_{a\text{-}final}$, displacement ductility μ_{final} and drift γ_{final}) obtained from the penultimate shaking table test were compared with the stability factor θ. These response quantities were also compared with the static stability limit μ_s, which is defined as the structure's ductility at ultimate displacement Δ_u. From the information given in Figure 1, μ_s can be shown to be the inverse of the stability factor. The following general observations can be made:

1. Elastic spectral acceleration S_a, ductility μ and percent drift γ were observed to have inverse relationships with θ. Spectral acceleration is plotted versus the stability factor in Figure 3 for the penultimate test (subscript "final"). The plot suggests that structures may be less able to undergo large inelastic excursions before imminent instability as the stability factor increases. Specimens 1 and 6, which had the lowest values of θ, were the only specimens able to withstand spectral accelerations greater than 0.75g.

2. Specimen 1 was the only specimen that underwent both a value of ductility greater than five (= 20.35) and a value of drift larger than 20% (= 64%) prior to collapse. It is recalled that specimen 1 is the only specimen whose value of θ is less than 0.10.

The static stability limit μ_s can be expressed as the inverse of the stability factor, as previously shown. The same parameters discussed above were compared with μ_s. A reverse trend from that shown in Figure 3 is observed, as expected. The ductility of each specimen's penultimate shaking table test is plotted versus its static stability limit in Figure 4. The line $\mu_{final} = \mu_s$ is shown for clarity. Only Specimen 1 was able to exceed its static stability limit.

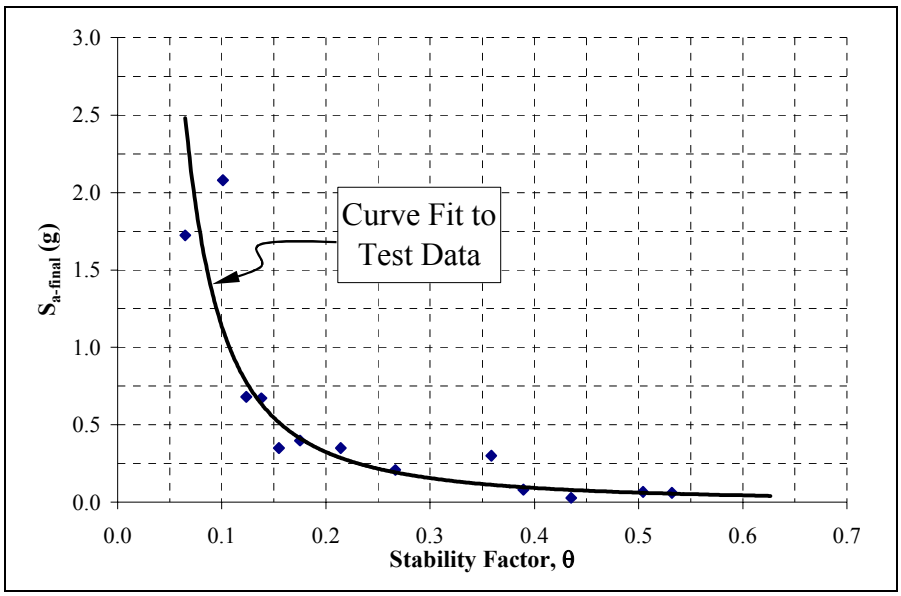

Figure 3. Spectral acceleration vs. stability factor

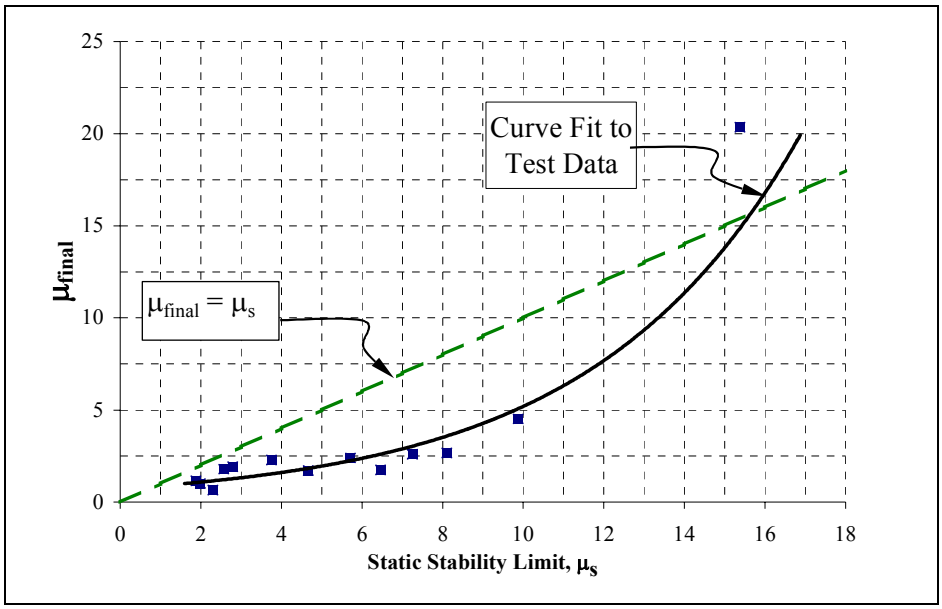

Figure 4. Displacement ductility vs. static stability limit

Overall, ultimate inelastic behavior is shown in this investigation to have a high dependence on the stability factor for a P-Δ affected structure. For the specimens tested in this research having a value of θ greater than 0.10, a relatively low level of inelastic behavior was exhibited before collapse. Specimens for which the value of θ is less than 0.10 were able to withstand ground motions with higher spectral accelerations, experience larger values of ductility and accumulate larger drifts than specimens having a value of θ greater than 0.10. Very slender structures, characterized by large values of θ, will undergo relatively small inelastic excursions prior to collapse.

Comparison with Proposed P-Δ Limits for Bridge Piers

The National Cooperative Highway Research Program (NCHRP), Project 12-49, under the auspices of the Transportation Research Board, is investigating the seismic design of bridges from all relevant aspects. At the conclusion of this project, proposed revisions to the current LRFD Specifications for Highway Bridges will be presented to the American Association of State Highway Transportation Organizations (AASHTO) for review and possible implementation. Studies on additional demands on the structure arising from P-Δ effect are included in the proposed revisions.

Figure 5 shows a comparison between the proposed drift limit and peak experimental responses. The estimated base shear coefficient C_s* is plotted as a function of the maximum drift γ (= Δ/*H*). Specimens for which the value of θ is less than 0.25 (specimens 1, 2, 4, 6, 7, 11 and 12) are shown in Figure 5a. None of these specimens failed during the initial tests, where the proposed drift limit was not exceeded. However, in the subsequent tests of the schedule, cumulative drifts of the specimens increased due to repeated inelastic action, which eventually caused progressive collapse and violation of the proposed drift limit. Collapse always occurred only after the drift limit was exceeded in a prior test, thus validating the proposed criterion.

As shown in Figure 5b, the remaining specimens, for which the value of θ is greater than 0.25, never satisfied the drift criterion, even for those tests that remained in the elastic range. However, values of θ for these specimens were well above the practical range discussed previously, hence violation of the drift limit is of no consequence.

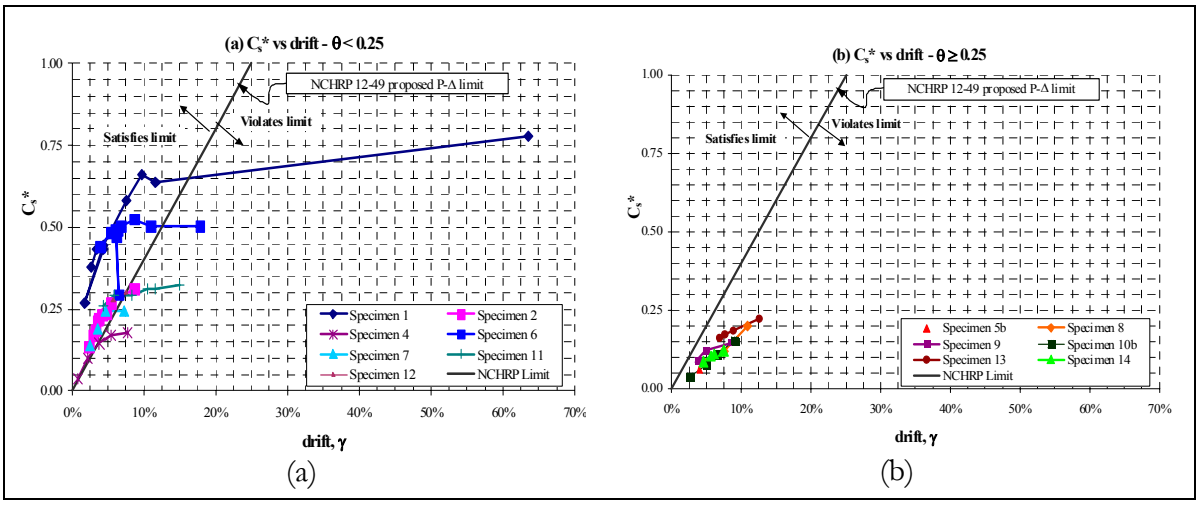

Figure 5. Comparison between test results and NCHRP 12-49 drift limits

Concluding Remarks

Data was gathered through an experimental shaking table test program of specimens subjected to earthquake ground motions up to collapse (Vian and Bruneau 2001). This type of experiment has previously not been carried out.

The stability factor θ was observed to have the most significant effect on the structure's propensity to collapse. As θ increases, the level of maximum attainable ductility, sustainable drift and spectral acceleration that can be withstood before collapse decrease. For values of θ larger than 0.10, ultimate values of maximum spectral acceleration, displacement ductility and drift reached before collapse were all grouped below values of 0.75 g, 5, and 20%, respectively. Stability factor values less than 0.10 tended to significantly increase each of the aforementioned response values. More tests should be performed to more accurately quantify the impact of the stability factor on the response quantities considered in this study and other possibly relevant response quantities.

Additional studies on the effect of nonlinear damping on the specimens, as well as on the comparison between the observed response and the response predicted by design equations, are beyond the scope of this paper but have been presented elsewhere (Vian and Bruneau 2001).

Acknowledgements

This research was carried out under the supervision of Professor Michel Bruneau and was supported in part by the Earthquake Engineering Research Centers Program of the National Science Foundation under Award Number ECC-9701471 granted to the Multidisciplinary Center for Earthquake Engineering Research.

References

MacRae GA, Priestley MJN, Tao J (1993): P-Δ effects in seismic design. *Report SSRP-93/05*, Department of Applied Mechanics and Engineering Sciences, University of California at San Diego, La Jolla, CA.

Vian D, Bruneau M (2001): Experimental investigation of P-Delta effects to collapse during earthquakes. *Technical Report MCEER-01-0001*, Multidisciplinary Center for Earthquake Engineering Research, Buffalo, NY.

14

Investigation of Principal Axes in a Linear MDOF Structure

Tsung Yuan "Tony" Yang

Department of Civil, Structural & Environmental Engineering, University at Buffalo

Research Supervisor: George C. Lee, Samuel P. Capen Professor

Summary

While it is well known that principal axes are nonexistent in asymmetric structures, they are usually recognized in the analysis and design of symmetric structures. However, imperfections in material properties and human errors during construction might lead to nonexistence of principal axes even if the structure is geometrically symmetric. This paper describes a research project intended to experimentally find the principal axes of a geometrically symmetric MDOF structure. Test results suggest that the experimental model indeed has no principal axes.

Introduction

Civil engineers typically accept large uncertainties in the design of structures by using a probabilistic safety factor to account for the uncertainties. However, large safety factors might not be an economical solution. Besides, probabilistic safety factors do not always lead to conservative designs. Since there are always imperfections in material properties and human errors during construction, structures cannot be symmetric with respect to any axis or plan. Consequently, the response of a structure to an external force applied in a given direction always has components in directions other than that of the external force. While this phenomenon has been realized by many engineers and researchers, proper identification of its causes has never been implemented. Most civil engineers believe that geometrically symmetric structures should have defined principal axes. This leads to the assumption that the response of the structure to a static load applied along one of the principal axes has no components in the direction perpendicular to that of the applied force. However, it has been proven mathematically that this phenomenon rarely exists in the real world even in the case of static forces. If the response in the direction perpendicular to that of the external force is small, then assuming principal axes exist might be conservative, but if the response in the perpendicular direction is large, traditional design practice needs to be revised. In the case of dynamic forces, the same phenomenon leads theoretically to an infinitely large response of undamped structures when the structure's natural period reaches resonance with the frequency of the external force. Hence, any minor imperfection leads the structure to suffer the effects of hugely uncertain design forces. In the past, researchers concluded that asymmetric structures have no principal axes and that their response could be calculated by considering torsional effects. This paper strongly emphasizes the idea that structures have no principal axes even if they are geometrically symmetric. In addition, it is shown that the dynamic response in the direction perpendicular to that of the excitation (cross effect) increases with the level of imperfections in structure properties.

Since structures can never be perfectly symmetric in the real world, cross effect always exists. Careful experimental tests have been conducted to verify its existence and to quantify its effects. In order to differentiate between cross coupling of asymmetric buildings and cross coupling effect in symmetric buildings with some engineering-tolerated imperfections, the experimental model was designed as symmetric as possible in order to avoid torsional cross effect.

Experimental Study

If the non-existence of principal axes in MDOF systems is theoretically shown, it is certain then that cross effect always occurs in the real world. In most cases, inputs along the x-axis cause response along the y-axis, and this response can sometimes be quite large. In other words, if the theory holds, then conventional earthquake engineering has to be improved in order to account for the coupling effect. Hence, by carefully conducting experimental tests, the idea of nonexistence of principal axes in MDOF systems under dynamic loads will be reinforced, and experimental results can then be used as evidence of theoretical results. Tests described in this paper are part of the first experimental research aimed to prove and quantify the existence of cross effect in linear MDOF systems under dynamic loads.

A 3-story steel model was built and its response under dynamic loads was carefully examined. The structure has two axes of geometrical symmetry. Since principal axes always lay in perpendicular directions, one of them must lay within 90º from any line passing through the center of geometry (if the structure has indeed any set of principal axes). Hence, experiments were setup to change the direction of the excitation from 0º to 100º. If the structure has any principal axis, the response in the direction perpendicular to that of the excitation should then be zero when the direction of the excitation is aligned with one of the principal axes.

Experimental Setup and Procedure

Recognizing the importance of experimental results, the structure was carefully designed so that it has two planes of geometric symmetry. No weight was added to the structure apart from the self-weight. The design dimensions of the structure are 5 ft long and 4 ft wide. Each floor is four ft tall. All connections are welded and assumed rigidly connected. Floor diaphragms are made with four L3x2.5x1/4 angles at the perimeter and four additional L2x2x1/8 angles were welded in parallel at the center of the diaphragm. The diaphragms are assumed rigid. The foundation of the structure was clamped at all times during all experiments. The lateral stiffness of the structure was provided by four C3x5 steel channels at the four exterior frames of the structure. The channels were originally aligned in such a way that the resulting weak axis is perpendicular to the loading direction. However, the channels were also designed to be able to rotate 360º vertically at each floor to allow for maximum change of the global stiffness matrix of the structure. In order to accommodate such design criteria, the steel channels and the rigid diaphragms were not connected with welds but with 5/8" diameter high strength bolts, post-tensioned with a 125 lb-ft torque to simulate rigid connections. Portions of the steel angles were cut off to allow 360º rotation of the steel channels. However, additional 10"x10" triangular steel plates (1.5" thick) were welded to the steel angles to prevent local yielding of the diaphragm. Since the steel channels were connected to the rigid diaphragms by bolts, 4"x3.5" (1/8" thick) steel plates were welded to the channels to allow for easy fastening of the channels to the rigid diaphragms.

The structure was designed to behave linearly under maximum design ground acceleration (0.353g) along the weak axis. SAP2000 nonlinear computer analysis program was used to check design

stresses. A safety factor equal to four was used in the design of the structure to account for the unforeseen dynamic amplification of structural response caused by cross effect.

Sixteen strain-gage type accelerometers manufactured by three different companies (Sensotec, Kulite and Endeveco) were used to monitor the response of the structure. The sensitivity of all strain gages is approximately equal to 30 mv/g. However, all accelerometers were calibrated to a sensitivity equal to 1v/g so that data obtained from each sensor are all in the same equivalent unit. The accelerometers could measure acceleration only in the direction along which they were mounted.

In order to identify the principal axes of the structure, a total of 21 tests were conducted varying the direction of the excitation at 5º intervals.

Summary of Results

Results obtained from the experiments are presented in three-dimensional plots. Figures 1-4 show the response of the structure in the direction perpendicular to that of the input excitation at the ground, 2nd, 3rd and 4th floor, respectively. Maximum structural responses (regardless of the corresponding frequency) are summarized in Figure 5. Y_{1max}, Y_{2max}, Y_{3max} and Y_{4max} in Figure 5 are the maximum response of the structure in the direction perpendicular to that of the input excitation at the ground, 2nd, 3rd and the 4th floor, respectively.

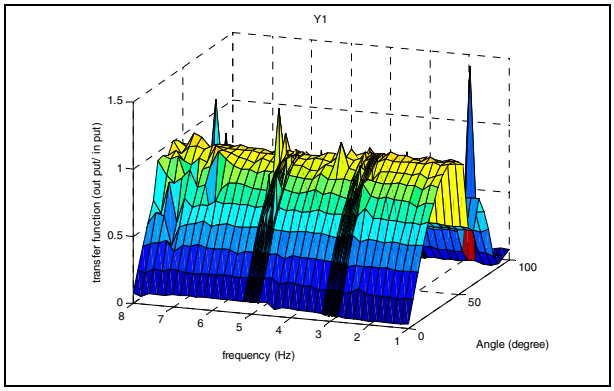

Figure 1. Perpendicular response of the structure at the ground floor

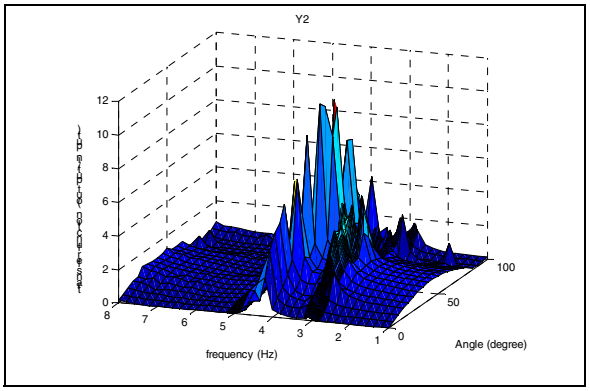

Figure 2. Perpendicular response of the structure at the 2nd floor

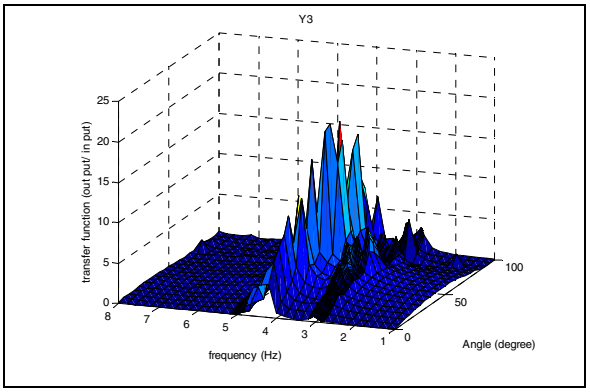

Figure 3. Perpendicular response of the structure at the 3rd floor

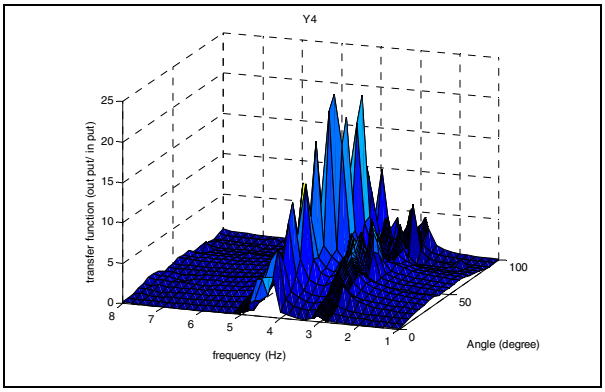

Figure 4. Perpendicular response of the structure at the 4th floor

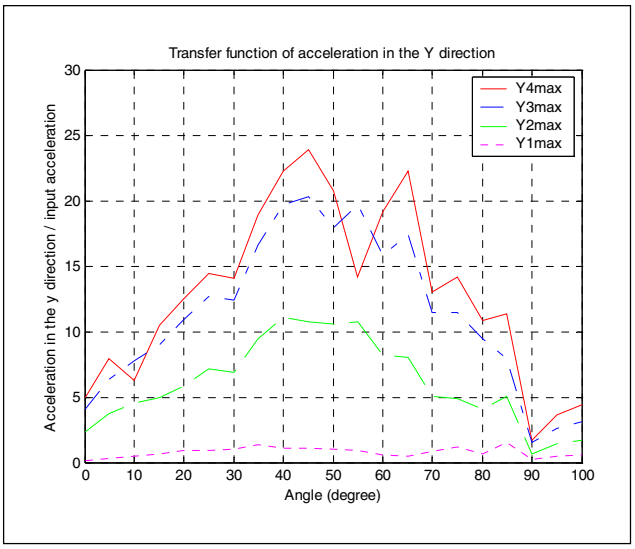

Figure 5. Transfer function of acceleration in the Y direction

Discussion of Results

Based on the results shown in Figure 5, none of the responses in the direction perpendicular to that of the ground excitation reaches zero in the 0º - 100º range considered. This indicates that the structure does not have principal axes under dynamic loads.

Conclusions

Cross effect always exists even if the structure is designed with two axes of geometric symmetry. This leads to the conclusion that principal axes do not exist in MDOF systems. Since results show promising repeatability, they are convincing, and the experiments can be considered valid. Experimental results not only prove the non-existence of principal axes in MDOF systems, but also indicate the amount of structural response amplification at the resonance frequency.

Acknowledgements

This research was carried out under the supervision of Dr. George Lee, and supported in part by the Multidisciplinary Center for Earthquake Engineering Research.

15

MCEER Hospital Demonstration Project

Tsung Yuan "Tony" Yang

Department of Civil, Structural & Environmental Engineering, University of Buffalo

Research Supervisor: Andrew S. Whittaker, Associate Professor

Summary

The MCEER Demonstration Hospital Project is intended to facilitate integration of MCEER research on characterization and retrofit of structural and nonstructural components and systems in mission-critical structures such as hospitals. The baseline hospital was constructed in the mid 1970's and is located in Southern California. This paper presents structural engineering information on three medical facilities: the original facility and two derivative facilities, one representing 1960's West Coast construction and one representing 1970's East Coast construction. Construction data were obtained for the design of the derivative facilities and the three building models were analyzed by nonlinear static analysis.

Introduction

The MCEER Demonstration Hospital Project is intended to facilitate integration of MCEER research on characterization and retrofit of structural and nonstructural components and systems in mission-critical structures such as hospitals. A complete description of this project can be found on the world wide web at *http://civil.eng.buffalo.edu/hospital/*.

The baseline hospital was constructed in the mid 1970's and is located in Southern California. This hospital was most likely designed to meet the seismic requirements of the 1976 Uniform Building Code. The mathematical model of this structure was simplified by assuming a rectangular plan and by replacing the penthouse at the top of the actual facility and the vertical shafts for mechanical and vertical transportation systems by typical floor framing. The resulting building model is termed West Coast 1970's (WC70).

The Uniform Building Code has been used for seismic design in California from the late 1920's until the introduction of the 2000 International Building Code in 2001. The Uniform Building Code was substantially revised in the 1960's, and many of these revisions were proposed by expert earthquake engineers in California. Limits on allowable displacements in buildings were introduced in the 1976 edition. These limits led to substantial increases in the required lateral stiffness of flexible buildings such as steel moment frames. Consequently, the lateral strength of moment-frame buildings increased. As such, the stiffness and strength of 1970's moment-frame construction are significantly greater than those of 1960's construction. In order to contribute to the development of retrofit strategies for structural components and systems typical of weak and flexible buildings similar to those constructed on the West Coast in the early to mid 1960's, a framing system that complies with the gravity-load and seismic requirements of the 1964 Uniform Building Code was developed. This

framing system was designed for the same gravity loads considered in the design of the baseline facility. The resulting model is termed West Coast 1960's (WC60).

Medical facilities on the West Coast have been designed for earthquake effects for more than 60 years. Such effects were not considered in the design of East Coast medical facilities until the 1990's. Consequently, a large number of medical facilities on the East Coast have minimal resistance to earthquake effects. In order to facilitate the preparation of retrofit strategies for a typical (vulnerable) 1970's East Coast medical facility, a second derivative framing system was developed. Structural members of this model were sized according to the requirements of the 1970 Building Code of New York City. Since this code did not include seismic requirements, framing systems complying with the Code were designed for gravity and wind loads only. The framing system developed for this project was designed for the same gravity loads considered for models WC70 and WC60. The resulting model is termed East Coast 1970 (EC70).

Description of the Existing Facility

The existing facility, modified as described in the introduction, is a 4-story steel frame building whose plan dimensions are equal to 275 ft in the east-west direction and 56.5 ft in the north-south direction. The height of the building, from grade level to the roof, is equal to 51 ft. A plan view of the building showing the grid lines in the NS and EW directions can be seen in Figure 1.

The floor framing consists of 5.5" thick concrete slabs on metal decking that span east-west to floor beams. These beams span north-south to steel girders, which in turn span east-west to steel columns. The gravity load resisting columns are supported on piled foundations. The lateral force resisting system consists of four moment-resisting frames in the north-south direction and two perimeter moment-resisting frames in the east-west direction. The three-bay north-south moment frames are located on Lines B, F, J, and N (Figure 1). The east-west moment frames are located on Lines 2 and 5. The moment frames are constructed with ASTM A572 and A588 Grade 50 steel. ASTM A36 steel was used for the remaining steel beams, girders, and columns. The foundation system beneath the moment-frames columns consists of 54" deep grade beams spanning to piles located on Lines 2, 5, B, F, J and N. Piles have a 12"x12" square cross-section and are typically 50 ft long. Piles are embedded 6" at the bottom of the pile cap. Pile caps have typically a 66"x66" square cross-section and are 60" deep. Pile caps are reinforced with bottom rebars only. The typical pile cap reinforcement consists of #10 bars at 12" on center, each way.

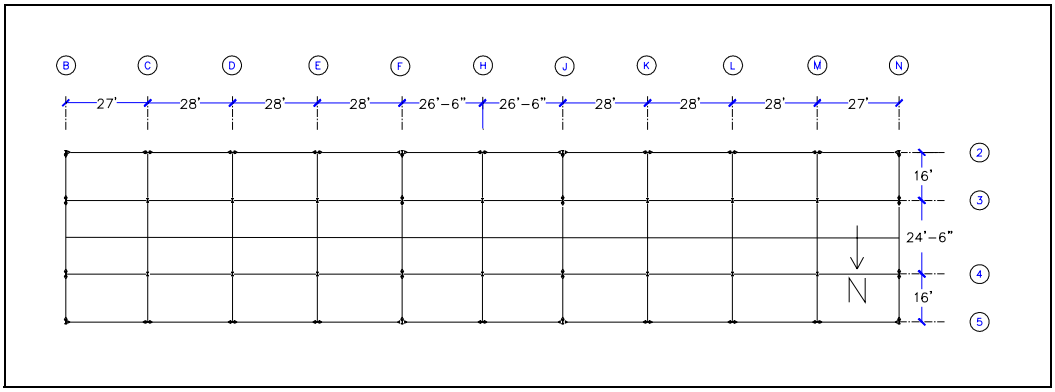

Figure 1. Plan view of the existing facility

Analysis and Design of Building WC70

The computer program SAP 2000 was used to model and analyze the existing facility (WC70). Centerline dimensions were used to define the lengths of the beams and columns; rigid end offsets were not considered. Only frames 2 & 5, B & N and F & J were modeled with rigid beam-column connections. All other beam-column connections were assumed pinned.

Reactive weights were calculated for each floor and story of the building. Calculations were based on a review of architectural and structural drawings of the building. Typical floor and roof loads are equal to 120 psf. The exterior wall was calculated to weigh 17.5 psf. Live loads were assumed equal to 40 psf for the typical floors and 20 psf for the roof. Live load reductions were considered when checking structural members.

Lateral (earthquake) forces were established as follows. The design base shear V was calculated as:

$$V = Z\,I\,K\,C\,S\,W \tag{1}$$

where Z is a seismic zone factor (= 1), I is an importance factor (= 1.5 for a hospital), K is a site base numerical coefficient (= 0.67 for a moment-resisting frame), S is a soil factor (= 1.5 for default soil condition), W is the reactive weight (= 9,800 kips for WC70), and CS_{max} = 0.14. The resulting design base shear (at the allowable stress level) is then equal to 1374 kips in both principal directions. Base shear V was distributed over the height of the building using the following equation from the 1976 Uniform Building Code:

$$F_i = \frac{w_i\,h_i}{\sum_{j=1}^{n} w_j h_j} V \tag{2}$$

where F_i is the design lateral force at level i, w_j is the reactive weight at level j, and h_j is the height of level j above grade.

Components were checked for the following load combinations required by the 1976 Uniform Building Code:

$$D + L \tag{3}$$

$$D + L + E \tag{4}$$

where D, L, and E are dead, live, and earthquake loads, respectively. A one-third increase in allowable stresses was considered when checking components under earthquake effects.

Analysis and Design of Building WC60

The framing system of the 1960's West Coast version of WC70 was established by modifying the size of beams and columns in moment-resisting frames (Lines 2, 5, B, F, J, and N) in such a way that they comply with the minimum requirements of the 1964 Uniform Building Code. New sizes were established in three steps as follows:

1. Beams and columns in moment-resisting frames were sized to resist gravity-load effects only.

2. Lateral (earthquake) loads were calculated per the 1964 UBC and imposed on the building frame.

3. The sizes of the beams and columns in the moment-resisting frames were increased from those calculated in step 1 as required to resist the forces induced by the load combinations of the 1964 UBC.

Lateral (earthquake) forces were established using the 1964 UBC as follows. The design base shear V was calculated as:

$$V = Z\,K\,C\,W = 0.045\,W \tag{5}$$

where Z is a seismic zone factor (= 1.0 for Zone 3 [Los Angeles]), K is a structural system factor (= 0.67 for moment resisting frame), W is the reactive weight (= 9,300 kips for WC60), and $C = 0.05 \,/\sqrt[3]{T} = 0.068$ (T = 0.40 sec) represents the spectral shape. The resulting design base shear (at the allowable stress level) is equal to 423 kips in both principal directions. Base shear V was distributed over the height of the building using Eq. 2, which is also included in the 1964 Uniform Building Code. Components were selected and checked for the load combinations specified in Eqs. 3 and 4, which also apply for the 1964 Uniform Building Code. Again, a one-third increase in allowable stresses was considered when checking components under earthquake effects. Grade A36 steel was assumed for all members of model WC60.

Analysis and Design of Building EC70

The framing system for the 1970's East Coast version of WC70 was established by modifying the size of beams and columns in moment-resisting frames (Lines 2, 5, B, N, F, and J) in such a way that they comply with the minimum requirements of the 1970 Building Code of New York City. New sizes were established in three steps as follows:

1. Beams and columns in moment-resisting frames were sized to resist gravity-load effects only.

2. Lateral (wind) loads were calculated per the 1970 BCNY and imposed on the building frame.

3. The size of beams and columns in moment-resisting frames were increased from those calculated in step 1 as required to resist the forces induced by the load combinations of the 1970 BCNY.

Following the 1970 BCNY, the structural frame was designed for a lateral (horizontal) wind pressure equal to 20 psf on the vertical projected surface. Components were selected and checked for the following load combinations per the requirements of the 1970 Building Code of New York:

$$D + L \tag{6}$$

$$0.75\,(D + L + W) \tag{7}$$

where D, L, and W are dead, live, and wind loads, respectively. Grade A36 steel was assumed for all members in model EC70. Live load reduction was considered for the design of beams and columns under gravity loads.

Summary of Results

Maximum horizontal story drifts (expressed as a decimal fraction of the story height) under the action of code lateral forces are summarized in Table 1. Modal properties of the three mathematical models are summarized in Table 2. Base shear vs. lateral displacement ("pushover") curves obtained from nonlinear static analysis, along with estimates of the lateral strength of the buildings obtained from plastic analysis, are presented in Figure 2.

Table 1. Interstory drifts under lateral loads

Story	WC70	WC60	EC70
1	0.0024 h_1	0.0033 h_1	0.0030 h_1
2	0.0033 h_2	0.0046 h_2	0.0040 h_2
3	0.0031 h_3	0.0049 h_3	0.0065 h_3
4	0.0021 h_4	0.0035 h_4	0.0060 h_4

Table 2. Results of eigenvalue analysis

Building model	Mode	Period	Frequency	Participating mass ratio (EW direction)	Participating mass ratio (NS direction)
WC70	1	0.87 sec	1.15 Hz	82.72%	0.00%
	2	0.82 sec	1.22 Hz	82.72%	82.87%
WC60	1	1.86 sec	0.54 Hz	0.00%	80.43%
	2	1.76 sec	0.57 Hz	83.09%	80.43%
EC70	1	2.50 sec	0.4 Hz	0.00%	81.23%
	3	2.06 sec	0.46 Hz	85.45%	81.23%

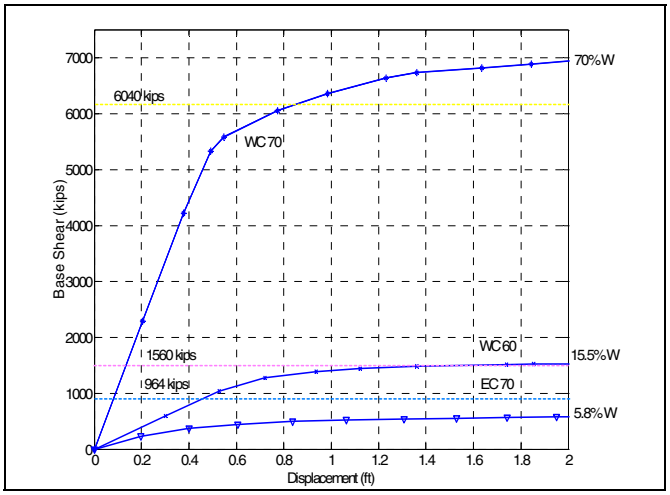

Figure 2. Pushover curves for the three building models

Acknowledgements

This research was carried out under the supervision of Dr. Andrew S. Whittaker, and supported in part by the Multidisciplinary Center for Earthquake Engineering Research. The author thanks Messrs. Tom Hale, S.E., and Chris Tokas, S.E., of the California Office of Statewide Health, Planning, and Design, for providing information on the construction of typical hospital buildings in California in the 1970's. The author also thanks Mr. Ton Wosser, S.E., of Degenkolb Engineers in San Francisco, California, for advice on design and construction practice in California in the 1960's.

16

The Impact of the Y2K Threat on Hospital Emergency Preparedness

Rory Connell

Disaster Research Center, University of Delaware

Research Supervisor: Kathleen Tierney, Director

Summary

The Y2K threat provides an excellent case study of organizational perception of and adjustment to risks. Utilizing qualitative data collected from focus group interviews with thirteen health care organizations, this paper examines hospital risk perception and preparedness for the Y2K computer problem. The potential for a date-specific failure of technological systems required hospitals to identify shortcomings of their emergency preparedness by significantly reassessing contingency plans, critical-care technology, and emergency supplies. The Y2K threat required a multi-departmental focus on emergency preparedness. In addition, many hospitals indicated that emergency plans were coordinated with external organizations, such as other hospitals and vendors. The paper concludes by suggesting implications of the Y2K case study for earthquake and natural hazard preparedness in hospitals. The manner in which hospitals responded to the Y2K problem suggests the potential for these organizations to effectively mitigate against perceived risks.

Introduction

While the potential impact of the Y2K problem on computer systems was a focus for many organizations during the late 1990s, the health care industry was particularly concerned about how the millennium bug could affect organizational functionality. Hospitals were vulnerable to the Y2K threat for two primary reasons. First, the majority of the daily functions of hospitals are intrinsically linked to computer systems, from the health-related services that hospitals provide to the basic operations of facilities. Second, because hospitals serve as key elements of a community's infrastructure, their continued functionality during disasters is an essential component to disaster resistant communities. In times of crisis, hospitals must provide medical service to those that were hospitalized before the disaster event as well as those that need medical attention as a result of the event (Alesch and Petak 2002). Quite often, hospitals are expected to function *more efficiently* in these times of crisis due to the heightened level of importance of hospital services in the disaster period (Whitney et al., 2001, Giacopetti 1999, Howe 1998).

Although the darkest prophecies of the Y2K doomsayers did not materialize, the Y2K threat does provide an excellent case study of organizational perception of and adjustment to risks. Unlike most disaster events, the Y2K problem represented a *time-specific* and *date-certain* event. Because of the hard deadline for systems compliance to the threat, Y2K focused the attention of both organizations and the media. Y2K was also an unprecedented organizational problem due to the potential for *failures in multiple systems*. The worst-case scenario projections for Y2K warned that a disruption to one system could affect countless other systems. Because of their dependence on public infrastructure systems

as well as organizations such as medical insurer payers, banks, and medical suppliers (Goldberg 1997), hospitals were also vulnerable to the malfunctions in external computer systems. Therefore, from an organizational perspective, Y2K could be considered both an internal and an external risk (Goldberg 1997). Finally, the Y2K threat was not limited to a specific geographic area; therefore, the *scope* of the potential impact was significantly larger than most risk events.

This paper will examine hospital risk perception and preparedness for the Y2K computer problem. The paper utilizes data on hospital mitigation collected by the Disaster Research Center (DRC) at the University of Delaware as part of its research on rehabilitation impediments and incentives. In the interviews, the focus groups were asked to relate recent experiences with hazard events and to discuss the impacts those events had on their preparedness and mitigation decision-making, including their decisions with respect to earthquake hazards.

Based on focus group interviews, this paper will identify common themes in the Y2K experiences of hospitals. The paper has three sections. First, it will provide a description of the study and the methodology utilized in the research, as well as a brief description of the study participants. Second, it will discuss three common themes in Y2K experiences of hospitals: (1) that the Y2K threat significantly influenced hospital preparedness; (2) that, unlike some threats, Y2K preparations required participation from entire organizations; and (3) that hospitals often coordinated their emergency plans with other organizations. Third, it will discuss why health care organizations were more likely to adopt mitigation measures for the Y2K problem than for natural hazard threats.

Methodology

Funding for the research was provided by the Multidisciplinary Center for Earthquake Engineering Research (MCEER). Researchers from the DRC (including the author) visited hospitals in three regions of the United States that faced three different levels of seismic risk (Southern California, which has a high level of risk, Tennessee, which has a moderate risk of seismic activity, and the New York metropolitan area, which has a low level of risk). While the research methodology was constructed around the level of seismic risk, the interview guide that was used for the focus groups was developed to address all of the internal and external risks that these organizations may face.

Hospital Selection

The study sample consisted of a total of thirteen hospitals: four California hospitals, five Tennessee hospitals, and four New York hospitals. Several criteria were used to select the study hospitals. First, the hospitals were required to be acute-care facilities with emergency rooms or trauma centers. Second, hospitals in each region were selected based on the size of the hospital organization, as measured by the number of beds. For the purpose of our study, a hospital with less than 150 beds was considered small, a hospital with 151 to 300 beds was considered medium-sized, and a hospital with 301 or more beds was considered a large facility. Third, hospitals with different types of ownership were selected. Study hospitals included public facilities, proprietary (or private) organizations, and nonproprietary (or not-for-profit) organizations. Fourth, while most of the selected hospitals were in a major metropolitan city in each of the three regions, a hospital in a smaller city in the same county was selected for each of the regions. The non-metropolitan facilities were selected in order to study the impact of city safety and building codes on hospital mitigation, as well as the role that hospital networks and associations in the city may play in risk perception and preparedness.

Focus Group Interviews

Once the hospitals were selected, DRC researchers contacted hospital administration in order to organize focus groups with key decision-makers within the hospitals. The focus group interviews included a diverse group of hospital employees. Typical focus groups included at least one representative from each of the following four groups: hospital administration, physicians, nursing, and engineers.

A total of seventy-six subjects participated in the study, representing a diverse range of professions. Typically, the focus group participants were also active members of their hospital's safety committee. As a result, the majority of the focus group participants had been involved in safety issues and emergency preparedness policies in their hospitals.

Hospital Experiences with the Y2K Problem

The media provided extensive coverage of Y2K preparations in hospitals and endless speculation about the possible outcomes of the event. When the transition into the new year occurred without any major incidents, the media provided little to no follow up on the impact of Y2K preparations on hospitals. Views of the Y2K threat in hospitals quickly shifted from a potentially life-threatening problem to the depiction of the Y2K problem as a media fabrication that was characterized more by hype than risk. While the media focus on Y2K quickly tailed off after January 1, 2000, hospitals were significantly altered as a result of their Y2K preparations. As a consequence of Y2K, hospitals revised their contingency plans, established task forces to combat the Y2K problem, replaced non-compliant technology, and increased emergency supplies.

Based on the focus group data, this section will show how Y2K preparations affected hospitals, focusing on: (1) the impact on hospital preparedness for emergency events; (2) the multi-departmental focus on Y2K preparations in hospitals; and (3) hospital emergency coordination with other organizations.

The Impact of Y2K on Emergency Preparedness

Study participants indicated that Y2K required extensive emergency planning. The potential for a date-specific failure of technological systems required hospitals to critically examine the shortcomings of their emergency preparedness by significantly reassessing contingency plans, critical-care technology, and emergency supplies.

Contingency Plans: The majority of the thirteen study hospitals indicated that their existing contingency plans were altered in preparation for Y2K. While hospitals are required by the Joint Commission on Accreditation of Health Care Organizations and other regulatory agencies to plan for disasters (JCAHO 2002), hospitals were not prepared for an emergency event such as Y2K. As a result, the study participants reported developing contingency plans to account for the unique aspects of the Y2K threat. Because hospital facilities are comprised of a diverse group of departments, the failure of one of these systems could impact the functionality of the entire system (Delevett 1999). Several study participants observed that the Y2K threat forced hospitals to consider how a localized systems failure could impact the entire organization. As a participant from a California hospital observed:

> *There are some things out of the box that you have to have up and running from a financial perspective. Then along those lines we determine if the [operating room] is going to be functional, who*

depends on the OR? The orderlies depend on the OR. What do you need to make everything a whole?

The Y2K threat required hospitals to plan for emergencies during periods of low staffing. The fact that the transition into the new year would occur during a holiday night shift indicated that employee resources could be somewhat limited. One hospital representative indicated that these off-hour emergency plans were later enacted during a computer failure on the night shift. The Y2K threat also demonstrated to hospitals their dependency on technology. Hospitals observed that the Y2K threat required their organizations to consider operating without computers. As a hospital representative from Tennessee stated:

I think in that same vein, Y2K probably helped us get better prepared, because we looked at every process that goes on in the hospital, and what will happen to this process, if this one doesn't have power or you know if these computers are not available, how are you going to do this process, so we look at every process and how are you going to do it, all the way down to the utilities and everything. How are you going to process the patients, how are you going to process the papers along with the patients and all that.

While none of the study hospitals experienced Y2K related problems, multiple hospitals reported that the Y2K contingency plans were utilized in other emergency events. The plans were enacted in response to small-magnitude internal emergencies; specifically, a flood, a computer failure, and a disruption in water service. The Safety Officer from a California hospital recalled his organization's experiences utilizing Y2K plans in response to an internal flood:

When we looked specifically at the issues that would arise under Y2K, we identified what we would need. You know, potential for the generator to go down under Y2K and the potential that we needed a back up small generator to back up our emergency room. That is where we purchased all that equipment as part of the Y2K. Just right after that in March when [the flood occurred]…and in turn everybody reacted and we went into the internal disaster [mode] and it was just one thing right after another. It was very smooth and we kept the lab up and running. And we were able to move some of our patients to some of the areas.

The hospitals that utilized their Y2K contingency plans in smaller internal events indicated that the plans improved organizational coordination and employee knowledge about safety. Several study representatives noted that their experiences in responding to these events communicated the ongoing value of the Y2K contingency plans.

One study hospital from California indicated that the hospital was revising its emergency plans in order to meet the standards established by the Y2K preparations. As the Director of Support Services from the hospital observed:

[The Emergency Preparedness Committee is] doing some revisions on our management plans….Part of [the committee was involved in] the Y2K Committee, which was a fairly large body also. They developed some really nice emergency preparedness plans. And with that I think there's some things that we wanted to change and implement all that work that went into the Y2K preparation, implement that into our…grander emergency preparedness plans….They're meeting and revising the management plans.

As this observation indicates, for many of the study hospitals, the contingency plans developed for Y2K were not considered irrelevant following the uneventful transfer into the new year. The Y2K

contingency plans were seen by hospitals as applicable to other emergency events, and, as one hospital noted, served as the benchmark for future emergency planning.

Technological Improvements: The threat of technological failure motivated many health care organizations to update or replace non-compliant computers and equipment. The Y2K threat required hospitals to assess the risks of technological failure in their organizations: including, cataloging computer systems; determining the Y2K compliance of equipment; prioritizing and planning equipment replacement or updates; and performing an impact analyses for mission-critical systems and applications (AAMC 1998). For many hospitals the process of assessing risks in technological systems was complex; for example, representatives from a New York hospital pointed out that computers stored inpatient and outpatient information as well as an automated system to order medication.

According to the study hospitals, the threat of Y2K related systems disruptions resulted in the upgrading of critical equipment. The hospitals listed a number of technological equipment that was either replaced or upgraded in order to meet Y2K compliance, including defibrillators, biomedical equipment, personal computers, and elevators. Indeed, many study hospitals expressed concern about the compliance of defibrillators, the medical units utilized in cases of cardiac arrest.

While the hospitals acknowledged that the Y2K threat improved the quality of many mission-critical systems, the study participants observed that budgeting for technological improvements was restricted. Accordingly, focus groups reported that only a few essential items were replaced or upgraded in the hospitals. In fact, a study hospital from New York indicated that it had rented some equipment such as emergency radios in order to save money.

Essential Supplies: In addition to upgrading equipment to meet compliance with Y2K, hospitals also increased the number of essential supplies in case of an emergency. Study participants observed that certain goods and supplies would be critical in a systems failure, and hospitals cited a number of essential supplies that were stockpiled in preparation for the Y2K threat, including medications, flashlights, batteries, bottled water, and antibacterial hand sanitizer.

The majority of hospitals stated that their organizations stored bottled water for use in the case of failures in the public infrastructure. One study participant from a New York hospital made light of the sizeable reserve of water in his facility, "We have enough bottled water to put out the Chicago fire." Several hospitals indicated that they had not stored bottled water due to internal and external backup sources of water. A few hospitals noted that emergency water could be provided by water towers located on the hospital premises. Representatives from a Tennessee hospital discussed their negotiations with the National Guard for that agency to provide truckloads of water to the facility in the case of Y2K failure.

Because many hospitals increased the supply of non-perishable and general use items, emergency reserves proved to be useful in facility operations following the passing of the Y2K threat. Indeed, many of the items that were stockpiled for Y2K were those that are typically purchased by the hospital. A hospital from New York noted that the increase in essential supplies alleviated the need for the hospital to purchase these supplies for everyday use, thereby making funds available for the next fiscal year. In the hospitals that experienced small internal disasters following Y2K, the reserve of emergency supplies assisted in the organizational responses to these events. Stockpiles of water were utilized in one hospital that experienced a disruption in water services due to an internal

construction accident. As a representative from another hospital that utilized essential supplies in an internal disaster observed, the value of Y2K emergency supplies was demonstrated in that emergency event:

> *Well, I think with the example of the flood, probably two weeks prior to [the internal flood], the answer would have been, 'Yes, we spent too much money.' The day after [the flood], I think the answer would have been we just spent enough. I think we used every bit of supplies.*

Intraorganizational Participation in Y2K Preparedness

Study participants noted that the Y2K problem required a multi-departmental focus in their organizations, and the participation of a diverse collection of individuals, committees, and departments in Y2K preparations. Quite often, hospital safety committees played a central role in developing Y2K emergency procedures, partly due to the pre-existing operational responsibilities of those committees (Brown 1979). However, due to the scope of the threat, the Y2K problem required participation from employees throughout the hospital. Therefore, Y2K was not simply viewed as an information technology problem. Because many hospitals viewed Y2K as a risk management problem rather than strictly a technological problem, the threat was defined as requiring a comprehensive organizational emergency plan (AAMC 1998).

A common theme that was evident in the focus groups was the high level of participation from hospital administrative personnel in Y2K preparations. Some study participants attributed the administrative focus on Y2K to the ambiguous nature of the problem and its potential to cause a significant organizational emergency. A study participant from a California hospital observed that the potential for liability for Y2K damages might have motivated the high level of participation on the part of the administration:

> *I think it has to do with potential. The administration would surely put more money into earthquake preparedness here then maybe a bomb threat or something like that because of the role of responsibility.*

However, a representative from the same California hospital noted that the administration typically participated in emergency planning and safety drills. The administration focus on safety in this hospital may be indicative of a greater focus on risk in California hospitals, due in large part to the region's high seismic risk.

Study participants noted that, in addition to participating in the planning process, hospital administration were an active presence on New Year's Eve. In a hospital from New York, every level of hospital administration was required to report to work on New Year's evening in case Y2K problems materialized. The Vice President of Operations from a Tennessee hospital commented on the importance of administration involvement in Y2K:

> *We were all here 12 [o'clock] on New Years Eve, every manager that works in this facility was not allowed off. So, I mean that said to the folks, when we are in this situation, these are the things you will have to do and are responsible. Each person had stations in the hospital that they were responsible to go to. And, so I mean everybody understood the impact that could happen.*

Interorganizational Preparedness for Y2K

In addition to discussing the intraorganizational focus on Y2K preparations, the hospitals also mentioned the coordination of hospital Y2K plans with other organizations. Hospital emergency planning was defined as dependent upon the level of preparation in the community, other critical care facilities, public infrastructures, and medical supply and equipment vendors. Of particular note were activities that focused on coordination between hospitals and vendors and between individual hospitals and other hospital facilities.

Coordination with Vendors: The hospitals interviewed for the study reported contacting local medical vendors and suppliers in order to determine whether or not technological systems were Y2K compatible. Quite often, the information provided by the vendors served as the foundation for the hospital's assessment of its vulnerability to Y2K. A representative from a Tennessee hospital described this process:

> *We also got a hold of every one of the vendors or everybody we were doing business with to make sure that they were in compliance. And, if not, what their progress was as a timetable in order to convert their systems to be compliant.*

In some instances, the vendors did indicate that equipment was not Y2K compliant, requiring hospitals to purchase new equipment.

Interestingly, one California hospital made arrangements with a vendor to continue receiving essential supplies in the event of Y2K malfunctions. The hospital has decided to continue this arrangement, possibly as a preparedness measure for a seismic event. The hospital's Director of Radiology discussed this process:

> *Purchasing has stuff set up even as far down as housekeeping supplies. You know just plain old toilet paper can get real important when you don't have any in a disaster. Through the Y2K scenario, material purchasing has developed with their key vendors contingency plan that and we have basically orders placed that if you do not hear from us within an allotted time then you are to ship this order.*

Interestingly, the study hospitals did not indicate whether they had tried to determine if vendors were compliant with respect to the Y2K threat. Clearly, a malfunction in a vendor's computer system could have hindered the automatic shipment of supplies to hospitals. Similarly, only one hospital indicated that it had contacted local public utilities about potential disruptions to essential services such as electrical power and water.

Coordination with Other Hospitals: According to focus group interviews, local and state governmental agencies in California and New York attempted to coordinate Y2K preparedness among hospitals. In California, the State Department of Health Services responded to the Y2K threat by organizing the first statewide disaster drills in health care facilities. Representatives from focus groups in California noted that the coordination of emergency drills in all of the state's health care facility was a significant undertaking. As a hospital representative stated:

> *Realize that California is two states without a boundary, Northern California and Southern California. They don't communicate; they're two totally different states. And to have pulled this off really speaks very great volumes of the State Department of Health Services that they were able to do that.*

Following the success of these inaugural statewide drills, the state of California now plans annual disaster drills for the state's hospitals. The focus of the second statewide disaster drill was bioterrorism.

According to the Director of Emergency Services of a New York hospital, the New York City Mayor's Office of Emergency Management was responsible for coordinating the city's hospitals in the event of a Y2K emergency event. The contingency plans stated that the Mayor's Office of Emergency Management was responsible for assessing damages to hospital, coordinating the flow of patients into health care facilities, and communicating with hospitals.

Implication for Earthquake and Natural Hazard Preparedness

According to the focus group interviews, hospital preparations for Y2K resulted in numerous short-term and long-term organizational changes. Clearly, the Y2K threat served to focus hospital attention on mitigating against potential Y2K related risks. The level of Y2K preparedness in the health care industry is notable because natural hazard risk management has typically been a difficult sell for most hospitals. Even in Southern California, where the structural integrity of hospitals has been considerably affected (most significantly in the 1971 San Fernando and 1994 Northridge earthquakes), the adoption of loss reduction measures for natural hazards has met with resistance (Alesch and Petak 2002). In an industry where mergers, acquisitions, and increased competition have highlighted the need for cost reduction, hospitals are less likely to adopt expensive risk management measures (Howe 1998). The organizational resistance to the adoption of loss reduction measures for natural hazards can be effectively understood through Cohen, March, and Olsen's "Garbage Can Model." In this conception, organizational choices are viewed as crowded into a garbage can, where the various problems, solutions, participants, and organizational choice opportunities influence the decision-making process (1972). The garbage can model views choice as embedded in an organizational context of other choices, actors, and relations (March 1978). Clearly, preparation for emergency events must often take a backseat to more urgent financial and organizational issues.

The health care industry's widespread acceptance of Y2K preparation measures raises two important questions. First, what was it that caused hospitals to focus so much on the Y2K threat? Second, why did Y2K have such an impact on hospital operations, when health care organizations continually face natural hazard threats, but do not generally commit significant organizational resources and funds to their mitigation? For example, hospitals in the Central United States prepared for the potential impacts of Y2K; in contrast, hospitals in this region have done little to address seismic risk despite the continual threat of earthquake hazards on the New Madrid fault.

Hospitals throughout the United States devoted significant organizational resources to mitigating the Y2K threat for several key reasons. First, because Y2K was a date certain event, health care organizations were forced to mitigate against its risks in a specified timeframe. In contrast, natural hazard events are difficult to predict, and, as a result, there is rarely a perceived deadline for compliance to mitigation measures. Instead, the mitigation of natural hazard risks is most likely to occur when "windows of opportunity" for policy change present themselves. For example, in the case of earthquake hazard mitigation, the occurrence of high magnitude seismic events facilitates the opening of the windows (Alesch and Petak 1986). Second, Y2K received massive media coverage and scrutiny. The level of media coverage devoted to Y2K is generally not present for natural hazard events. Third, because the Y2K threat had the potential to disrupt the functionality of countless systems, mitigation efforts in health care organization involved the participation of a diverse group

of departments and occupations. In contrast, the responsibility for mitigating natural hazards is typically assigned to disaster coordinators and members of the hospital safety committee. As a result, Y2K was a risk issue that was relevant to entire organizations rather than a specialized department or group of risk decision-makers. Fourth, because existing regulations and codes such as JCAHO safety standards address the mitigation of natural hazards, there is little incentive for organizations to exceed these compliance guidelines. However, the lack of industry-wide guidelines for Y2K compliance required health care organizations to independently assess their vulnerability to the millennium bug. As a result, many hospitals were aware of their vulnerabilities to the Y2K threat and mitigated against these risks. The manner in which hospitals responded to the Y2K problem suggests the potential for these organizations to effectively mitigate against risks. Clearly, if hospitals were inclined to devote the same degree of attention and resources to the natural hazard risks that continually threaten their functionality, these organizations would significantly decrease their risk to seismic events and other hazards.

References

AAMC (1998): Medical schools and teaching hospitals grapple with 'Y2K'. *AAMC Reporter*, http://www.aamc.org/newsroom/reporter/july98/y2k.htm.

Alesch DJ, Petak WJ (1986): *The politics and economics of earthquake hazard mitigation: unreinforced masonry buildings in Southern California*. Institute of Behavioral Science, University of Colorado, Boulder, CO.

Alesch DJ, Petak WJ (2002): *The troubled road from adoption to implementation: hospital seismic retrofit in California*. Presentation given at the MCEER 2002 Annual Meeting, Buffalo, NY.

Brown Jr. BL (1979): *Risk management for hospitals: a practical approach*. Aspen, Germantown, MD.

Cohen MD, March JG, Olsen JP (1972): A garbage can model of organizational choice. *Administrative Science Quarterly*, **17** (1), 1-25.

Delevett P (1999): Rx for Y2K: hospitals spending millions. *Silicon Valley/San Jose Business Journal*, http://sanjose.bizjournals.com/sanjose/stories/1999/02/15/story1.html.

Giacopetti RJ (1999): *Year 2000 implications for Philadelphia hospitals, health systems and provider organizations*. Delaware Valey Healthcare Council, http://www.dvhc.org/rr/Y2K.htm.

Goldberg SH (1997): *Managing 'Year 2000' business and legal risks for hospitals and health care systems*. http://www.comlinks.com/legal/gold1.htm.

Howe A (1998): *Millennium bug puts hospitals in intensive care*. http://www.info-sec.com/y2k/y2k_062698b_j.html-ssi.

JCAHO (2002): *Facts about Patient Safety*. Joint Commission on Accreditation of Healthcare Organizations, http://www.jcaho.org/general+public/patient+safety/index.htm.

March JG (1978): Bounded rationality, ambiguity, and the engineering of choice. *Bell Journal of Economics*, **9** (2), 587-608.

Whitney DJ, Dickerson A, Lindell MK (2001): Nonstructural seismic preparedness of Southern California hospitals. *Earthquake Spectra*, **17** (1), 153-172.

17

Elements of Community Resilience in the World Trade Center Attack

James Kendra and Tricia Wachtendorf

Disaster Research Center, University of Delaware

Principal Investigator: Kathleen Tierney, Director

Summary

In this paper we examine how New York City coped with the destruction of its Emergency Operations Center following the World Trade Center attack and how it reconstituted that center in a new location. We make the observation that, although the physical facility was destroyed, the organization that had been established to manage crises in New York City remained substantially intact, enabling a response that drew on the resources of New York City and neighboring communities, states, and the federal government. A resilient emergency response was achieved through integrating the adaptive capacity of the response organization with the resources of New York City, private entities, and government at all levels. Availability of resources (which fostered redundancy of capability), pre-existing relationships that eased communication challenges as the emergency developed, and the continuation of organizational patterns of response integration and role assignments were among the factors that contributed to resilience following the attack.

Introduction

In this paper, we examine how organizational resilience was reflected in the activities of New York City departments as they responded to the World Trade Center attack in September, 2001 while at the same time losing their primary emergency operations center (EOC) facility at 7 World Trade Center. Our focus lies primarily on the reestablishment of the EOC in the days that followed the attack. Data for this analysis were gathered during exploratory fieldwork commencing within two days of the attack and continuing for two months thereafter, totaling over 750 collective hours of systematic field observations. In particular, we observed key planning meetings at highly secured facilities, including the EOC and incident command posts; we spent extensive periods observing operations at supply and food staging areas, the "Ground Zero" area, family service centers that were established for victims' families, and respite centers that were established for rescue workers. These observations yielded voluminous field notes as well as over 500 photographs. Additionally, we collected reports, schedules, meeting agendas, and maps, and we sketched or collected floor plans of various facilities to track spatial- organizational changes over time. Through these data-gathering efforts we were able to document the evolution of the re-established emergency operations center from very early stages.

The response to the attacks on the Twin Towers necessitated the coordination and interdependency of hundreds of organizations within and outside the City of New York. Our focus of analysis, however, is on the Emergency Operations Center, the facility at which emergency operations are coordinated in disasters of all types. We consider the EOC not only as a physical space but as an

organization that facilitates and oversees the City's multi-organizational disaster response, and that has its own set of protocols, functional responsibilities, and organizational structure. Because the Office of Emergency Management (OEM) permanently staffs the EOC space and plays an instrumental role in its activation, the resilience of the EOC as an organization during an emergency is more tightly coupled to OEM's robustness than it is to other departments within the city. At the same time, the instrumental roles key City departments play in the EOC organization should not be understated. In a later section we distinguish *robustness* and *resilience*.

The Emergency Operations Center

One key function of an emergency operations center is to centralize at one location the personnel and equipment that are needed to manage a response to diverse types of emergencies. The New York City Emergency Operations Center occupied much of the 23rd floor of 7 World Trade Center and boasted an array of technological capabilities. There were computer-equipped workstations for up to 68 agencies, arranged into groups called *pods* (Health & Medical, Utilities, Public Safety, Infrastructure, Human Services, Transportation, Government, and Administration) with an ability to expand by another 40 workstations if the need arose (OEM, 2001). Workstations were equipped with software that made it possible to perform the specialized tasks of the various constituent agencies. The site was equipped with computer messaging systems for communicating among staff, a phone system with provision for microwave back-up, separate systems for Fire, Police, and EMS communications, Coast Guard-operated video monitoring of New York's waterways, and traffic monitoring of the city's streets. In addition, a raised "podium" provided selected staff an overview of the EOC and its operations and allowed for access to a variety of sources of weather information—including direct National Weather Service feeds—video conferencing, and ARCVIEW and MAPINFO GIS packages. Podium staff could also view the location of critical systems and facilities, such as the electric grid, the water system, and hospitals (OEM, 2001).

The Destruction of the Emergency Operations Center

The broad outlines of the events of September 11, 2001 are now widely known, featured as they have been on television and in other media. 7WTC was among the buildings evacuated after the second airplane strike because of the extreme hazard caused by its close proximity to the towers. In addition, early reports of a possible third hijacked aircraft with an unknown destination contributed to the decision to evacuate. The evacuation of the facility was very rapid, and little or no equipment or documentation was saved. 7WTC collapsed in late afternoon on September 11 as a result of fire that had engulfed the structure. Emergency managers, along with the mayor and some agency representatives, kept falling back from the attack area to intermediate sites in order to set up a command post. Before long each of these sites also proved hazardous or otherwise untenable. During the initial period after the attack, the City made use of a mobile emergency operations unit that was able to provide a base for initial reestablishment of the EOC. Preliminary accounts differ regarding the nature of communications difficulties during this early time; most communications were down, but one OEM official has stated that the 800Mhz capability remained and OEM personnel could communicate with other staff. Eventually OEM personnel reached the library of the Police Academy but they soon found its configuration and communications capability to be inadequate. Meanwhile, a parallel operations center was established at a nearby high school to serve as a forward staging area. This was an improvised arrangement, with cafeteria tables being used for meetings, wires running everywhere, and very old telephones. Nevertheless, this site was set up to resemble the spatial organization of the original EOC, with workstations and a command table. During the night of September 13th, approximately 60 hours after the attack, the operations at the

Police Academy moved to a large cruise ship facility at Pier 92 on the Hudson River. This semi-permanent facility still housed the EOC until mid-February 2002, when OEM moved to a facility in Brooklyn.

Resilience in New York City

One key aspect of the response to the September 11 attack is that, although the emergency operations center was destroyed, the emergency management organization was not. Rather, the organization itself exhibited resilient, adaptive behavior. When we arrived at the new EOC, some 96 hours after the attack, we found not a makeshift facility, but a two-city-block long space already half-filled with an expanding number of people, work-tables, copy machines, maps, charts, and over two hundred computers, all networked and functioning—a number which was to grow during the period of our observations. The facility did lack the well-appointed furnishings, lighting, and acoustics of 7WTC and it did bear abundant evidence of its rapid assembly, but it was nevertheless a functioning, continually maturing site for the performance of all necessary emergency management functions.

What occurred in the aftermath of the September 11 attacks can by analyzed using the definitions and dimensions of resilience developed by MCEER researchers. MCEER (Bruneau et al. 2002) defines resilience as "the ability of [a] system to reduce the chances of a shock, to absorb a shock if it occurs (abrupt reduction of performance) and to recover quickly after a shock (re-establish normal performance). Dimensions of resilience include *robustness*, *redundancy*, *resourcefulness*, and *rapidity*.

Robustness is "…the ability of elements, systems, or other units of analysis to withstand a given level of stress or demand without suffering degradation or loss of function" (Bruneau et al. 2002: 6). While the physical structure housing the EOC was not sufficiently robust to survive the September 11th attack, in contrast OEM did exhibit considerable robustness *as an organization*, demonstrating an ability to continue to function even after losing its facility and a great deal of its communications and information technology infrastructure.

Redundancy is "the extent to which elements, systems, or other units of analysis exist that are substitutable, i.e., capable [of] satisfying functional requirements in the event of disruption, degradation, or loss of functionality" (Bruneau et al. 2002: 6). Resourcefulness is the "capacity to identify problems, establish priorities, and mobilize resources when conditions exist that threaten to disrupt some element, system, or other unit of analysis" (Bruneau et al. 2002: 6). Rapidity is the "capacity to meet priorities and achieve goals in a timely manner in order to contain losses and avoid future disruption" (Bruneau et al. 2002: 6). The features of redundancy, resourcefulness and rapidity are well illustrated in the re-establishment of the EOC. In addition the WTC case demonstrates that the qualities of redundancy and resourcefulness are strongly interrelated. Resources, and resourcefulness, can create redundancies that did not exist previously. For example, one of the major concerns with the increasingly intensive use of technology in emergency management is the possibility of over-reliance on those tools, so that if technology fails or is destroyed the response falters. To forestall this possibility, many planners advocate redundancy. In the World Trade Center attack, the EOC was completely destroyed; everything was lost. Emergency managers thus were faced with two requirements: new space, and new tools.

A major impediment in meeting this suddenly emergent need was that there was no pre-established back-up facility at which OEM staff and other responding departments could conduct operations even on an interim basis. Any back-up facility should also have been geographically removed from the primary center. This might have increased the City's resilience, and therefore response capacity,

at least in the short term. Instead, OEM staff had to seek space at several intermediate locations, eventually settling on the Police Academy, where they had to jury-rig telephone lines, for two to three days. Nevertheless, events would later demonstrate that any back-up facility would probably have been inadequate given the wide-ranging demands of this disaster. Improvisation on a large scale would still have been necessary, as was seen at the site that became the EOC for the next five months.

OEM compensated for a lack of robustness and redundancy in physical systems through strategies that not only succeeded in mobilizing resources but also created an alternative physical facility where none had existed before. A pier on the Hudson River, which had been scheduled to be used for a bioterrorism drill on September 12, was leased for long-term usage. OEM staff then arranged for the delivery of hundreds of computers; these were installed and networked within 36 hours, with more arriving thereafter. With space as well as computing and communications equipment, OEM staff were able to establish a functioning replica of the old facility. There was no pre-existing redundancy for the EOC. Rather, with access to resources from within the city and relationships with the private sector, the Office of Emergency Management created redundancy. Obviously, one source of this enormous capacity for resilience inheres in the City itself. New York City alone, even without recourse to external sources of assistance, possesses immense capacity, with emergency services departments equaling the population of a small city, and a resident citizenry possessing every art and talent.

New York was also the focus of an outpouring of support that further enhanced its resilience. Resources of nearly every description arrived, with convergence becoming at times a management problem in itself. This convergence of volunteers and equipment is well documented in reports of other disasters as well (see, for example, Neal (1992, 1994). See Kendra and Wachtendorf (2001) for a discussion of convergence in New York City.). In terms of the community aspect of resilience, New York participated not only in formal mutual aid agreements, but also there was a network of personal contacts between the emergency managers in OEM and their colleagues in other nearby communities. They knew each other and often attended meetings and conferences together, and thus they were able to ask for and give assistance more readily. For example, personnel from nearby Nassau County worked at the logistics station, augmenting the existing staff. Police officers from New York State Police staffed barricades and checkpoints. National Guard personnel and police from well beyond the city's borders—and ultimately from across the country—also arrived to provide help in a similar capacity. The role these assisting officers and military personnel played enabled New York City's officers to work at tasks requiring more local knowledge. Such emergent redundancy was not limited to the police force but also seen in a variety of areas such as logistic offices and fire departments.

Another large source of personnel were the Red Cross volunteers who served hot meals (prepared by a commercial caterer) in the EOC and in respite facilities established close to Ground Zero – at first near forward staging areas in outdoor tents and then later at the Marriot Financial Hotel and St. John's University. In these respite centers established at the latter two facilities were cots, easy chairs, showers, dining halls, televisions, and computers with Internet and email access. They also provided such services as massage therapy and chiropractic care, counseling, and first aid. Urban Search and Rescue teams arrived from across the United States. Nextel supplied thousands of radiotelephones. Other Hudson River piers were pressed into service for Federal Emergency Management Agency (FEMA) office space and the establishment of the Family Service Center, where relatives of victims and survivors displaced from their homes or jobs could find assistance

with the many administrative processes. New York City and Company, the visitors' bureau, helped volunteer and other relief workers find accommodations. Hewlett Packard, ESRI, and professors and graduate students from local colleges were among those who supplied GIS support and equipment. As these examples suggest, a large influx of materials can, at least in some instances, counteract a lack of redundancy.

Mirroring the original EOC, which as indicated earlier was organized by function into working modules called pods, staff established comparable pods at the new EOC. It is important to stress, particularly in terms of the rapidity dimension of resilience, that the improvised EOC that was set up within 48-72 hours of the attack was already twice the size of the original, both in size and in terms of the number of organizations represented and computers involved. Over two hundred fifty computers and a comparable number of organizations were eventually present in the EOC, and some 700 people worked there or passed through during the day. One senior OEM official said, in fact, that the city would have been unable to manage the event entirely from 7WTC even if it hadn't been destroyed.

None of OEM's regular staff was killed, though its members were dispersed and out of regular contact with one another for several hours after the attack. Some were temporarily trapped or missing or had been injured. Nevertheless, OEM was able to preserve its organization, even though it had to reconstitute that organization in an entirely new location. OEM's creativity lay not so much in creating something new, but rather in reproducing what it had lost: the familiar sociotechnical system in which personnel had worked and trained in previously. Physical elements of the EOC, such as the workgroup pods, the podium, the raised platform for the watch officers, were replicated. The ability to re-establish that level of familiarity with respect to physical facilities and arrangements helped to maintain the shared vision that most researchers agree is important to a resilient organization and, in this case, a resilient community. OEM did not merely use what it already knew; it drew upon resources in order to duplicate familiar operational patterns. When existing procedures were destabilized in the face of unexpected catastrophe, OEM created the operational context for maintaining them. This was possible because, through training, frequent drills, and exercises that often involved the mayor, OEM had developed a capacity for adaptive behavior that was not dependent on either specific physical facilities or specific technological systems. As one senior official said, "It [the organization] was in my head." OEM thus created, not a new "shared vision," but the means of preserving the vision that had guided its activities prior to September 11.

Conclusion

Our findings with respect to the response to the World Trade Center attack support conceptions of resilience that are found in the existing literature, but we also find some divergences, especially with regard to the anticipation-resilience dichotomy presented by Wildavsky (1991). Anticipation is the perspective he prefers only for situations in which there is "considerable knowledge" and change is "predictable" (1991: 123). These are the minority of situations. In other situations, he argues, problems are addressed through actions that demonstrate resilience. We argue, however, that resilience and anticipation are not polar opposites or mutually exclusive characteristics or states. Indeed, Wildavsky himself often conflated resilience and anticipation, probably because they are so closely related. Resilience is achieved by preparing, not for a particular event, but rather for the maintenance of a range of capabilities. "The organization was in my head," the statement made by the OEM official, is a key phrase in this respect, because the organizational outline or template "in his head" was a schematic of tasks to be performed and the interorganizational relationships that

would accomplish them. Anticipation lay in the design of an organization that would focus on the dimensions of the response—what, how, where, who—and that would be able to "think" about needs and then fulfill them.

The case of New York demonstrates that, rather than being conceptually distinct, anticipation is an integral dimension of resilience. The distinguishing feature concerns what is to be anticipated. NYC certainly devoted attention to anticipating, and preparing against, a certain range of expected hazards, biological attack among them. Researchers from DRC attended a bio-warfare exercise just a few months prior to the attack and were again scheduled to observe another bio-terrorism exercise on September 12. There is a strong measure of anticipation evident in NYC's resilience: in its previous training and drills, and in the organization itself, which was able to expand dramatically to cope with new demands. Importantly, there were no rigid boundaries that excluded new agencies from participating.

Given the foregoing, we return to what the case of New York City can tell us about resilience or, stated more generally, about socially constituted adaptability to unpredictable ambient forces. Clearly, an organization involved in emergency response wants to maintain the established and known aspects of its operations, such as policies, procedures, practices, or tools. Yet, as illustrated by the World Trade Center attack, such organizational features can fail or prove inadequate to deal with the emerging disaster situation. It is at these times that resilience proves instrumental for bolstering effective response efforts. We see from New York that craftsmanship with respect to problem solving—almost an artisanal quality—allows people to deploy rapidly adaptive strategies. Like any craftsmanship, activities associated with emergency response derive from training, experience, and the ability to become inspired by features in the surrounding environment and to translate those inspirations into creative and innovative actions. Inspiration here is not meant in an ephemeral sense. Instead, it implies that the craftsman has taken note of a feature or features in the surrounding environment, engaged in a cognitive process of interpretation of that feature to produce a vision of a new goal or a previously unthought-of way to achieve an existing goal, and redirected his or her actions. Just as an artist may employ a new tool, new material, or new strategies, so too do decision makers in a resilient organization invoke new tools, materials, and strategies to rebound when established methods fail or when unanticipated circumstances arise. In both cases, training and preparation remain fundamental, but creative thinking, flexibility, and the ability to improvise in newly emergent situations are vital.

Acknowledgements

This research is supported by grants from the Multidisciplinary Center for Earthquake Engineering Research (MCEER), New Technologies in Emergency Management, No. 00-10-81 and Measures of Resilience, No. 99-32-01, and by special supplemental funding provided by the National Science Foundation following the September 11 attacks. An earlier version of this paper was presented at the 48th North American Meetings of the Regional Science Association International. Charleston, SC, USA. November 15-17, 2001. We are grateful to Professor Kathleen Tierney for her comments and suggestions on successive drafts of this paper.

References

Bruneau M, Chang S, Eguchi RT, Lee GC, O'Rourke TD, Reinhorn AM, Shinozuka M, Tierney K, Wallace WA, von Winterfelt D (2002): *A framework to quantitatively assess and enhance seismic resilience of communities*. Multidisciplinary Center for Earthquake Engineering Research, Buffalo, NY.

Kendra J, Wachtendorf T (2001): Rebel food…renegade supplies: convergence after the World Trade Center attack. *Preliminary Paper #316*, Disaster Research Center, University of Delaware, Newark, DE.

Neal DM (1992): *Issues of donations following hurricane Andrew*. International Sociological Association's Disaster Research Meeting.

Neal DM (1994): The consequences of excessive unrequested donations: the case of hurricane Andrew. *Disaster Management*, **6**, 23-28.

OEM (2001): Web page. Content revised or discontinued.

Wildavsky A (1991): *Searching for Safety*. Transaction Publishers, New Brunswick, NJ.

18

Analysis of a Damaged Building near Ground Zero

Jeffrey Berman and Gordon P. Warn

Department of Civil, Structural & Environmental Engineering, University at Buffalo

Research Supervisors: Michel Bruneau, Professor, and Andrew S. Whittaker, Associate Professor

Summary

An NSF-funded MCEER research team visited Ground Zero twice in the two weeks following the attacks of September 11, 2001, to collect perishable data related to the collapse of the two 110 story towers and collateral damage to buildings and infrastructure surrounding the World Trade Center complex. The visit on September 23 involved a walk-through of one high-rise building that was badly damaged by large pieces of debris that were ejected from World Trade Center Tower 2 as it collapsed. This summary report presents information from the subsequent analysis of a building frame with properties similar to those of the damaged building. Linear and nonlinear analyses were undertaken, however, only the linear analyses are presented here. Such analyses shows that the use of rigid beam-to-column connections in the building frame enabled gravity loads in the frame above the segment of the building that partially collapsed to be transferred to adjacent undamaged vertical components.

Introduction

The observation that the subject building did not collapse despite the loss of key structural elements and severe damage (Figure 1) motivated the research team to analyze the building to understand the cause of the observed behavior. Standard tools for linear and nonlinear analysis of buildings subjected to earthquake shaking were employed for these studies. Linear analysis was performed to determine demand to capacity ratios for an undamaged state as well as for three damage states, one of which corresponds to the observed damage. Linear analysis also provided an estimate of the elastic limit of the framing system for each of the damage states considered. Two-dimensional and three-dimensional linear analyses were performed. Small displacement theory was employed for these analyses.

Detailed information on the structural framing system was not available to the research team, although approximate sizes were noted during the building reconnaissance. In order to facilitate linear and nonlinear analysis of the building, sizes of the beams and columns in the moment-resisting frame were estimated by analysis of the building frame for gravity and winds loads as prescribed by the 1970 Building Code of the City of New York (BCCNY 1970). All beam-to-column connections were assumed to be moment resisting. The estimated sizes of the WF beams and columns were checked against the approximate sizes noted during the building reconnaissance. Because no information was available on the steel braced core, sizes were not estimated for the steel braces. Figure 2 shows the resulting section sizes and grid lines on floor 25 just above the damaged section of the building.

Figure 1. Building damage to northern façade and column on line D

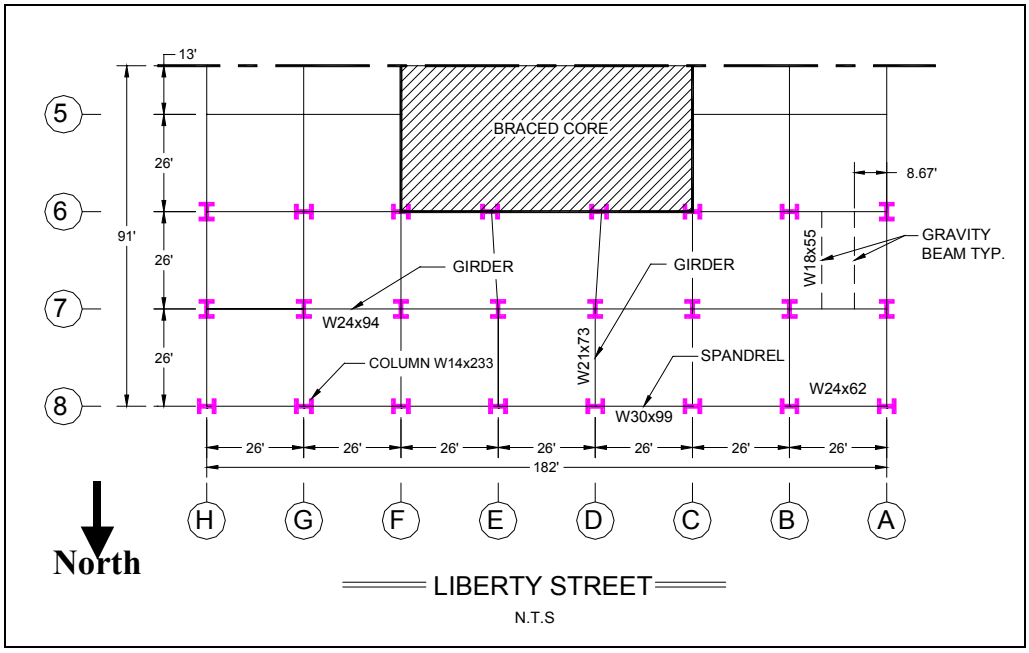

Figure 2. Framing on floor 25 and grid lines

Building Analysis

Two- and three-dimensional finite element models were constructed using SAP2000 (CSI 2000). Firstly, a two-dimensional model (Figure 3a) was prepared considering the structural framing over all 39 stories along Line 8 (Figure 2). This model was constructed to study the response of a single frame with varying degrees of damage (or damage states). Secondly, a three-dimensional model was prepared considering the structural framing over all 39 stories along Lines 6, 7, and 8, including intermediate perpendicular framing. This model was prepared to better understand the response of the building for the observed damage state and to compare the results of two- and three-dimensional analysis.

The analyses presented below considered only gravity loads with dead load and reduced live load equal to 50 psf each. A uniform distributed load of 260 lb/ft per story was assumed to account for the curtain wall loading. Mathematical models were analyzed for the undamaged state, denoted ND, and three damage states, one of which corresponds to the existing damage shown in Figure 1. Each damage state involved the removal of columns on Line 8 from Tenant Level 7 to Tenant Level 25. The three damage states involved the removal of: (1) the column on Line D (the observed damage per Figure 3b); (2) the columns on Lines D and E; and (3) the columns in Lines C, D, and E, denoted DS1, DS2, and DS3 respectively. Maximum member actions under gravity loads were calculated for the undamaged state and the three damage states.

Figures 4 and 5 present some results of the two- and three-dimensional analyses, respectively. Shown in these figures are moments normalized by the yield moment for the assumed beam section sizes at Tenant Level 25 (the floor level immediately above the observed damage). The spandrel beam designation (e.g., DE) refers to the grid lines between which the beam spans (e.g., Lines D and E).

The girder designation (e.g., E87) refers to the grid line along which the girder is aligned (e.g., Line E) and the grid lines between which the girder spans (e.g., Lines 8 and 7). Such normalized moments represent demand-to-capacity (D/C) ratios for these elements, albeit not exactly, because M_y is used in lieu of ϕM_{nx} and each beam is assumed to be fully braced.

Consider first damage state DS1 (the observed damage) and the two-dimensional analysis. All D/C ratios are substantially less than unity. The three-dimensional analysis shows similar results. These results provide an explanation for the observed behavior of the framing along Line 8 following the impact of debris from Tower 2 and the loss of a column on Line D, namely, that the moment-resisting framing above Tenant Level 25 provided an alternate (redundant) path for gravity loads around Line D and to the foundation without distress of the structural framing. As observed from DS1, models with increasing levels of damage (i.e., DS2 and DS3) show that the moment resisting framing above the damage provided an alternate path for gravity loads. However, for DS2 and DS3, Vierendeel truss action become more apparent.

The mathematical models for damage states DS2 and DS3 were prepared to evaluate the robustness of a building frame with characteristics similar to those of 130 Liberty Plaza, where robustness herein is judged by the ability of the framing system to support gravity loads following the loss of multiple perimeter columns. Results of the two-dimensional analysis of the DS2 model show that the frame on Line 8 would have been compromised by the loss of columns on Lines D and E unless the moment-resisting connections were ductile (i.e., they possess some degree of inelastic rotation

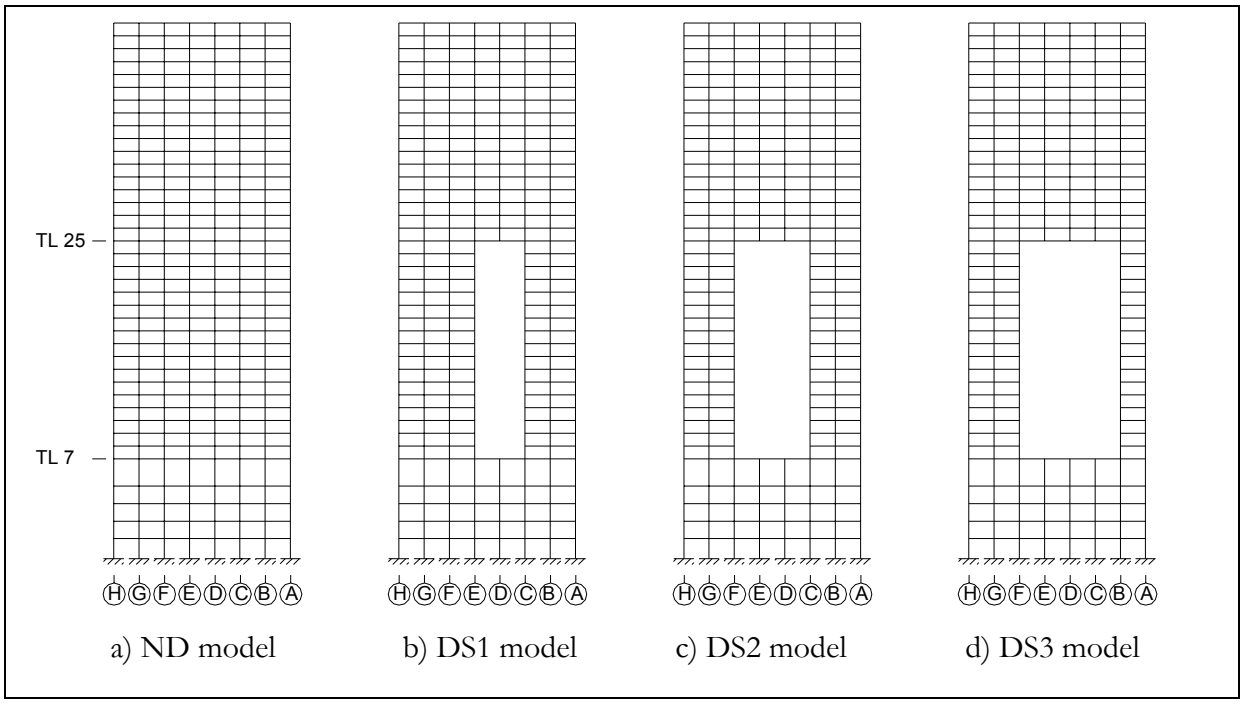

Figure 3. Two dimensional model of framing on line 8

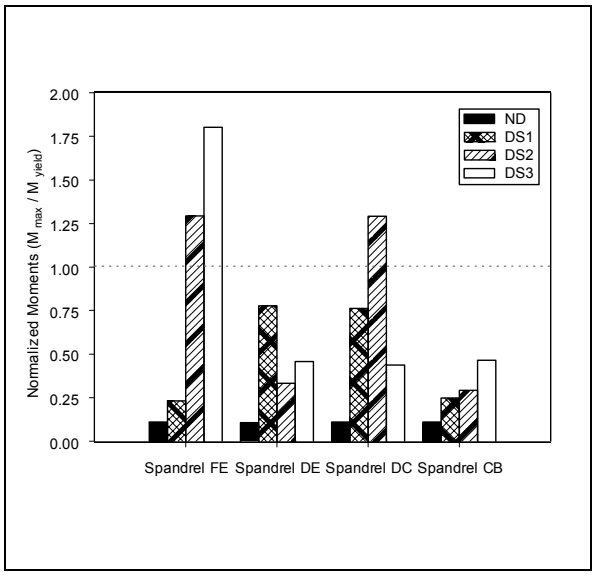

Figure 4. D/C ratios for 2-D analysis

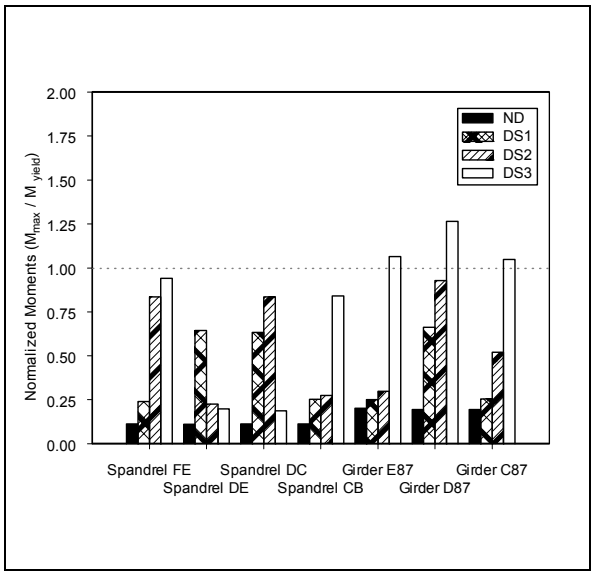

Figure 5. D/C ratios for 3-D analysis

capacity). Review of the three-dimensional analysis results of Figure 5, however, shows that the use of the results of the two-dimensional analysis leads to conservative conclusions and that moment-resisting framing perpendicular to Line 8 also participated in the redistribution of load around the lost columns on Lines D and E. Analyses for both the two- and three-dimensional models of DS3 (the loss of columns on Lines C, D, and E) show modest overloads in both instances. For the three-dimensional analysis, the D/C ratios are greatest in the framing perpendicular to Line 8, namely, Girders C87, D87, and E87.

Demand-to-capacity ratios were calculated for columns on Line 8 between Tenant Levels 24 and 25 (Figure 3) for both two- and three-dimensional analyses. The column designation (e.g., F8) in Figures 6 and 7 refers to the column between Tenant Levels 24 and 25 at the intersection of Lines F and 8. Shown in Figures 6 and 7 are column D/C ratios. These ratios were calculated using the nominal strength equation for members under combined forces included in the 1998 Edition of the AISC Manual of Steel Construction, Load and Resistance Factor Design (AISC 1998). To facilitate calculation of D/C ratios and comparison of analysis results, the value of the effective length factor was assumed equal to 1.0 for all columns. This value is the largest assuming that side-sway is prevented, which is a reasonable assumption for the moment frame when considering the lateral stiffness of the braced core (significantly greater than that of the moment frame) and the presence of rigid floor diaphragms.

Results of the two-dimensional analysis shown in Figure 6 indicate D/C ratios less than unity for the undamaged state ND and the damage states DS1 and DS2. For damage state DS3, the D/C ratios for columns F8 and B8 exceed unity. Ratios greater than unity can be attributed to an increase in both axial forces and moments due to the removal of columns C8, D8 and E8. This observed increase in bending moment for the two-dimensional analyses ranged from essentially zero for ND to approximately 0.25 M_p (plastic moment of section) for DS3. Noting that the span between adjacent columns for DS3 is four times the span in the undamaged state ND, an increase in moment demand is expected. The D/C ratios for the three-dimensional model (Figure 7) are less than unity for ND and DS1, DS2, and DS3. Again, results of the three-dimensional analysis indicate that the use of two-dimensional analysis leads to conservative conclusions and that the presence of perpendicular framing provides additional redundancy and capability for gravity loads to be redistributed to adjacent framing.

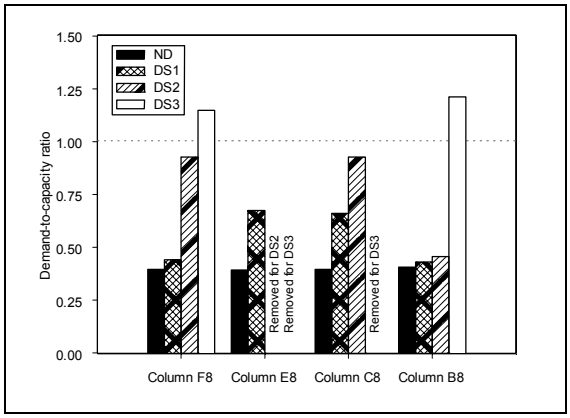

Figure 6. D/C ratios for 2-D analysis

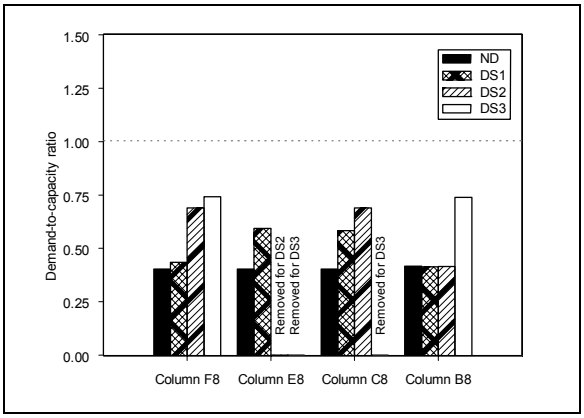

Figure 7. D/C ratios for 3-D analysis

Conclusions

The 130 Liberty Plaza building sustained severe damage from falling debris during the collapse of the World Trade Center Tower 2. Reconnaissance efforts on September 21 and 23, 2001, documented the exterior and interior damage to the building. Despite the loss of a perimeter column over a 17-story height, the building did not collapse because the lateral and gravity load resisting systems were highly redundant. The redundant structural systems permitted gravity loads to be redistributed around the badly damaged region, an observation supported by preliminary elastic and plastic analyses of a building frame with characteristics similar to those of the damaged building. Key observations from the work to date include:

1. Highly redundant gravity and lateral-force resisting systems are key to the construction of damage tolerant buildings.

2. The use of ductile details (ability to deform well into the inelastic range) improves the damage tolerance of buildings.

3. Simple framing systems such as unreinforced slabs on metal decking can span substantially further than what is assumed in design and such capabilities should be included in the evaluation of buildings for damage tolerance. Addition of inexpensive details (such as continuous slab reinforcement and continuity in the metal decking) further enhances building performance and prevents partial collapses.

4. Simple two- and three-dimensional analysis tools such as those adopted for the work presented in this summary report can be used to judge, in a preliminary sense, the damage tolerance of buildings.

For a more complete report of the reconnaissance and analysis of this building, the reader is referred to Berman et al., (2002).

Acknowledgements

The authors wish to acknowledge the substantial technical contributions of the expert structural engineering staff at LZA Technology of New York, a division of the Thornton/Tomasetti Group. Special thanks are due to Mr. Edward Sweirtz (Associate Partner, Chicago), Mr. Daniel Cuoco (Managing Principal, New York), and Mr. Emmanuel Velivasakis (Managing Principal, New York).

This work was supported in whole by the Multidisciplinary Center for Earthquake Engineering Research and was carried out under the supervision of Professors M. Bruneau and A. Whittaker.

References

AISC (1998): *Manual of steel construction – Load and resistance factor design*. American Institute of Steel Construction, Chicago, IL.

Berman J, Warn GP, Whittaker AS, Bruneau M (2002): Reconnaissance and Preliminary Assessment of a Damaged Building Near Ground Zero. *Report MCEER-02-SP03*, Multidisciplinary Center for Earthquake Engineering Research, Buffalo, NY.

BCCNY (1970): *Building Code of the City of New York*. Van Nostrand Reinhold Company, New York, NY.

CSI (2000): *SAP2000 - Integrated Finite Element Analysis and Design of Structures (Version 7.4*). Computers and Structures, Inc, Berkeley, CA.

Kim T, Whittaker AS, Gilani ASJ, Bertero VV, Takhirov SM, Shakhzod M (2000): Cover-plate and flange-plate reinforced steel moment connections. *Report PEER-2000/07*, Pacific Earthquake Engineering Research Center, Richmond, CA.

19

Frictional Properties of Non-Metallic Materials for Use in Sliding Bearings: An Experimental Study

Daniel Fenz

Department of Civil, Structural & Environmental Engineering, University at Buffalo

Research Supervisor: Michael C. Constantinou, Professor and Chairman

Summary

The purpose of this study is to investigate the frictional properties of several low-friction, non-metallic materials in contact with stainless steel in order to determine their usefulness for base isolation systems. In addition, modifications made to the lateral bracing of the existing isolation testing machine constructed in 1999 at the University at Buffalo's Structural Engineering and Earthquake Simulation Laboratory are discussed as well. Several tests were performed using the improved isolation testing machine to measure dynamic coefficients of friction and their relationships with sliding velocity and normal pressure. Results will be used to evaluate the potential of the materials for use in seismic applications, where low friction and acceptable wear characteristics are desirable.

Introduction

Sliding bearings with a restoring force element are a very useful type of isolation hardware. During earthquakes, they transmit shear force from the ground to the structure above up to the point at which sliding initiates. After this point, the force transmitted depends on the dynamic coefficient of friction of the sliding interface, not on the magnitude of the earthquake itself. This is a very attractive property, as it allows structures to be designed independently of the seismicity of the area. By lowering the friction of the sliding interface, forces transmitted to the structure are lowered as well.

In this study, friction in Axon bearings was tested. Small scale Axon bearings, previously used in the shaking table tests performed by Wolff (2001), consist of a flat sliding interface and a urethane ring to provide damping and restoring force. Past studies of the sliding interface have focused on the use of high friction materials in hopes of providing increased energy dissipation. Instead, this study concentrates on low friction materials, which provide a greater reduction of transmitted forces.

Behavior of PTFE in Contact with Stainless Steel

The most common interface in sliding bearings consists of sheet-type PTFE (Teflon^{TM}) in contact with polished stainless steel. Constantinou et al., (1987) and Mokha et al., (1988) were among the first to report extensively on the behavior of the PTFE – stainless steel interface under dynamic conditions. They determined that the sliding velocity and normal pressure are the two key parameters affecting friction at the sliding interface. Their major conclusions, summarized in Figures 1 and 2, are the following:

1. Friction increases with increasing sliding velocity up to a certain point after which it remains constant. The point at which friction plateaus is dependent on the normal pressure.

2. Friction decreases with increasing normal pressure.

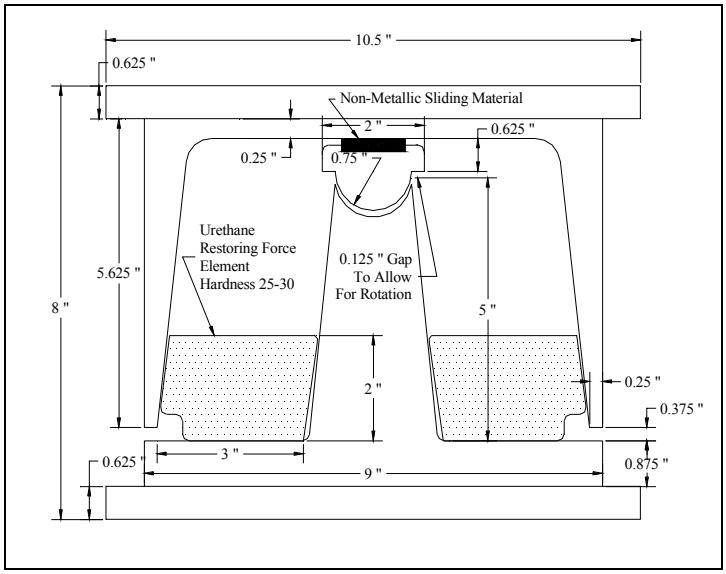

Figure 1. The small scale Axon sliding bearing

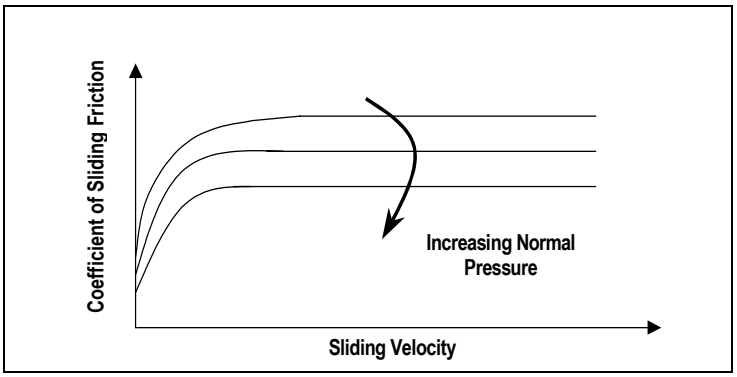

Figure 2. Dependence of friction at the PTFE stainless steel interface on sliding velocity and normal load.

Test Apparatus

The original configuration of the isolator testing machine is shown in Figure 3. The key components are the horizontal actuator (used to impose a predefined displacement history), the two vertical actuators (used to apply normal loads) and the reaction load cell (which measures shear and normal forces at the bearing). The original lateral bracing scheme, also shown in Figure 3, consisted of two sleeved threaded rods attached only at the top flange of the loading beam. They were connected to a weak steel frame made of Uni-Struts.

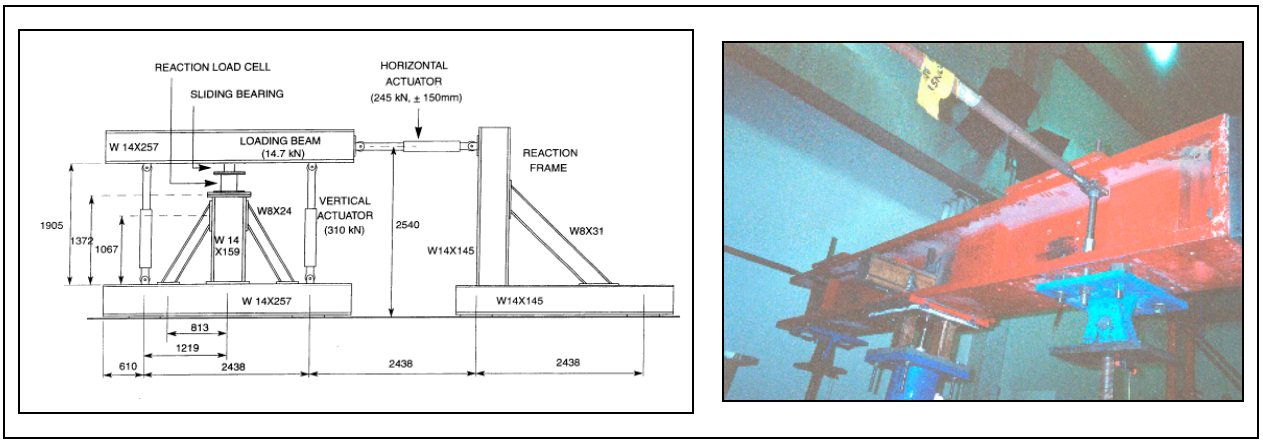

Figure 3. Schematic of the original configuration of the isolator testing machine (all dimensions in mm) and a photograph of the original lateral bracing configuration. Note the connection only at the top flange of the loading beam.

Due to a combination of factors, namely the eccentricity and small point of application of the bearing's reaction force as well as the low friction of the sliding interface, the original lateral bracing proved insufficient to prevent rotation of the loading beam. Since the force that could be exerted by the bracing was limited by the friction at the sliding interface, the reaction couple was insufficient and resulted in a near disastrous rotation of the beam. This is shown in the free body diagram in Figure 4.

Consequently, a new lateral bracing configuration was developed with emphasis on preventing rotation of the loading beam. The new system had to be able to permit horizontal and vertical displacements of the loading beam in addition to being rotationally adjustable. Furthermore, the new system could not interfere with existing components in a manner that would constrain the apparatus' performance. For example, it was necessary to maintain the proper clearance around the vertical actuators needed for the loading beam's maximum 6" displacement.

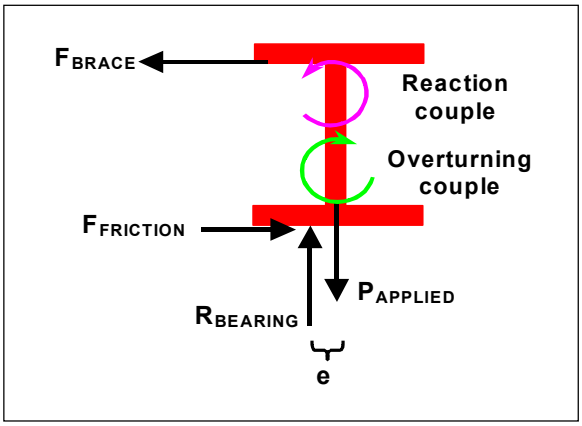

Figure 4. Free body diagram demonstrating how the small frictional force of the sliding interface limited the reaction couple and led to rotation of the loading beam

In the new scheme, shown in Figure 5, bracing is provided at eight points by spherical rollers mounted at the top and bottom flanges on opposing sides of the loading beam. This configuration prevents rotation and transverse movement while providing minimal opposition to vertical and horizontal displacements during testing. In addition, the rotational capability of the loading beam is still maintained by mounting the rollers on adjustable threaded rods. The bracing's supporting structure consists of two stiff U-shaped frames. Vertical members are 6"x4"x3/16" steel tubing oriented along the strong axis in the transverse direction. These are welded to a 4"x4"x1/2" bottom cross member and the entire frame is bolted to the existing bottom support beam. Furthermore, a length of 1' square tubing is welded at mid-height to provide further stiffening. The system is prestressed with Dywidag bars against the strong floor to prevent rigid body rotation.

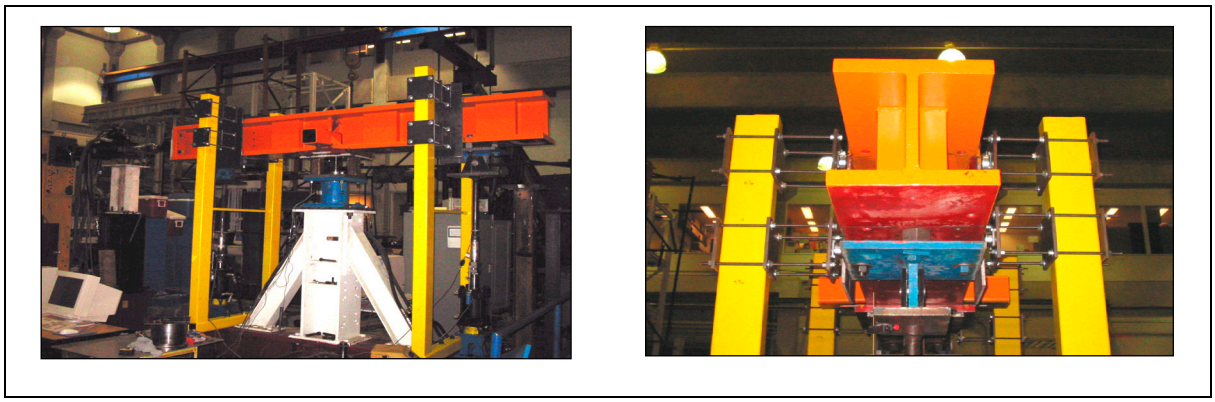

Figure 5. Photographs of the improved lateral bracing scheme

Test Specimens

In all, thirteen different specimens having a wide range of commercially available low friction materials were tested. However, the experiments focused on woven PTFE (Teflon™) composites and self-lubricating cast nylon specimens (see Figure 6). PTFE composites are manufactured by weaving PTFE fibers together with other strengthening fibers and by embedding the resulting fabric in an epoxy resin matrix. Three different strengthening fibers were tested: glass, polyester and Nomex, a very strong heat-resistant material. Self-lubricated cast nylon specimens have liquid or a combination of liquid and solid lubricants embedded during the manufacturing process.

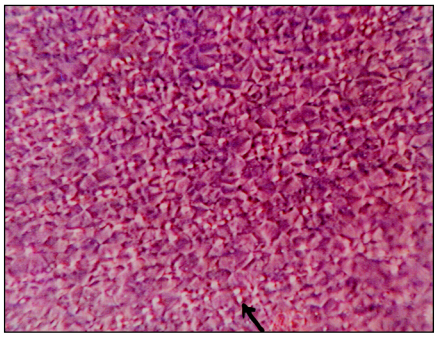

Figure 6. A microscopic view of self-lubricated cast nylon. The highlighted circles are internally embedded lubricant. (Courtesy Nylacast Ltd.)

Testing Procedure

Several tests were required to completely capture each material's behavior regarding the dependence of friction on sliding velocity and normal load. Twelve tests were performed on each specimen, and the sliding coefficient of friction was measured at four velocities for each of three levels of normal load (Table 1). The interface was cleaned with a dry rag after every four tests to prevent any wear debris from affecting the test results. Normal pressures were chosen to be representative of the service loads that the bearing may be subjected to and sliding velocities were chosen over a broad range to completely capture the material's behavior. Sliding velocities were based on a sinusoidal displacement history of 1" amplitude and varying frequency. In addition, each specimen's thickness was also measured prior to and upon completion of testing. This gave information on the wear characteristics of the material in order to evaluate its suitability for various seismic applications. Data analysis entailed plotting normalized friction force (i.e., the coefficient of friction) vs. displacement loops and then extracting the dynamic coefficient of friction. Plots showing the sliding (dynamic) coefficient of friction vs. sliding velocity were then made.

Experimental Results

The frictional behavior of woven PTFE in contact with polished stainless steel is similar to the behavior of plain sheet-type Teflon. Tests show that the coefficient of friction initially increases with increasing sliding velocity and decreases with increasing normal pressure, as shown in Figure 2. Mokha et al., (1988) have shown that friction becomes independent of the sliding velocity above a certain "threshold" velocity. This study found that no such plateau exists for woven PTFE composites. Instead, friction actually decreases at higher sliding velocities. This is attributed to frictional heating, which led to a deposition of PTFE film on the stainless steel plate. In essence, the frictional interface consists of PTFE sliding over PTFE at this point, which results in lower friction.

Table 1. Summary of tests performed on each specimen.

Normal load [kips]	Pressure [psi]	Amplitude [in]	Frequency [Hz]	Peak velocity [in/sec]	Number of Cycles
4.42	2,500	1.0	0.01	0.06	1.5
			0.20	1.25	3.0
			1.00	6.28	3.0
			2.00	18.85	3.0
8.84	5,000	1.0	0.01	0.06	1.5
			0.20	1.25	3.0
			1.00	6.28	3.0
			2.00	18.85	3.0
17.68	10,000	1.0	0.01	0.06	1.5
			0.20	1.25	3.0
			1.00	6.28	3.0
			2.00	18.85	3.0

Not surprisingly, the use of different strengthening fibers does affect the frictional properties of the composite. The results of testing the woven PTFE composites (see Figure 7) are the following:

1. Qualitatively, polyester and glass composites behave similarly. Their behavior is characterized by an increase in friction with increasing sliding velocity and by a slight

decrease at higher sliding velocities. In the case of the Nomex composite, friction increases slightly with increasing velocity and then levels out at higher sliding velocity. Friction decreases with increasing pressure for all fibers.

2. Friction in the polyester composite was slightly less than that in the glass composite. Wear however, was significantly greater in the polyester. The Nomex composite exhibits the highest friction coupled with less wear than those for glass and polyester composites from the same manufacturer.

3. Woven PTFE/glass composites from different manufacturers exhibited essentially the same frictional behavior with respect to dependence on sliding velocity and normal pressure. However, the sample from one manufacturer had only a 10% reduction in thickness contrasted to a 35% reduction in wear for the other manufacturer's sample.

Frictional behavior of cast nylon specimens (see figure 8) is markedly different from that of woven PTFE. These specimens show a very small dependence of friction on sliding velocity. The gap between the minimum and maximum values of friction is much smaller than that in woven PTFE samples. In addition, friction varied much more in cast nylon specimens as the normal load increased. At lower pressure, friction in cast nylon is comparable to that in woven PTFE. At higher pressures, however, cast nylon demonstrates much lower friction than woven PTFE.

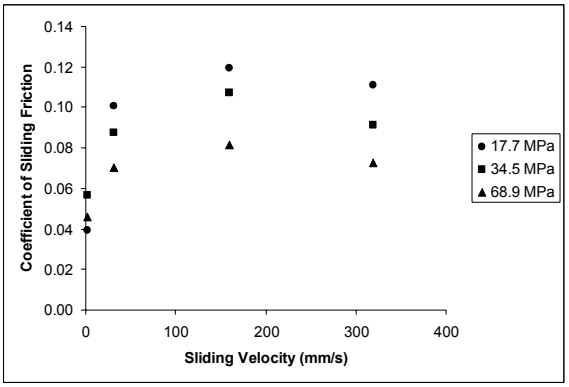

Figure 7. Typical behavior of a woven PTFE composite material (PTFE/glass/phenolic)

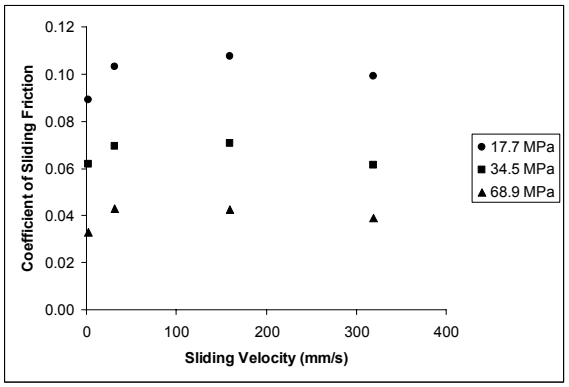

Figure 8. Typical behavior of a cast nylon material

References

Constantinou MC, Caccese J, Harris HG (1987): Frictional characteristics of teflon-steel interfaces under dynamic conditions. *Earthquake Engineering and Structural Dynamics*, **15** (6), 751-759.

Mokha A, Constantinou MC, Reinhorn AM (1988): Teflon bearings in aseismic base isolation: experimental studies and mathematical modeling. *Technical Report NCEER-88-0038*, Multidisciplinary Center for Earthquake Engineering Research, Buffalo, NY.

Wolff ED (2001): Large scale experimental study of the Axon seismic isolation system. *Ph.D. Dissertation (draft)*, Department of Civil, Structural & Environmental Engineering, University at Buffalo, Buffalo, NY.

20

Damping of Frame Structures: An Educational Shake Table Test

Nishadi Karunarathne

Department of Civil Engineering, Catholic University of America

Research Supervisor: Andrei M. Reinhorn, Clifford C. Furnas Professor, University at Buffalo

Summary

This paper describes an experimental study on the effects of viscous damping walls on structures. The experimental tests were performed using an instructional shake table developed by the University Consortium on Instructional Shake Tables (UCIST). A simple model of a viscous wall, created using a Plexiglas container and a steel blade, was attached to a building model. The container was filled with different liquids and the structure-wall system was subjected to free-vibration excitation. In order to increase the damping provided by the wall, fins were added at the bottom of the steel blade. The damping coefficient, the logarithmic decrement and the structural period of the building-wall model were obtained for the original and the modified wall (i.e., before and after adding the fins) and for the different viscous fluids used to fill the wall container. Results indicate that a fluid with higher viscosity and a smaller gap between the container and the blade increase the effectiveness of the viscous wall to dissipate energy.

Introduction

Although nothing can be done to prevent earthquakes, precautions can be taken to mitigate their destructive effects. In order to reduce damage caused by seismic events, civil engineers incorporate a variety of technologies into structures. Many techniques can be used either individually or in combination to reduce external forces and to control deformations caused by earthquakes.

An available seismic protection method consists of incorporating any of several types of energy dissipation devices. Friction dampers have moving parts that slide over each other to create friction, which is used to dissipate the seismic energy (Li and Reinhorn 1995). Metallic dampers dissipate energy through plastic deformation of metal elements (MCEER Information Service 2001). Viscous dampers are hydraulic devices that dissipate energy when a fluid is forced to pass through an orifice (Constantinou 1994).

Damping is the process by which vibration steadily decreases its amplitude (Chopra 1995). It occurs when the kinetic and strain energy of the vibrating system are dissipated by various mechanisms such as heat and friction. Figure 1 displays the displacement response of undamped and damped structures. The undamped structure keeps oscillating forever with the same amplitude and period, while the vibration amplitude of the damped structure gradually decays with time. The motion of most freely oscillating systems eventually dies out and reduces to zero with time. Free vibration occurs when a structure is disturbed from its static equilibrium and is then allowed to vibrate without the interference of external forces (Chopra 1995).

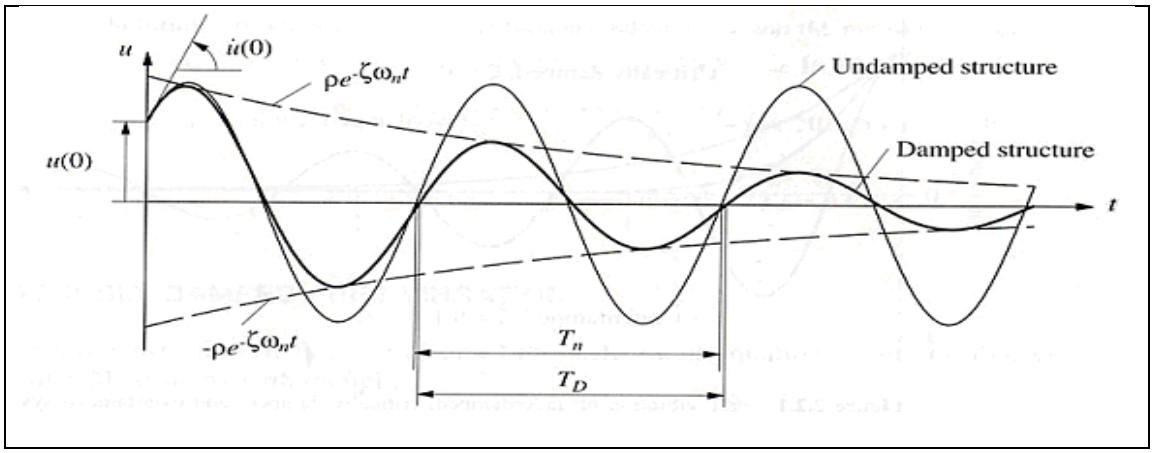

Figure 1. Effects of damping on free vibration (Chopra 1995)

Also illustrated in Figure 1 are the so-called envelope curves (dotted lines). They touch the displacement-time curve at points slightly to the right of its peak values (Chopra 1995). The equation $\pm \rho e^{-\zeta \omega_n t}$ denotes the decay for the envelope curves. The natural period T of the system can be determined from the displacement-time plot by measuring the time required to complete one cycle of vibration.

The rate at which the motion decays in free vibration is controlled by the damping ratio ζ, which is a dimensionless measure of damping expressed as a percentage of the critical damping. Figure 2 displays the free-vibration response of several systems with varying levels of damping ratios. It can be observed that the amplitude of the vibration decays more rapidly as the value of the damping ratio increases.

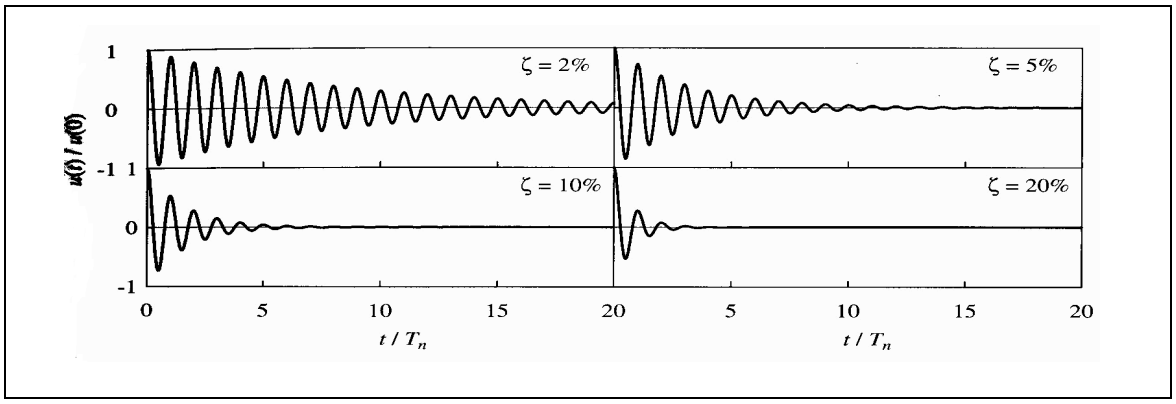

Figure 2. Free vibration of systems with different levels of damping (Chopra 1995)

The logarithmic decrement δ is a measure of the mechanical damping (Chopra 1995). It is calculated from the natural logarithm of the ratio of the amplitudes of any two oscillations (u_i and u_{i+j}) and is directly correlated to the damping ratio:

$$\delta = \ln \frac{u_i}{u_{i+j}} = 2\,\pi\,\zeta \qquad (1)$$

Background

The research project described in this paper is based on previous studies by Reinhorn and Li (1995), who conducted extensive research on the effect of viscous damping walls on structures. A concrete structural model 1:3 in length scale with different damping devices (fluid viscous, friction and viscous wall dampers) was tested in a shake table. Results (Table 1) indicated that dampers have the potential to significantly diminish inelastic deformation demands and damage to the structure. The damping ratio of the bare structure was less than 10%. It increased to 20%-30% with the addition of fluid or friction dampers and to nearly 50% when the viscous damping walls were added. Viscous walls were by far the most effective damper tested, which indicate the great potential of this kind of dampers to reduce structural damage during earthquakes.

Table 1. Dynamic characteristics of the structure (Reinhorn and Li 1995)

Ground motion	PGA	Damping (% of critical)			Fundamental period	
	[g]	Low amplitude testing	Strong motion testing	Approximated analytically	Low amplitude testing	Strong motion testing
Without dampers						
El Centro S00E	0.30	3	6	6	0.62 sec	0.76 sec
Taft N21E	0.20	3	5	5	0.62 sec	0.76 sec
With fluid dampers (Taylor)						
El Centro S00E	0.30	16	28	26	0.53 sec	0.62 sec
Taft N21E	0.20	16	26	25	0.50 sec	0.55 sec
With friction dampers (Sumitono)						
El Centro S00E	0.30	7	23	28	0.31 sec	0.42 sec
Taft N21E	0.20	7	26	22	0.31 sec	0.50 sec
With viscous damping walls						
El Centro S00E	0.30	50	46	44	0.25 sec	0.27 sec
Taft N21E	0.20	49	47	44	0.25 sec	0.27 sec

Testing

As illustrated in Figure 3, a viscous wall consists of a plate floating in a thin container filled with a highly viscous fluid. Damping provided by viscous walls protects the structure from seismic events as well as from other natural occurrences such as winds and heat.

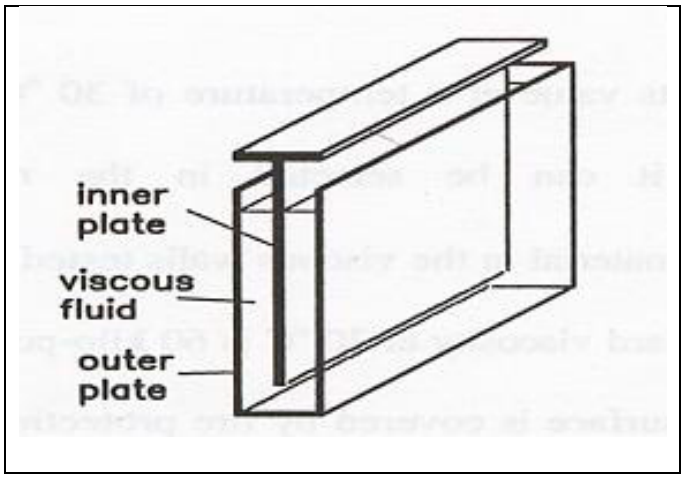

Figure 3. Viscous wall (Reinhorn and Li 1995)

An experiment on viscous damping was designed and implemented using an instructional shake table developed by the University Consortium on Instructional Shake Tables (UCIST), which is intended to introduce structural dynamics and earthquake engineering to undergraduate students. The shake table "package" includes a power module to drive the shake table, a data acquisition board to collect data and drive the power amplifier, a portable pendant capable of generating pre-programmed earthquakes, a 2-story test building, three accelerometers (one for the shake table and one on each floor of the structure) and a Pentium-class computer. WinCon realtime software, along with computer programs MATLAB and SIMULINK, controls the shake table. Figure 4 contains pictures of the shake table hardware.

A container was constructed with Plexiglas and bolted to the shake table. The dimensions of the contained were 4.25" wide, 11.5" long and 8" high. In order to emulate a 1-story viscous wall, the first floor of the test structure and its accelerometer were removed and then a steel plate was hung from the top floor and inserted into the container. An approximately 1" gap was provided between the edge of the steel plate and the bottom of the container. An accelerometer was attached to the steel plate at the top of the structure. The test setup is illustrated in Figure 5.

The container was filled with several viscous fluids in order to test the corresponding damping effects. Water, soap water, oil and detergent were used. Free vibrations were induced by tapping the structure at the top. The structure was then allowed to vibrate freely until motion stopped. The data was collected using Wincon software and analyzed using MATLAB.

Viscous resistance is the resulting force of the viscous fluid in the container against the moving steel plate (Reinhorn and Li 1995). The frictional force resists the movement of the steel plate in the fluid. The smaller the gap between the plate and the wall, the higher the resistance provided by the fluid. This concept (illustrated in Figures 6 and 7) led to make some modifications in the initial test structure. In order to obtain a larger damping ratio, the container must be slimmer or the plate wider. To resolve the conflict, two U-shaped metal fins (Figure 8) were added at each side of the steel plate and bolted to the bottom portion of the steel plate.

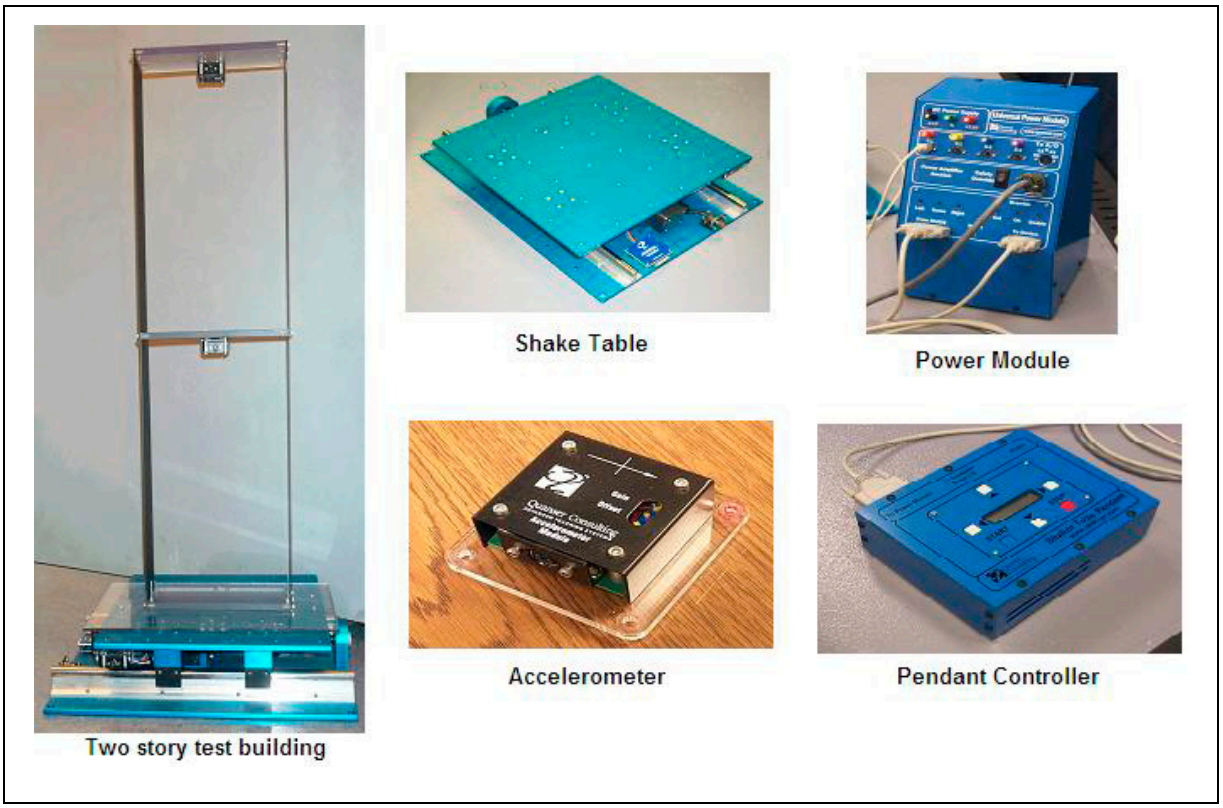

Figure 4. The instructional shake table (UCIST)

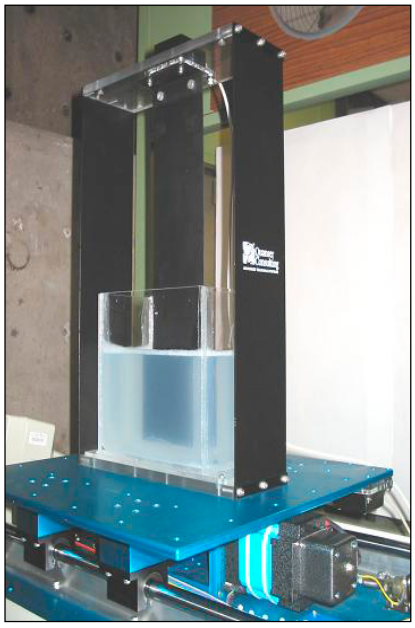

Figure 5. Test setup: A simplified model of a viscous wall

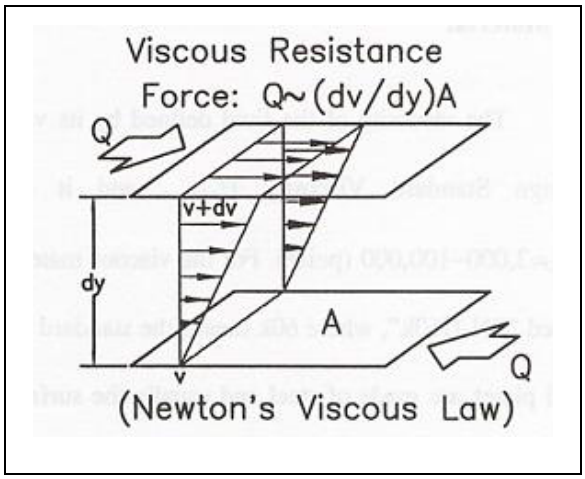

Figure 6. Viscous resistance

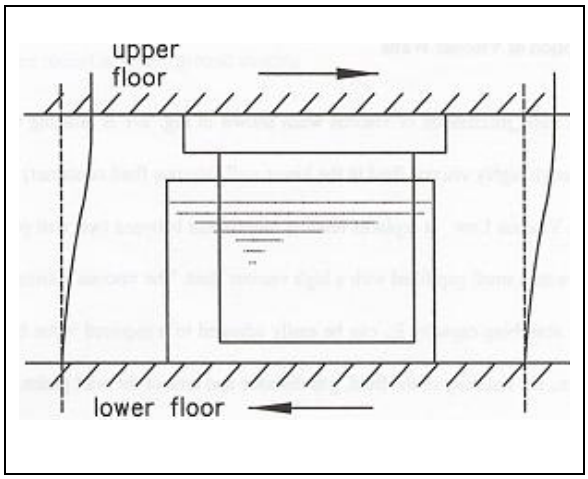

Figure 7. Viscous wall

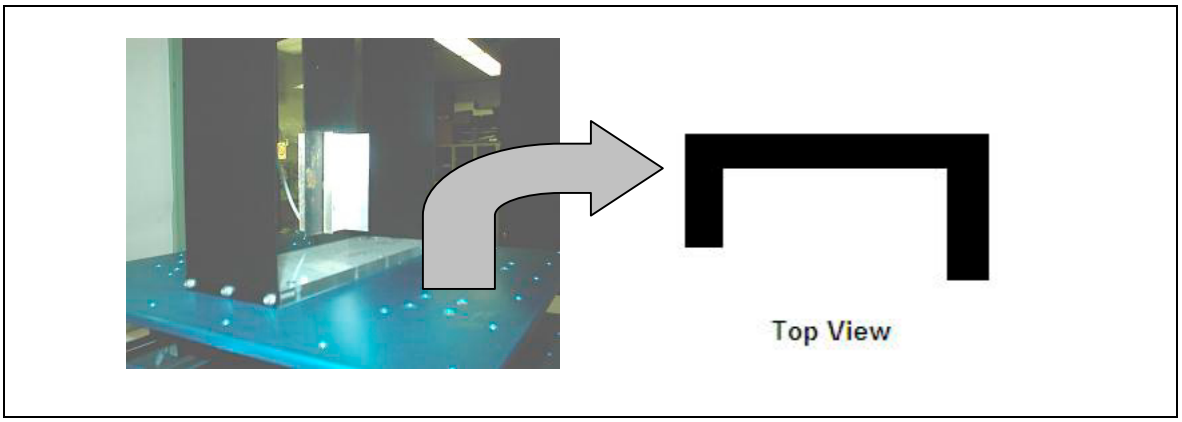

Figure 8. Steel plate with added fins

The structure with the modified walls was then re-tested. In addition to free vibration testing, records from the Kobe and Northridge earthquakes were also simulated. However, the corresponding results did not prove to be of much use on their own since the earthquakes were not simulated when testing the original walls.

Results

The response of the table and the steel plate was collected from the accelerometers and plotted. The plot was then saved as an m-file and then MATLAB was used to evaluate the plot and determine the period (frequency) of the structure, the damping ratio and the damping coefficient. Results are presented in Table 2, whose are the average of results from three tests. While the results of each of the three tests were in most cases similar to each other, some of them showed erratic behavior. Since only three tests were performed per fluid, even one test could alter the average. This observation could explain the fact that the damping ratios were different from what was expected and from what should possibly have been. Due to a shortage of time and resources, tests with the added fins and oil were not conducted.

Table 2. Test results

Viscous fluid	Damping ratio ζ [%] (before/after)	Logarithmic decrement δ (before/after)	Period [sec] (before/after)	Frequency [Hz] (before/after)
Nothing	1.55 / 1.79	13.37 / 11.26	0.32 / 0.32	3.18 / 3.10
Water	1.97 / 6.61	12.39 / 41.54	0.32 / 0.33	3.15 / 3.10
Soap	1.80 / 7.86	11.28 / 49.35	0.32 / 0.43	3.15 / 2.41
Oil	1.86 / NA	11.66 / NA	0.32 / NA	3.12 / NA
Detergent	3.54 / 7.08	22.25 / 44.51	0.32 / 0.37	3.12 / 2.72

Figure 9 shows the damping ratios of the model viscous wall before and after the modification. There is a significant contrast between the two conditions. The damping ratios increased once the extra fins were added to the steel plate. The most significant change occurred between the damping ratios of the soap water. It increased from 1.8% to 7.8%, a 6% increase in damping. This is illustrated in Figure 10, where the response of the original viscous wall is compared with the response of the wall with the fins added to the steel plate.

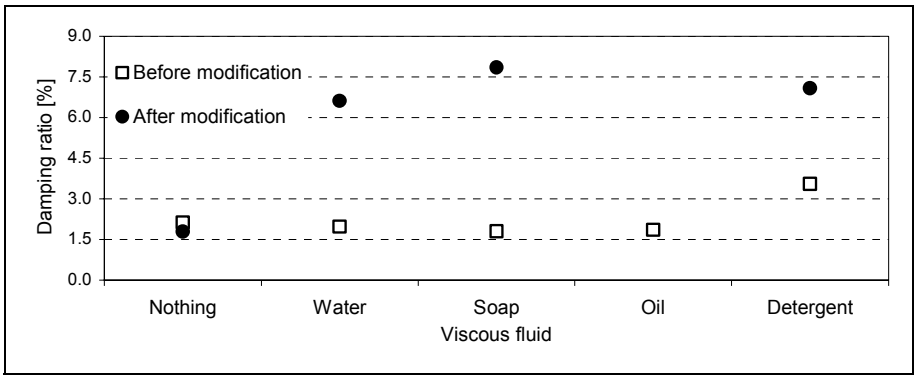

Figure 9. Comparison of damping ratios

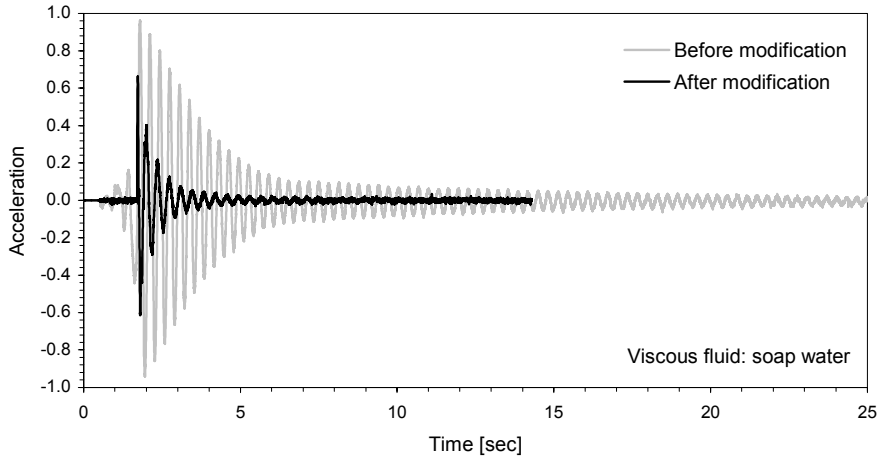

Figure 10. Response before and after adding fins to the plate of the viscous wall

Conclusion

Due to an oversight in the original test setup, the model viscous wall had to be modified. Viscous resistance was brought into focus and the damping characteristics of the viscous wall were improved. As results clearly show, there was a significant increase in damping once the fins were added to the viscous wall. Once the length of the gap between the wall of the container and the steel blade was reduced, the friction between the fluid and the blade increased. Because of that, the movement of the blade was dampened at a faster rate. Besides, thicker and more viscous fluids proved to provide better damping characteristics as opposed to fluids with lower viscosity.

Possible future work includes the development of a better version of the viscous wall. Comparison between the response of the modified viscous wall tested in this study and that of a viscous wall with a slimmer container will indicate which approach is more effective. Future tests should include several earthquake simulations. Other possibilities include test of viscous walls of different size, different amount of fluid and different (new) types of fluids.

The experiments described in this paper were intended as an introductory experience about structural dampers in general and viscous damping walls in particular. Although the device tested is a simplified model of an actual viscous wall, it nevertheless operates on the same principles. It allows the building to move during an earthquake and quickly dampens the vibrations so that structural damage is minimized.

Acknowledgements

I would like to thank my advisor, Dr. Andrei Reinhorn, for guiding me through this research experience. I acquired a vast amount of knowledge on earthquake engineering in a short period. It was an honor to work with him and I am grateful for the opportunity. I would also like to acknowledge everyone at MCEER, especially Mrs. Andrea Dargush, for her help. In addition, I wish to acknowledge the lab technicians Mark Pitman, Scott Weinreber and Duane Kozlowski for their time and assistance. Finally, my acknowledgments to the National Science Foundation for providing the opportunity to participate in the REU program.

References

Chopra AK (1995): *Dynamics of Structures: Theory and Applications to Earthquake Engineering*. Prentice Hall, Englewood Cliffs, NJ.

Constantinou MC (1994): Application of fluid viscous dampers to earthquake resistant design. *Research Accomplishments: 1986-1994*, National Center for Earthquake Engineering Research, Buffalo, NY.

Li C, Reinhorn AM (1995): Experimental and analytical investigation of seismic retrofit of structures with supplemental damping: Part II - Friction Devices. *Technical Report NCEER-95-0009*, National Center for Earthquake Engineering Research, Buffalo, NY.

MCEER Information Service (2001): *What are some Advanced Earthquake Resistant Techniques?* http://mceer.buffalo.edu/infoservice/faqs/asdesign.asp.

Reinhorn AM, Li C (1995): Experimental and analytical investigation of seismic retrofit of structures with supplemental damping: Part III – Viscous damping walls. *Technical Report NCEER-95-0013*, National Center for Earthquake Engineering Research, Buffalo, NY.

21

Tri-Center Field Mission 2002: Taiwan

Diego Lopez Garcia

Department of Civil, Structural & Environmental Engineering, University at Buffalo

Summary

This paper presents some examples of civil engineering structures that were damaged or destroyed by the 1999 Chi-Chi earthquake and have been repaired or rebuilt, as well as examples of structures not affected by the earthquake but retrofitted for damage mitigation during future seismic events. It is shown that non-engineered retrofit measures are often implemented in typical residential buildings, while more rational procedures are followed for public buildings such as schools. In the case of bridges, it is shown that simply-supported spans are no longer used and have been replaced by continuous girders connected to the substructure through elastomeric bearings. All the examples have been observed and evaluated during a recent visit (Field Mission) to Taiwan made by the author and other graduate students from U.S. universities. The Field Mission was supported by the three U.S. Earthquake Engineering Research Centers (MAE, MCEER and PEER) and was coordinated by Taiwan's National Center for Research in Earthquake Engineering (NCREE).

Introduction

The central region of Taiwan was struck by a magnitude 7.6 (Richter scale) earthquake on September 21, 1999, at 1:47 a.m. local time (September 20, 5:47 p.m. Universal Time). The earthquake was caused primarily by a rupture of the Chelungpu fault and its epicenter was located close to the town of Chi-Chi, in the Nantou County. The earthquake generated a surface fault rupture of about 100 km, and the maximum offsets were among the largest ever observed: about 11 m (vertical) and 10 m (horizontal) in the northern part of the Chelungpu fault. Peak ground accelerations were of the order of 0.30–0.50 g, while peak ground velocities were between 40–80 cm/sec.

A large number of engineering structures were located in the densely populated area around the epicenter and the surface rupture. It is not surprising then that the Chi-Chi earthquake caused a vast amount of damage. Around 2400 lives were lost, about 10,000 people were injured and approximately 100,000 people were left homeless. Many kinds of structures (buildings, bridges, dams, tunnels, transmission towers, etc) were destroyed or damaged by strong shaking, large ground offsets or landslides.

Most of the damaged structures have been repaired or rebuilt, and most of the structures that collapsed have been removed and replaced by new constructions. The objective of this paper is to present some examples of engineering structures affected by the Chi-Chi earthquake that have been repaired or rebuilt. The examples were observed and selected during the recent Tri-Center Field Mission 2002 in Taiwan, where a group of eight graduate students from the three U.S. Earthquake Engineering Research Centers (MAE, MCEER and PEER) visited the Chi-Chi area. The author of

this paper was a member of the group and represented MCEER. The Field Mission was coordinated by Taiwan's National Center for Research in Earthquake Engineering (NCREE), whose members provided comprehensive background information through a series of seminars and logistic support for the field trip.

Building Structures

The typical residential building in Taiwan is a 2-to-5-story reinforced concrete frame structure with masonry infill partitions and exterior walls. Since the first story is in most cases occupied by small stores, these buildings have a pedestrian corridor and open front at the side facing the street (Figure 1a). As a result, the first floor is weaker and more flexible than the upper floors, a structural deficiency that is often made worse by the stiffness eccentricity in the direction parallel to the street. These undesirable features were responsible for most of the collapses suffered by these kinds of buildings (Figure 1b). Other deficiencies (short column effect, lack of adequate transverse reinforcement, etc.) also contributed to the poor performance of this type of construction.

Photograph by Lopez Garcia

a)

Photograph by Bruneau/MCEER

b)

Figure 1. Typical residential building in Taiwan: (a) pedestrian corridor and open front; (b) soft story damage

Most of the buildings that did not collapse but suffered some damage have been repaired (Figure 2a) and many more have been retrofitted, mainly by incorporation of new structural members (beams and columns). In most cases, these new structural members are steel elements (Figure 2b, Figure 3). Unfortunately, the majority of these retrofit measures are non-engineered and their utility in improving the seismic behavior of typical residential buildings is difficult to evaluate.

School buildings were also severely affected by the Chi-Chi earthquake and many of them collapsed (Figure 4a). An example of retrofitting measures can be seen in Figure 4b, where metallic dampers have been added to an existing steel structure. Figure 5 shows a new school building under construction, where frames are made up of composite RC-steel members.

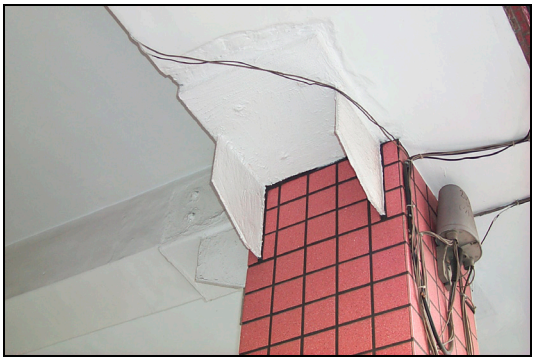

Photograph by Lopez Garcia

a)

Photograph by Lopez Garcia

b)

Figure 2. Non-engineered retrofit of residential buildings: (a) beam-column joint retrofitted with steel plates; (b) structure strengthened by a new column

Photograph by Lopez Garcia

a)

Photograph by Lopez Garcia

b)

Figure 3. Non-engineered retrofit of residential buildings: (a) RC beam strengthened by a steel beam; (b) eccentric RC beam-column joint supported by a steel column

Photograph by Lopez Garcia

a)

Photograph by Lopez Garcia

b)

Figure 4. (a) Collapse of school building; (b) Library building retrofitted with metallic dampers

Photograph by Lopez Garcia

a)

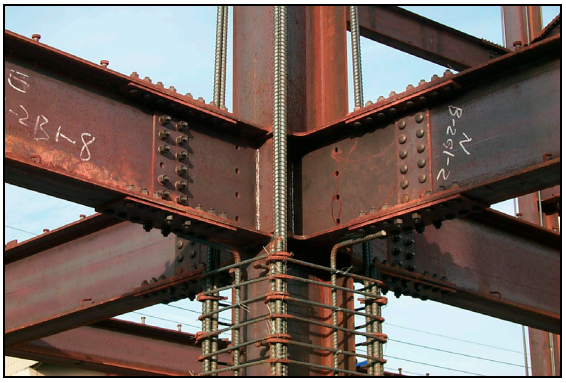

Photograph by Lopez Garcia

b)

Figure 5. New school building under construction: composite RC-steel frame

Bridge Structures

The Chi-Chi earthquake caused many bridge structures to collapse. Many bridges were directly affected by surface rupture and the consequent ground movement. These bridges collapsed due in large part to unseating of one or more simply supported spans (Figure 6a, Figure 7a), which was the typical structural configuration for bridges in service at the time of the earthquake. Other kinds of failures were also observed (Figure 8a). These bridges have been reconstructed, either partially (Figure 6b) or totally (Figure 7b, Figure 8b). An example of partial reconstruction is the Bei-Feng bridge (Figure 6), where some of the original columns were not demolished and were used to support the new bridge. The slope of part of the new bridge (Figure 6b) is a consequence of vertical offset. Most of the completely rebuilt bridges have composite decks supported by continuous steel girders (Figure 7b, Figure 8b), which seems to be the preferred structural configuration for new bridge structures in Taiwan. Joints between continuous segments are located at pier locations (Figure 9a) and the superstructure is supported through elastomeric bearings (Figure 9b). Restrainers against both longitudinal and transverse displacements are usually provided at pier and abutment locations (Figure 9).

Some bridges not affected by surface rupture were also damaged by strong ground shaking. An example of a repaired bridge structure is shown in Figure 10, where it is shown that a wide column damaged at the connection with the superstructure has been retrofitted by steel jacketing. The column-to-cap beam connection has also been improved by adding steel plates and post-tensioned rods.

Photograph by Shen/MCEER

a)

Photograph by Lopez Garcia

b)

Figure 6. Bei-Feng bridge: (a) collapse of end spans; (b) after reconstruction

Photograph by Buckle/MCEER

a)

Photograph by Lopez Garcia

b)

Figure 7. Shi-Wei bridge: (a) collapse of the middle span; (b) after reconstruction

Photograph by Buckle/MCEER

a)

Photograph by Lopez Garcia

b)

Figure 8. Wu-Shi bridge: (a) diaphragm and shear key failures; (b) after reconstruction

Photograph by Lopez Garcia

a)

Photograph by Lopez Garcia

b)

Figure 9. Typical details of new bridge structures: (a) longitudinal restrainer at joint between continuous segments; (b) restrainer at abutment location

Photograph by Buckle/MCEER

a)

Photograph by Chadwell/PEER

b)

Figure 10. Mao-Lou-Shi bridge: (a) distress in eccentric connection; (b) column retrofitted with steel jackets

Concluding Remarks

The examples shown in this paper indicate that rational procedures have been followed in either repairing or rebuilding structures such as highway bridges and public buildings such as schools. Unfortunately, this does not seem to be the case of typical residential buildings, whose structural deficiencies (soft/weak story, eccentricity) make them prone to earthquake damage. The effectiveness of non-engineered retrofit measures typically implemented in this type of buildings is somewhat uncertain and should be carefully evaluated.

Acknowledgements

The author's Field Mission in Taiwan was fully supported by the Multidisciplinary Center for Earthquake Engineering Research. Valuable assistance was provided by Andrea Dargush, MCEER's Assistant Director for Education and Research Administration, and by various staff members of MCEER Information Service. The author's observations were greatly enriched by several individual and group discussions with the other members of the Field Mission Team: Stephanie Arbogast (Southern Illinois University at Edwardsville), Cale Ash (University of Illinois at Urbana-Champaign), Charles Chadwell (University of California at Berkeley), Constantine Christopoulos (University of California at San Diego), Shana Crane (Washington State University), Amber Grubbs (Texas A&M University), Jennifer Knapp (Georgia Institute of Technology) and the Field Mission Team Leader, Professor Paul Roschke of Texas A&M University. The author also wishes to thank the various members of Taiwan's National Center for Research in Earthquake Engineering (NCREE) who contributed in one way or another to the success of the Field Mission. The dedication and patience of the Field Mission Coordinator, Dr. Jiun-Fu Chai, is particularly acknowledged.

22

An Earthquake Analysis of an Existing Structure in the Southeast Region of the United States

Terri Norton

Department of Civil and Environmental Engineering, Florida A&M University

Research Supervisor: Makola M. Abdullah, Assistant Professor

Summary

Earthquakes can and do happen in the Southeastern United States. In areas where earthquakes are likely to occur, knowledge of where and how to build structures can be helpful in reducing property damage. In this study, a detailed earthquake analysis of an existing high-rise structure located in the southeast region of the United States is performed. The analysis is based on the effects of past earthquakes in the Eastern United States. The probability of structural and nonstructural damage due to displacements imposed by seismic excitations was approximated through fragility curves. Repair costs were estimated based on the probability of exceedance of each damage state. Passive control devices were used to improve the response of the building and to reduce the extent of damage. Findings of this study will be used to educate both students and professionals on the importance of earthquake hazard in the southeast region.

Background

While hurricanes have historically been the main cause of damage to structures located in the Eastern and Southeastern United States during the June-November period, the probability of earthquakes in this region cannot be ignored. Believe it or not, earthquake hazard is prevalent in this area. Figure 1 shows the seismic hazard map for the Eastern United States. Of this area, South Carolina, Tennessee, Arkansas, Missouri, and Kentucky have a high probability of earthquake occurrence.

Although most earthquakes occur at the boundaries of tectonic plates (e.g., California), they can occur in inner zones. This is most likely caused by the build-up of strains from pressures developed at the plate boundaries (Hu 1996). The most notable events of this type were the New Madrid earthquakes of 1811-1812 and the Charleston earthquake of 1886. The four New Madrid earthquakes were the largest intraplate earthquakes in the world. The Mississippi River changed its course, the land surface sunk to form new lakes and the violent shaking snapped off trees. The Charleston earthquake, whose maximum intensity and magnitude were equal to X and 7.3, respectively, caused damage for an estimated $5,000,000 and was felt as far as 160 km away from the epicenter. This was the most damaging earthquake ever to strike the Eastern United States. To date, there have been more than 60 earthquakes in the Charleston area. On April 13, 1998, a small earthquake of magnitude 3.9 shook Kershaw County, SC, and on May 8, 2001, the Monticello Reservoir experienced a 3.26 magnitude earthquake. The quake was felt throughout the whole state.

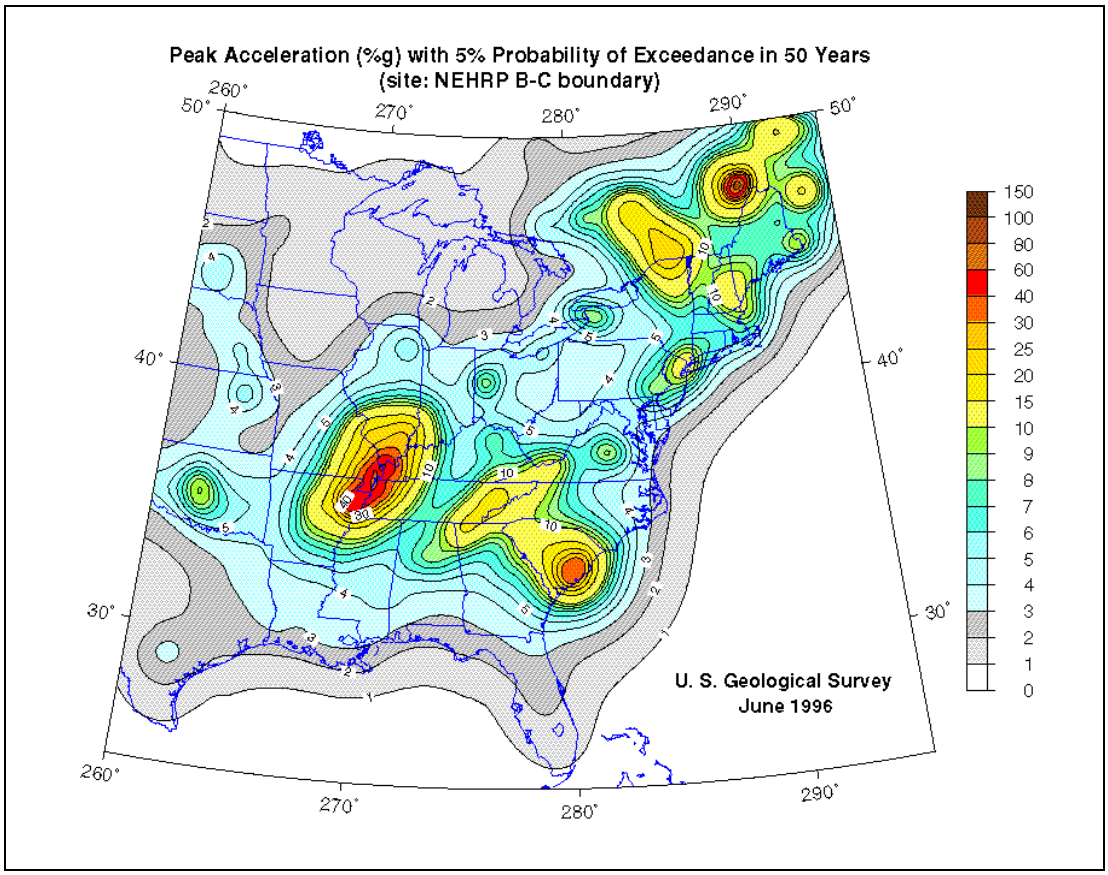

Figure 1. Seismic hazard in the Eastern United States

The probability of another event like the 1886 earthquake occurring somewhere in the Eastern United States is equal to 40-60% in the next 30 years (Nishenko and Bollinger 1990, Sibol et al., 1990). Mitigation of the effects of earthquakes is no longer a goal in earthquake-prone areas only. Therefore, there is a need to develop a methodology to guide future decision-making regarding seismic hazard.

The primary objective of this study is to analyze the effects of an earthquake on an existing structure constructed in the Southeastern region of the United States. This research also aims to relate building motion to probability of damage, which can be used to obtain approximate amounts of earthquake damage in terms of monetary cost. In addition, this study is intended to develop a methodology for the reduction of structural and nonstructural damage.

Literature Review

Recent advancements in structural dynamics have allowed civil engineers to better understand and control the vibrations of civil engineering structures due to earthquakes. This knowledge allows engineers to more readily control the vibration of high-rise structures caused by natural hazards such as earthquakes and hurricanes. Social and economic impacts of natural disasters are continually increasing due to factors such as population growth, increasing capital investment in urban areas and the inevitable increasing number of older buildings with time (Liu 1996). Therefore, there is a

growing need to mitigate the effects of natural disasters on civil engineering structures. In recent years, civil engineering applications of methods for structural control have been developed (Fujino et al., 1996).

Passive control is a widely used method of structural control. Passive control devices include base isolators and tuned mass dampers. Other passive devices are liquid column vibration absorbers and gyrostabilizers (Chang and Hsu 1998, Higashiyama et al., 1998). Base isolation was utilized in an experiment conducted on a 4-story building in Santiago, Chile. The experiment showed that the base isolation system was effective in reducing the building's peak acceleration (Moroni et al., 1998). In recent years, tuned mass dampers have been installed in a number of buildings worldwide to reduce building vibration. A tuned mass damper has been installed in the Citicorp Center in New York City (Peterson 1980).

Methodology

The structure considered for this study is the Turlington building located in downtown Tallahassee. It is a federal building housing the Florida Department of Education and Board of Regents. Therefore, it falls into the occupancy class "governmental structure." Although this study focuses on South Carolina, a structure located in Florida was chosen because building designers were accessible and because the structure was designed using a regional building code (SBC). The present worth of this building is $39,624,000.

Since the structure consists mainly of 3-bay frames, the dynamic behavior of one frame can be considered representative of the dynamic behavior of the whole structure. A 2-D finite element model of one of the N-S frames was developed. Since torsion effects were not considered, 3-D analysis was not necessary. The model has 104 nodes and 312 DOFs. Each node was assigned three DOFs: horizontal displacement, vertical displacement and rotation. Nodes were also assigned at splice locations at floors 4, 6, 8, 10, 12, 14, and 16. The model has 154 elements separated by beam-to-column connections at each node. The number of DOFs of the model was reduced using a Guyan reduction technique but the relevant dynamic characteristics of the full model were maintained (Spencer et al., 1998). The damping matrix was determined from the reduced mass and stiffness matrices.

Two types of control devices were considered: passive tuned mass damper and base isolators. The devices were designed considering the natural frequency of the uncontrolled structure. The tuned mass damper was incorporated at the top floor of the structure, while the base isolation system was modeled by adding supplemental masses at the base of the first story columns and by modeling rubber bearing pads between the new floor masses and the ground.

In this study, the HAZUS approach for damage assessment was followed, according to which estimates of earthquake damage in buildings can be made given the building type and the level of ground motion. Damage functions or fragility curves are used to define the probability of reach or exceedance for different damage states given the peak building response. Damage states include slight, moderate, extensive, and complete damage.

According to the building types presented by HAZUS, the structure considered in this study is labeled as S1H, which means high-rise steel moment frame with 8+ stories. This kind of structures, like others, might experience both structural and non-structural damage.

Economic loss is derived from building damage estimates. These estimates, which depend on the structural type and/or the occupancy class, are expressed in terms of the probability of occurrence of a particular damage state. Using inventory information and economic data, monetary loss can be derived from the damage state probabilities. Building repair and replacement costs are estimated as the product of the floor area of each building type within the given occupancy class, the corresponding probability of occurrence of the given damage state, and repair costs of the building type per square foot for the given damage state.

Results

Three input loads were considered for this analysis. The first input load used in the analysis is the acceleration record of the 1988 Saguenay earthquake (Quebec, Canada), whose magnitude and intensity were equal to 5.9 and VII, respectively. This event was the largest earthquake in Eastern North America in 53 years. The next input load is a magnitude 7.3, "Charleston-like" synthetic ground acceleration, which was developed by the Engineering Seismology Laboratory at the University at Buffalo using a stochastic model. The final input load considered for the analysis is a synthetic representation of the New Madrid earthquakes that shook the western part of Tennessee in 1811-1812. The magnitude 8 earthquake is one of the largest ever felt in the United States.

For each control approach considered (i.e., tuned mass damper and base isolation), the uncontrolled response of the structure was compared with the controlled response. Results proved that the control methods were successful in reducing the floor displacements of the structure. The tuned mass damper was found to be more effective in reducing the response of the upper floors, while base isolation was most effective in reducing the response of the lower floors. Overall, separation of the superstructure from its foundation (base isolation) achieved higher reductions of building motion.

Static analysis was performed and accurate approximations of the structural response were obtained considering the first five modes only. The probabilities of damage for the five modes were used to approximately calculate the cost of damage to the structure. In the worst-case scenario, a magnitude 8 earthquake will damage 30% of a structure such as the one considered in this study (i.e., the building designed without seismic provisions) and repairs will cost $12,000,000. Structures located in the low seismic zone of South Carolina might experience as much as $10,000,000 worth of damage if exposed to a large magnitude earthquake. These amounts are considerable compared to the $7,000,000 damage expected in High-Code design regions such as California. While none of the seismic designs considered made the structure resilient to damage, consideration of seismic effects always reduce the likelihood of structural collapse and personal injuries.

Conclusion

Cost of damage repair can be reduced by as much as 70% by incorporating either a TMD or a base isolation system. The TMD was not as effective as the base isolation system in reducing the damage to the post-earthquake model. Control devices not only reduce the response of the structure to earthquakes but also reduce the amount of damage. Therefore, control devices might be a good supplement for existing structures designed without considering seismic provisions and located in regions with seismic history.

Future Work

Consideration of nonstructural damage and damage to the building contents due to ground accelerations might be important and should be considered in further studies. In addition, 3-D models might be necessary to perform more realistic analyses. While this study considered structural damage caused by strong ground motion only, future work should account for other causes of damage. The methodology developed in this study should also be used to evaluate damage caused by other phenomena such as hurricanes.

Acknowledgements

This research was carried out under the supervision of Professor Makola M. Abdullah, and supported in part by the Multidisciplinary Center for Earthquake Engineering Research.

References

Chang CC, Hsu CT (1998): Control performance of liquid column vibration absorbers. *Engineering Structures*, **20** (7), 580-586.

Fujino Y, Soong TT, Spencer Jr. BF (1996): Structural control: basic concepts and applications. *Proceedings of Structures Congress XIV*, American Society of Civil Engineers, New York, NY.

Higashiyama H, Yamada M, Kazao Y, Namiki M (1998): Characteristics of active vibration control system using gyro-stabilizer. *Engineering Structures*, **20** (3), 176-183.

Hu YH (1996): *Earthquake engineering.* E & FN Spon, London, UK.

Liu A (1996): Regional Loss Estimation in Earthquakes. *Ph.D. Dissertation*, Department of Civil Engineering, Johns Hopkins University, Baltimore, MD.

Moroni MO, Sarrazin M, Boroschek R (1998): Experiments on a base-isolated building in Santiago, Chile. *Engineering Structures*, **20** (8), 720-725.

Nishenko SP, Bollinger GA (1990): Forcasting damaging earthquakes in the Central and Eastern United States. *Science*, **249** (4975), 1412-1416.

Peterson N (1980): Design of large scale tuned mass dampers. *Structural control: Proceedings of the International IUTAM Symposium on Structural Control*, North-Holland Publishing Co., New York, NY.

Sibol MS, Snoke JA, Bollinger GA, Chapman MC, Birch JB, Johnston AC (1990): The probability of a major earthquake in the Eastern United States. *Seismological Research Letters*, **61** (2), 131-136.

Spencer Jr. BF, Christenson RE, Dyke SJ (1998): Next generation benchmark control problem for seismically excited buildings. *Proceedings of the Second World Conference on Structural Control*, Wiley, Chichester, UK.

Production Staff

- Jane E. Stoyle, Managing Editor
- Michelle A. Zuppa, Layout and Design

Cover Images

Cover Images (from top left, then clockwise): Jeffrey Berman and Gordon Warn, University at Buffalo, analyze damage to the Liberty Building following the attack on the World Trade Center complex; Group photograph from the 2002 SLC retreat held in August in Buffalo, NY; Diego Lopez Garcia (right) and Dr. Juin-Fu Chai, NCREE, (left) are pictured during the Tri-Center Field Mission to Taiwan; Computational model for connectivity used by Dyah Kusumastuti, University at Buffalo; Experimental model of transformer-bushing on shaking table, used in research by S. Ali Ashrafi, New Jersey Institute of Technology; Group photograph from the 2002 SLC retreat held in August in Buffalo, NY; Daniel Fenz, REU student, studied the frictional properties of non-metallic materials for use in sliding bearings; Gordon Warn, University at Buffalo, discusses his research with researchers, students, and industry partners at the poster session portion of MCEER's 2002 Annual Meeting.

Acknowledgements

This work was supported primarily by the Earthquake Engineering Research Centers Program of the National Science Foundation under NSF Award Number EEC-9701471.

Any opinions, findings and conclusions or recommendations expressed in this material are those of the author(s) and do not necessarily reflect those of the National Science Foundation.

MULTIDISCIPLINARY CENTER FOR EARTHQUAKE ENGINEERING RESEARCH

A National Center of Excellence in Advanced Technology Applications

University at Buffalo, State University of New York
Red Jacket Quadrangle ▪ Buffalo, New York 14261-0025
Phone: 716/645-3391 ▪ Fax: 716/645-3399
E-mail: mceer@acsu.buffalo.edu ▪ WWW Site: http://mceer.buffalo.edu

Headquartered at the University at Buffalo